Defining the Use of Midazolam as a Probe of CYP3A4 Activity: Sensitive Quantitation of the Metabolites and Characterization of Mechanism-Based Inactivation

by

Terry D. Podoll

A dissertation submitted in partial fulfillment
of the requirements for the degree of

Doctor of Philosophy

University of Washington

1996

Approved by William F. Trager
(Chairperson of Supervisory Committee)

Program Authorized to Offer Degree Medicinal Chemistry

Date January 30, 1996

In presenting this dissertation in partial fulfillment of the requirements for the Doctoral degree at the University of Washington, I agree that the Library shall make its copies freely available for inspection. I further agree that extensive copying of this dissertation is allowed for scholarly purposes, consistent with "fair use" as prescribed in the U.S. Copyright Law. Requests for copying or reproduction of this dissertation may be referred to University Microfilms, 1490 Eisenhower Place, P.O. Box 975, Ann Arbor, MI 48106, to whom the author has granted "the right to reproduce and sell (a) copies of the manuscript in microfilm and/or (b) printed copies of the manuscript made from microfilm."

Signature Jeffrey D Fiedoll

Date Jan. 31 1996

University of Washington

Abstract

Defining the Use of Midazolam as a Probe of CYP3A4 Activity: Sensitive Quantitation of the Metabolites and Characterization of Mechanism-Based Inactivation

by Terry D. Podoll

Chairperson of the Supervisory Committee:
Professor William F. Trager
Department of Medicinal Chemistry

A highly sensitive GC NCI/MS assay was developed for midazolam metabolites. The limit of quantitation was 0.3 ng/mL. This assay allowed the determination of kinetic parameters for metabolite formation from *in vitro* incubations that contained only 250 fmol/mL CYP3A4 and included midazolam concentrations as low as 200 nM (similar to the *in vivo* concentrations of this drug). Time-dependent metabolite formation was found to be limited to only 4 minutes for the calculation of initial rates of product formation, and the reasons for this were investigated.

During these investigations, evidence that midazolam is a selective mechanism-based inactivator of CYP3A4 was obtained and can be summarized as follows:

1) Active site titration experiments gave linear results in both human liver microsomes and a cDNA-expressed CYP3A4 preparation, and the partition ratio was approximately 200 in both systems.
2) Pseudo-first order, saturable inactivation kinetics were observed, and a $K_I = 15.0 \pm 3.4$ μM and a $k_{inact} = 0.338 \pm 0.135$ min^{-1} were determined.
3) The requirement of catalytic turnover for inactivation was inferred from the observation that inactivation required NADPH.
4) Inactivation was not attenuated in the presence of superoxide dismutase, catalase, glutathione, or N-acetyl cysteine.

5) Inactivation was attenuated in the presence of a competing substrate, alfentanil.
6) A 1 to 1 correspondence between the level of NADPH-dependent ^{3}H-midazolam irreversible binding to microsomal protein and the level of inactivation of CYP3A4 was observed.

Therefore, all of the established criteria for mechanism-based inactivation were addressed.

Despite mechanism-based inactivation, midazolam can be used as an *in vitro* probe of CYP3A4 activity. When the midazolam concentrations used to determine K_m and V_{max} are ≤ 4 μM, the ratio, K_m/V_{max}, for 1′-hydroxylation was determined by the content of CYP3A4 in hepatic microsomes from a population of organ donors. Under these conditions inactivation did not significantly alter the kinetics of metabolite formation. However, when the concentrations of midazolam were ≥ 10 μM, inactivation significantly effected the relative rates observed for 1′- and 4-hydroxylation. The gross kinetic characteristics of 1′- and 4-hydroxylation at high midazolam concentrations were predicted by calculating the time-averaged levels of CYP3A4 remaining during the incubation.

TABLE OF CONTENTS

LIST OF FIGURES

Figure **Page**

LIST OF TABLES

Table **Page**

ACKNOWLEDGEMENTS

I would like to thank the chairman of my supervisory committee, Dr. William F. Trager, for his help and support in preparing this dissertation. I would also like to thank the other reading committee members, Dr. Sid Nelson and Dr. Gary Elmer, as well as the remaining members of the supervisory committee, Dr. Tom Baillie, Dr. Y. A. Pocker, and Dr. Rene Levy. Meeting the high standards of this committee was facillitated by a particularly enthusiastic group of scientists including Dr. Evan Kharasch, Dr. Kent Kunze, Dr. Allan Rettie, and Dr. Ken Thummel whose ideas helped fuel this dissertation. There are many contributors to the work in this dissertation including Miss. Justina Calamia, Dr. Eric Dietze, Mr. William Howald, and Dr. Raimond Peter. Furthermore, many people have made favorable contributions to my personal and professional growth over the last few years including Dr. Bill Atkins, Mr. Ben Amore, Mr. Andy Bird, Dr. Tim Carlson, Mr. Mike Dabrowski, Dr. John Darbyshire, Mr. Mike Fisher, Mrs. Jeanine Fisher, Mr. Shane Hendrickson, Dr. Krishna Iyer, Mr. Luke Koenigs, Dr. Debra Mattiello, Miss Mary Paine, Mr. Mike Schrag, Dr. Larry Wienkers, and Mrs. Colleen Wurden. Without the continuing love and support of my family, Mr. Harvey Podoll, and "the sibs", Gaynelle, Jack, Doug, Cindy, and Ryan, this dissertation would not have been possible. Thank you, everyone!

Dedicated to mom, Bonnie J. Podoll
in loving memory

and

to my wife, Jill R. Arechiga
forever one of a kind in my heart.

CHAPTER ONE

INTRODUCTION

1.1. Cytochrome P450

Cytochrome P450 is a collective term for what is now known to be an important class of monooxygenase enzymes involved in the metabolism of numerous endobiotic and xenobiotic organic compounds [Guengerich, 1990]. The products of cytochrome P450 metabolism include biologically inactive, pharmacologically active, and toxic metabolites [Williams, 1959; Drayer, 1976; Nelson, 1982]. Mammalian cytochrome P450s are membrane bound, heme-containing monooxygenase proteins (45 - 60 kDa) localized in "microsomes", a cellular fraction derived from the endoplasmic reticulum [Guengerich, 1990]. Although these enzymes are located in many tissues in the body, metabolism of exogenous compounds predominantly occurs in the liver [Williams, 1971]. Cytochrome P450 converts lipophilic substrates to polar products by catalyzing the covalent transfer of an atom of oxygen to the substrate. This oxygen transfer reaction is the endpoint of a series of electron transfer reactions that require reduced nicotinamide adenine dinucleotide phosphate (NADPH), NADPH-cytochrome P450 reductase, and molecular oxygen (O_2). The present understanding of the sequential interactions of the monooxygenase system can be represented as a catalytic cycle (Fig. 1.1) [Ortiz de Montellano, 1986]. For each mole of hydroxylated product and water formed there is one mole of O_2 consumed and one mole of NADPH consumed. However, the catalytic cycle is

inherently inefficient and decoupling pathways are present in the cycle, one of which is shown in Fig. 1.1.

Recently, P450 has been described as a superfamily of related genes and a nomenclature system has been developed based on the divergent evolution of the genes [Nebert et al., 1993]. The authors listed 221 individual genes occuring in mammals, plants, and prokaryotes. The nomenclature system divides the genes into families and subfamilies by comparing the deduced amino acid sequences of the proteins. There are at least 17 human P450 subfamilies, seven of which participate in the hepatic metabolism of exogenous compounds. One subfamily that has been widely studied because of its clinical and toxicological importance is CYP3A [Wrighton and Stevens, 1992].

1.2. Cytochrome P450 3As

The CYP3A subfamily, at the time of the most recent report, was know to contain genes encoding 4 proteins: CYP3A3, CYP3A4, CYP3A5, and CYP3A7 [Nebert et al., 1993]. However, expression of CYP3A3 has never been demonstrated in human tissue [Gorski et al., 1994]. The deduced amino acid sequence of CYP3A3 is 97% similar to that of CYP3A4, and thus the difference between the genes encoding CYP3A3 and CYP3A4 may be the result of a cloning artifact [Gonzalez et al., 1988; Gorski et al., 1994]. CYP3A7 is expressed at relatively high levels in human fetal livers, but not in the normal livers of adult humans [Komori et al., 1990; Itoh et al., 1992]. Recently, however, detection of the mRNA of CYP3A7 in adult human liver was reported [Schuetz et al., 1994].

CYP3A5 is also expressed in most fetal livers while it is polymorphically expressed in only about 25% of adult human livers [Schuetz et al., 1994; Wrighton et al., 1989; Wrighton et al., 1990]. When CYP3A5 is expressed in adult livers, the levels found are usually about 30% of the amounts of the major, constitutive CYP3A, CYP3A4 [Wrighton et al., 1990; Bork et al., 1989].

CYP3A4 appears to be the major cytochrome P450 constitutively expressed in adult human liver, comprising as much as 50% of the total P450 in the liver [Guengerich and Turvey, 1991]. Additionally, it is the major P450 expressed in enterocyte cells of the small intestine [Kolars et al., 1992; Watkins et al., 1987]. The observed level of CYP3A4 in both liver and intestine is increased ("induced") in individuals exposed to glucocorticoids (e.g. dexamethasone), rifampin, phenytoin and other drugs [Watkins, 1992]. A distinguishing characteristic of the catalytic activity of the CYP3A subfamily is their apparent ability to exist in kinetically distinct conformations which can be modulated by allosteric effectors, or activators [Johnson et al., 1988; Shou et al., 1994; Koley et al., 1995]. Furthermore, the role of CYP3A4 in metabolizing a large and growing number of structurally diverse compounds including endogenous steroids, drugs, and environmental contaminants has been established (Table 1.1 and references within). Three of the substrates have also been described as selective inhibitors of CYP3A4 (Table 1.1 and references within).

Because the metabolism of so many drugs is mediated primarily by CYP3A4, the potential for clinically significant drug-drug interactions

to occur might be expected to be high. Indeed, interactions between cyclosporin and erythromycin, midazolam and erythromycin, and a life-threatening interaction between terfenadine and ketoconazole have been described [Godin et al., 1986; Olkkola et al., 1993; Monahan et al., 1990]. It is now known that the basis of the terfenadine-ketoconazole interaction, which precipitates increased plasma levels of terfenadine that lead to ventricular arrythmias, is inhibition of CYP3A4 by ketoconazole [Woosley et al., 1993]. Historically, as in the case of terfenadine, clinicians have been unaware of potentially adverse drug-drug interactions until they have been observed in a clinical setting. Recently, several investigators have suggested that *in vitro* metabolism studies should be rigorously pursued to allow anticipation of such metabolism-based interactions before clinical trials and marketing of new pharmaceuticals [Chiu, 1993; Gonzalez, 1992; Peck et al., 1993; Rodrigues, 1994].

Before accurate, quantitative predictions of the *in vivo* metabolic behavior of a drug candidate can be provided by *in vitro* metabolism studies, our knowledge of the determinants of metabolism in each system must be established. The objective of the studies presented in this dissertation is to establish the determinants of metabolism *in vitro*. Once established, assessment of their extention into the *in vivo* system can be undertaken. One approach to assessing P450 drug metabolism *in vitro* and *in vivo* is the development of molecular probes of the enzymes. Initial considerations in the selection of an appropriate probe of a P450 *in vitro* include:

1) Is the probe selectively metabolized by that single P450?
2) Does metabolite formation *in vitro* obey Michaelis-Menten kinetics?
3) Is the probe metabolized to a dominant, chemically and metabolically stable metabolite?

Furthermore, if these *in vitro* considerations of the potential probe are affirmed, then initial assessment of its metabolic properties *in vivo* should be made. Does metabolism of the probe *in vivo* resemble the metabolism observed *in vitro*? Is the measurement of the probe's *in vivo* metabolism relatively non-invasive and timely?

Currently, two molecular probes of CYP3A4 are being used *in vivo*. They are the erythromycin breath test (ERMBT) and urinary screening of 6ß-hydroxycortisol relative to cortisol [Watkins, 1992; Horsmans et al., 1992]. However, the appropriateness of neither of these probes has been established *in vitro*, and there appears to be problems with the selectivity of these probes *in vivo* [Thummel et al., 1994]. Because of the uncertainty of selectivity, and the clear need for a suitable *in vivo* probe, the development of such a probe with well established kinetic behavior *in vitro* would be highly desirable. To that end, the widely used anesthetic benzodiazepine, midazolam, was selected as a prime candidate (Fig. 1.2). The reasons for the selection are outlined below.

1.3. Midazolam

1) At low concentrations in human liver microsomes midazolam is predominantly metabolized *in vitro* by CYP3A4 [Fabre et al., 1988;

Kronbach et al., 1989]. These studies utilized several techniques, including antibody inhibition, chemical inhibition, correlative analyses, and cDNA-expressed CYP3A4 to show that P450 enzymes belonging to the CYP3A subfamily are major contributors to midazolam 1′- and 4-hydroxylation. CYP3A5 has also been shown to metabolize midazolam [Gorski et al., 1994]. However, because CYP3A5 is expressed polymorphically in only 25% of the population, and because CYP3A5 is expressed at levels ≤ 30% of CYP3A4 in individuals who do express CYP3A5, the contribution of CYP3A5 could be considered negligible in the population.

2) Although Kronbach et al. initially reported unusual, non-competetive substrate inhibition, other investigators later reported single-enzyme, Michaelis-Menten kinetics [Gascon et al., 1991; Gorski et al., 1994]. Michaelis-Menten kinetics provides a characteristic numerical definition of midazolam metabolism *in vitro*, through the V_{max}/K_m value of the selective CYP3A4-dependent metabolite, that allows direct comparison to its *in vivo* metabolism behavior via the intrinsic formation clearance for that metabolite. The critical observations which indicate that product formation via an enzyme catalyzed reaction obeys steady-state Michaelis-Menten kinetics are addressed in the opening sections of Chapters 2, 3 and 5.

3) Midazolam is predominantly metabolized *in vitro* to a single metabolite, 1′-hydroxymidazolam (1′-OH MDZ) that is chemically and metabolically stable [Woo et al., 1977; Gerecke, 1983]. These properties are suitable for sensitive quantitative analysis of product formation.

Furthermore, midazolam contains halogenated aromatic rings which provide a sensitive analytical handle. Analytical considerations are discussed in detail in Chapter 2.

In addition, midazolam is extensively and predominantly metabolized to 1′-OH MDZ *in vivo* [Puglisi et al., 1978], suggesting that CYP3A4 activity is the main determinant of metabolism both *in vitro* and *in vivo*. Although 1′-OH MDZ is at least partially glucuronidated before excretion, ß-glucuronidase treatment of the urine and plasma samples releases 1′-OH MDZ, allowing quantitation of the initial hydroxylation process. A non-sedating dose of midazolam can be administered either orally or in a non-irritating intravenous formulation, and exhibits a short elimination half-life (1 to 2 h) [Garzone et al., 1989]. Therefore, the contribution of both hepatic and intestinal metabolism could be conveniently assessed *in vivo* from blood samples obtained within a few hours.

Upon initial assessment, it appears that midazolam is well suited to be a probe of both the *in vitro* and *in vivo* system. Knowledge of the determinants of midazolam metabolism in the two systems could allow accurate, quantitative predictions of the *in vivo* metabolic behavior from *in vitro* metabolism studies. If so, then significant progress has been made toward using *in vitro* studies to anticipate CYP3A4-metabolism-mediated drug-drug interactions. This dissertation defines the determinants of the *in vitro* metabolism of midazolam.

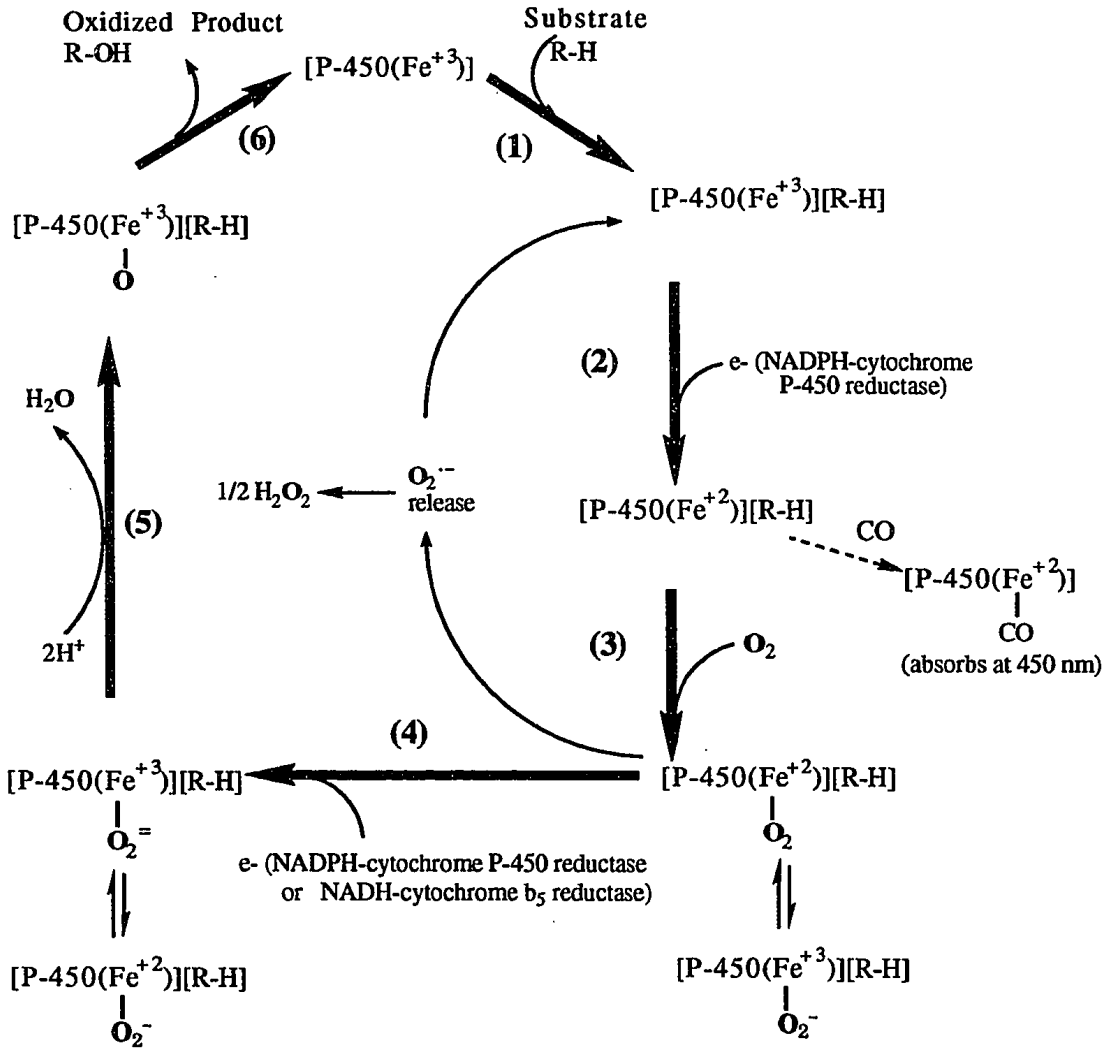

Figure 1.1. The catalytic cycle of cytochrome P450.

Table 1.1. Partial list of substrates for the CYP3A subfamily.

Steroids:	Testosterone	[Waxman et al., 1988]
	Cortisol	[Guengerich et al., 1986]
	Progesterone	[Waxman et al., 1988]
	Androstenedione	[Waxman et al., 1988]
	Estradiol	[Guengerich et al., 1986]
Drugs:	FK506	[Sattler et al., 1992]
	Cyclosporin A	[Kronbach et al., 1988]
	Rapamycin	[Sattler et al., 1992]
	Erythromycin	[Watkins et al., 1985]
	Ifosfamide	[Walker et al., 1994]
	Midazolam	[Kronbach et al., 1989]
	Warfarin	[Rettie etal., 1992]
	Alfentanil	[Kharasch et al., 1993]
	Quinidine	[Guengerich et al., 1986]
	Nifedipine	[Guengerich et al., 1986]
	Benzphetamine	[Guengerich et al., 1986]
	Acetaminophen	[Thummel et al., 1993]
	Terfenadine	[Yun et al., 1993]
Selective Inhibitors:	Troleandomycin	[Wrighton, et al., 1985]
	17α-ethynylestradiol	[Guengerich, 1988]
	Gestodene	[Guengerich, 1990]
Toxins:	Aflatoxins	[Ramsdell et al., 1991]
	1-Nitropyrene	[Silvers et al., 1992]

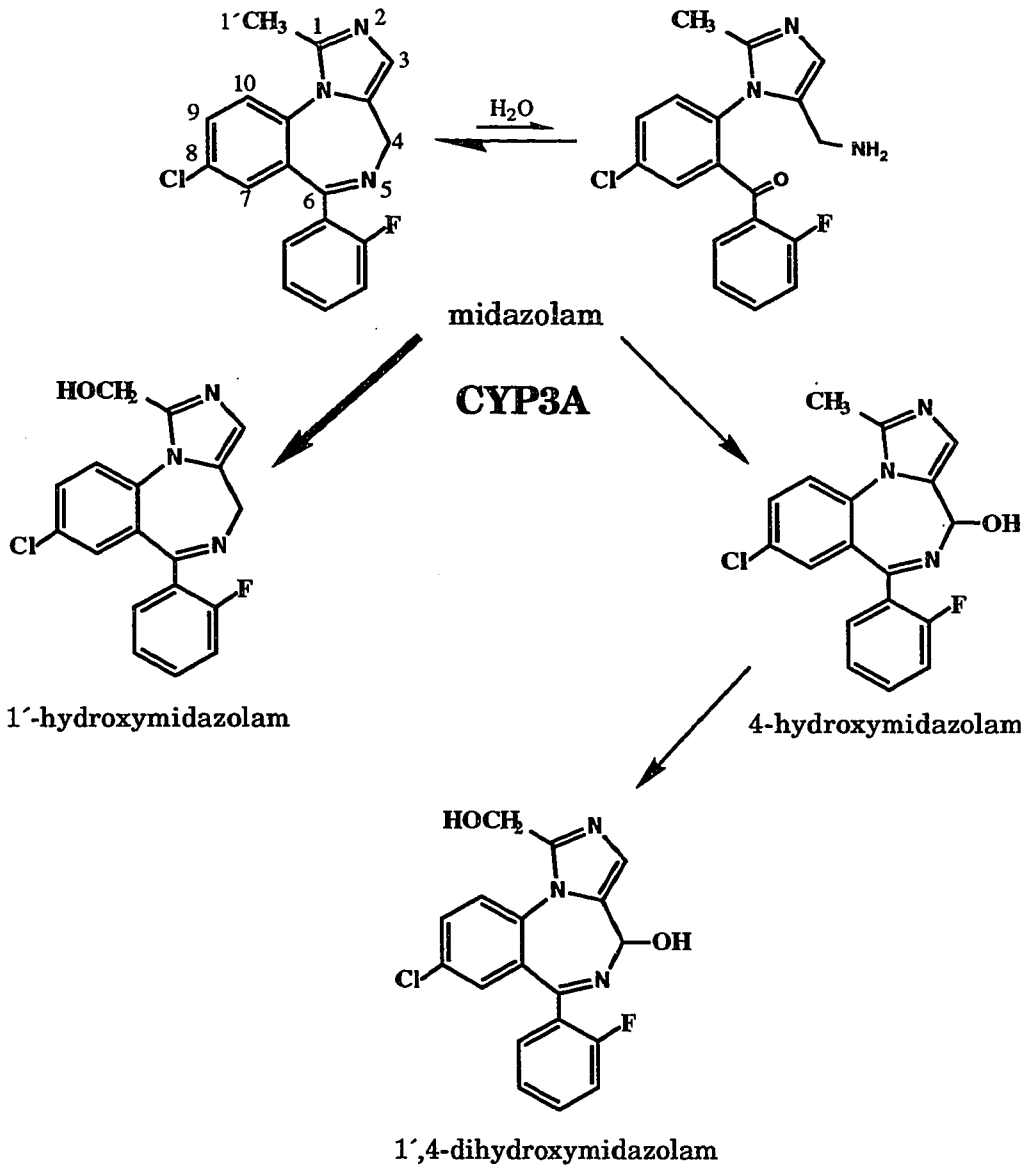

Figure 1.3. Metabolic pathway of midazolam hydroxylation.

CHAPTER TWO

THE QUANTITATIVE ASSAY OF MIDAZOLAM METABOLITES BY GAS CHROMATOGRAPHY NEGATIVE CHEMICAL IONIZATION MASS SPECTROMETRY

2.1 Goals for the Assay of Midazolam Metabolites

All studies concerned with the fate of midazolam in biological environments, whether they be forensic, clinical or research, require an adequate method for the determination of midazolam and its metabolites. One of the goals of the research presented in this thesis was to utilize midazolam as an *in vitro* probe to predict midazolam metabolism *in vivo*. If the *in vitro* system is to reflect *in vivo* metabolism, then drug concentrations used *in vitro* should be similar to those found *in vivo*. Midazolam is a very potent drug with plasma concentrations of only 50 to 100 ng/mL (~0.15 to 0.3 μM) required for pharmacologic effect [Allonen et al., 1981]. Utilization of such low concentrations *in vitro* demands a highly sensitive assay for the metabolites. Accurate measurement of K_m and V_{max} *in vitro* requires the observation of steady-state kinetics. The steady-state assumption is valid if < 5% of the substrate is consumed during *in vitro* metabolism experiments. Therefore, to accurately measure metabolites from a 100 ng/mL incubation *in vitro*, assuming steady-state kinetics, the metabolite assay sensitivity must be ≤ 5 ng/mL. Such an assay for midazolam metabolites was desired to allow characterization of the steady-state kinetic parameters of this drug at low, *in vivo*-like substrate concentrations in human liver microsomes. The following discussion

outlines the available assays for midazolam metabolites, current knowledge of *in vitro* midazolam metabolism, and the incentives and strategy for developing a highly sensitive assay for midazolam metabolites.

Published methodologies for the determination of midazolam and/or its metabolites include high-performance liquid chromatography (HPLC) [Blackett, 1988; Ha, 1993; Mastey, 1994; Puglisi, 1985], gas chromatography (GC) [Vasiliades, 1982; Puglisi, 1978; Greenblatt, 1981], gas chromatography interfaced with electron ionization mass spectrometry (GC/MS) [Fraser, 1991; Vasiliades, 1982], gas chromatography interfaced with negative chemical ionization mass spectrometry (GC/NCIMS) [Rubio, 1982], differential pulse polarography [Puglisi, 1978], fluorescence polarization immunoassay [Fraser, 1991], and radioimmunoassay [Dixon, 1982]. All of these assays were designed to measure the analytes extracted from plasma and/or urine. Limits of quantitation (LOQ) range from 1 to 100 ng/mL. Those studies measuring the minor metabolite, 4-hydroxymidazolam (4-OH MDZ), reported LOQ ranging from 5 to 50 ng/mL. However, 5 ng/mL LOQ for the minor metabolite was expected to be insufficient for our planned *in vitro* studies (*vide infra*). The most sensitive of all the published assays was that for 1′-hydroxy midazolam (1′-OH MDZ) developed by Rubio et al.using GC/NCIMS (LOQ 1 ng/mL). However, the report did not include determination of the minor metabolite.

Published studies of *in vitro* midazolam metabolism were reviewed with regard to the levels of metabolites that are typically generated at very low substrate concentrations.. Midazolam metabolism in human liver microsomes has been extensively characterized [Kronbach, 1989; Fabre, 1988; Gorski, 1994; Gascon, 1991]. These studies utilized HPLC analysis of

metabolites extracted from a 10 minute incubation of midazolam with microsomal P450, during which linear product formation was reported. The LOQ for these assays ranged from 5 to 30 ng/mL for both 1′-OH MDZ and 4-OH MDZ. Because the amounts of metabolites formed at each specific concentration were not reported explicitly, the amounts generated were calculated based on the reported parameters and conditions. Two of the citations above reported Michaelis-Menten parameters estimated by non-linear regression analysis of velocity vs. substrate concentration curves assuming single-enzyme kinetics. Metabolite formation in these studies was rapid and displayed a high interindividual variablity, V_{max} values ranged from ~200 to 2000 pmol/min/mg protein for both metabolites [Gascon et al., 1991; Gorski et al., 1994]. The apparent K_m s reported for 1′-OH MDZ and 4-OH MDZ formation ranged from 2.5 to 12.6 μM (average $K_m = 6.0 \pm 3.9$ μM) and 14.7 to 119 μM (average $K_m = 58.5 \pm 43.3$ μM) respectively. The lowest substrate concentration utilized in these studies was 0.5 μM midazolam while the microsomal protein concentration was 250 μg/mL and 500 μg/mL for Gorski and Gascon, respectively. Under these conditions, the single enzyme kinetic model rate equation used by these investigators:

$$v = \frac{V_{max} * [S]}{K_m + [S]}$$

predicts relative rates of formation of the metabolites at a 9:1 ratio of 1′-OH MDZ to 4-OH MDZ. The fastest conditions, achieved with microsomes from a liver that gave a high V_{max} for midazolam turnover and Gascon's relatively high protein concentration, gives a rate, v, that predicts complete depletion of the substrate after a 10 minute incubation. The slowest conditions, achieved with microsomes from a liver that gave a low

V_{max} for midazolam turnover and Gorski's relatively low protein concentration, give a rate that predicts 8% substrate depletion, and formation of 13 ng 1´-OH MDZ and 1.4 ng 4-OH MDZ. This analysis highlights two important factors regarding steady-state metabolism at low midazolam concentrations in human liver microsomes. The first factor is that substrate depletion may occur due to the high affinity and high rate of midazolam turnover to the 1´-OH MDZ metabolite. Lowering the protein concentration to avoid substrate depletion leads to the second factor. At low protein concentration incubations of midazolam sub-ng/mL concentrations of 4-OH MDZ are predicted. Therefore, the reported LOQ for 4-OH MDZ, at 5 ng/mL, is not sensitive enough to provide *in vitro* midazolam kinetics at the desired, low substrate, conditions and current midazolam metabolite assays are insufficient. In conclusion, the GC/NCIMS assay introduced by Rubio warranted further investigation in order for the kinetics of midazolam metabolism to be adequately determined.

Rubio et al. took advantage of one of the most sensitive techniques available for the determination of organic compounds, particularly those with high electron affinity. The technique is electron capture, coupled with a mass spectrometer operating in the negative ion detection mode, which provides a very sensitive means of detecting polyhalogenated organic compounds. Midazolam, as a polyhalogenated organic compound, is expected to have high electron affinity. Negative chemical ionization mass spectrometry has been reviewed [Budzikiewicz, 1986]. In short, negative chemical ionization provides a volume of low energy electrons (0 to 5 eV) which can interact with analytes introduced into the source of the

mass spectrometer. High energy (~70 eV) electrons emitted from a hot filament are thermalized by interacting with a moderating gas, such as methane or nitrogen, at a pressure of at least 10^{-4} Torr within the source. The moderating gas lowers the electron energy via ionization of gas molecules and electron collisions with neutral gas molecules. With low energy electrons, two types of electron-molecule interactions giving negative ions are possible:

$$\text{i) } AB + e^- \rightarrow AB^{-\cdot}$$

$$\text{ii) } AB + e^- \rightarrow A^- + B^{\cdot}$$

Negative molecular ions are generated via process i) at 0 to 2 eV and termed associative resonance electron capture; or one or more fragment ions can be generated via process ii) at up to 5 eV and termed dissociative resonance electron capture where AB represents the analyte and A or B are fragments thereof. Ions can also be generated by ion-molecule reactions, the most important of which is depicted in process iii) and involves proton transfer:

$$\text{iii) } ABH + X^- \rightarrow AB^- + XH$$

where X^- is an anion exhibiting a higher proton affinity than the analyte anion. Neutral loss from any of the negative ions generated in the processes outlined above generates a negative fragment ion. Rubio et al. observed an $M^{\cdot-}$ base-peak molecular ion for the trimethylsilated 1′-OH MDZ (m/z 413) and an $[M\text{-}(CH_3)_3SiOH]^{\cdot-}$ fragment ion (m/z 323). Derivatization of the midazolam alcohol to the trimethylsilyl (TMS) ether was shown by Rubio et al. to give suitable GC and fragmentation properties. The electron capture and fragmentation properties of the

derivatized 4-OH MDZ metabolite are expected to be similar to those of the 1′-OH MDZ metabolite.

Assuming similar GC/NCIMS properties for 4-OH MDZ, Rubio's report suggested that the LOQ for both metabolites might be < 1 ng/mL. Rubio et al. have reported a LOQ of 1 ng/mL for 1′-OH MDZ. The lowest calibration curve sample contained 2 ng/mL 1′-OH MDZ and accuracy and precision statistics were reported for a 5 ng/mL standard. They also reported that only 0.025 to 0.050 ng derivatized 1′-OH MDZ injected into the GC was required to give a signal-to-noise ratio of better than 5:1. These results suggest that a much lower LOQ for 1′-OHMDZ could have been obtained. Presumably, Rubio et al. had no need to drive the assay to a lower LOQ because of the abundance of 1′-OH MDZ appearing in the plasma of humans given a typical dose of midazolam. However, based on their reported results, further development of this assay for both metabolites could, in principle, provide the sensitivity and selectivity required for their determination from *in vitro* incubations designed to examine the steady-state kinetics of midazolam metabolism at low substrate concentrations.

This chapter will describe our efforts to extend Rubio's negative chemical ionization mass spectrometric assay for midazolam metabolites. The success of the extended assay for determining metabolite formation from dilute microsomal incubations with midazolam for both the major (1′-OH MDZ) and one of the minor metabolites (4-OH MDZ) with a high degree of precision and accuracy at 0.3 ng/mL is reported. Application of the assay to give steady-state kinetic parameters for product formation

from human liver microsomal tissue at midazolam concentrations as low as 0.2 μM is also reported.

2.2 Materials and Methods

Materials

Midazolam, 1′-hydroxymidazolam (1′-OH MDZ), 4-hydroxymidazolam (4-OH MDZ), and the deuterated internal standard, 1′-$^{2}H_{2}$-1′-hydroxy-midazolam (D_{2}-1′-OH MDZ) were gifts provided by Drs. William Garland and Bruce Mico, Roche Laboratories (Nutley, NJ). N-methyl-N-*tert*-butyl-dimethylsilyltrifluoroacetamide (MTBSTFA) was purchased from Pierce Chemical (Rockford, IL), NADPH (reduced form, tetrasodium salt) from Sigma Chemical Co. (St. Louis, MO), and ethyl acetate and acetonitrile from Fisher Scientific (Fair Lawn, NJ).

Standard and Sample Preparation

Stock solutions of 1′-OH MDZ, 4-OH MDZ, and D_{2}-1′-OH MDZ at concentrations of 0.1 mg/mL in methanol were prepared and stored in a dessicator at -20°C for periods of less than 2 months. For each standard curve, appropriate volumes of the 1′-OH MDZ stock solution and the 4-OH MDZ stock solution were initially diluted into 100 mL of distilled, deionized water at a 5 to 1 ratio, respectively. Subsequently, serial dilutions were made in water to give six known concentrations of metabolite standards. Microsomal standards were prepared by the addition 100 μL of the known standards to 900 μL control human liver microsomes diluted to 10 nM P450 in potassium phosphate buffer (100

mM, pH = 7.4) containing 1 mM EDTA. The final concentrations of the analytes used in the assay for 1′-OH MDZ were 0.3, 1.5, 3, 15, 30, and 45 ng/mL, and 0.06, 0.3, 0.6, 3, 6, and 9 ng/mL for 4-OH MDZ. The microsomal sample was basified with 1 mL of 100 mM Na_2CO_3 (final pH = 11). For each standard curve the D_2-1′-OH MDZ stock solution was diluted into water and 100 µL was added to each basified microsomal standard to give a final concentration of 20 ng/mL.

Extraction and Derivatization Procedure

The basified samples were extracted with 2 x 2 mL volumes of ethyl acetate by vortex mixing, centrifugation, and transfer of the upper, organic phase to 16×125 mm culture tubes. After extraction and separation, the samples were placed in a heated water bath at ≤ 40°C and solvent was removed under a slow stream of dry nitrogen. The concentrated extracts were dissolved in 80 µL of derivatizing reagent (20% MTBSTFA in acetonitrile) and vortexed 10 seconds. The samples were transferred to autoinjector vials equiped with 200 µL limited volume inserts and sealed before being heated at 80°C for 2 h prior to GC/NCIMS analysis.

GC/NCIMS Analysis

A VG-model Trio 1000 mass spectrometer interfaced to a Hewlett Packard 5890A gas chromatograph equipped with a Hewlett Packard 7376A autoinjector and a DB-17 fused capillary column (30 m x 0.32 mm i.d., 0.25 micron film thickness; J & W Scientific, Ventura, CA) was used for analysis. Helium carrier gas was used at a head pressure of 7 psi and injections were made in the splitless mode. The injector purge was opened

after 1 min. The injector and transfer line temperatures were held at 250°C and 290°C, respectively. The injection volume was 2 μL. The oven temperature was held at 160°C for 1 min, increased at 25°/min to 290°C, held for 5 min, and increased at 40°C/min to 300°C and held for a final 3 min.

Under these conditions the derivatives of 4-OH MDZ and 1′-OH MDZ eluted with retention times of 10.9 and 11.5 min, respectively. The D_2-1′-OH MDZ internal standard derivative also eluted at a retention time of 11.5 min while midazolam eluted at 8.2 min.

The mass spectrometer was operated in the negative chemical ionization mode. Methane was used as the moderating gas, the source temperature held at 200°C, and the source housing pressure at approximately $1 \times 10^{-3.8}$ Torr. The electron energy and photomultiplier settings were 70 eV and 400 mV, respectively.

Selected ion monitoring was employed using the base peak fragment ions $[M - t\text{Bu}(CH_3)_2\ SiOH]^-$ at m/z 323 for both metabolites. The internal standard was monitored at m/z 327, the base peak fragment ion of the ^{37}Cl isotopic species. The dwell and reset times were 120 ms and 10 ms, respectively. Concentrations of 1′-OH MDZ and 4-OH MDZ were quantified by comparing peak area ratios from peaks in the unknown samples to corresponding peaks in their respective standard curves calculated using least-squares regression.

Data Analysis

The intra-day assay precision was calculated from the agreement of duplicate determinations at each concentration in the calibration curve.

For each set of duplicates (n = 5), a ratio is calculated by dividing one of the duplicate determinations by the other. For each set of 5 ratios of duplicates at each 5 nominal concentrations on the calibration curve, the relative standard deviation (RSD = (standard deviation/mean) * 100%) was calculated.

The inter-day assay precision is a measurement of the day to day reproducibility of the determinations of concentration in the standards used for the calibration curve. For each point on the curve, for 5 successive calibration curves the means of the duplicate determinations were calculated. The means are summed and the mean, standard deviation and RSD determined at each concentration.

Midazolam Metabolism by Human Hepatic Biopsy Tissue

A liver biopsy sample, R-6, was obtained approximately 10 days after liver transplant surgery. The tissue sample was immediately placed on dry ice and held under these conditions for 1-12 hours while it was transported to our laboratory. Liver tissue was thawed, weighed and homogenized by brief sonication in 100 μL of buffer (50 mM KPi, pH 7.4, 0.25 M sucrose, 0.1 mM phenylmethylsulfonyl fluoride). After centrifugation at 13,000 × g for 10 minutes, at 4°C, the supernatant was removed and stored in air-tight vials at -70°C. Quantitation of CYP3A4 by Western blot analysis was performed as previously described [Thummel et. al., 1991]. The catalytic activity of the 13,000 × g supernates was stable for at least 6 months under these conditions.

S-13,000 × g supernatant from the liver biopsy sample was incubated in duplicate with midazolam at 0.2, 1, 4, 16, and 64 μM. The

subcellular fraction was thawed and suspended in cold potassium phosphate buffer (0.1 M, pH 7.4) to achieve a final CYP3A4 concentration of 250 fmol/mL (~30 μg/mL protein concentration). The total reaction volume was 1 mL. Incubation mixtures were gently agitated with midazolam in a Dubnoff metabolic shaking incubator at 37°C for 3 min. The reaction was started with the addition of NADPH (1 mM final concentration) and terminated after 4 min by the addition of 1 mL of 100 mM Na_2CO_3 (final pH 11). The basified incubation samples were spiked with 20 ng of D_2-1′-OH MDZ and extracted, derivatized and analyzed as described above.

2.3 Results

Fragmentation Patterns of the Derivatives

The negative chemical ionization mass spectrum of *t*-butyl-dimethlysilyl (TBDMS) 1′-OH MDZ consisted of two fragment ions, the $[M-H]^-$ proton transfer ion (m/z 454) and the base peak fragment ion $[M - t\text{Bu}(CH_3)_2\ SiOH]^{--}$ (m/z323, Fig. 2.1), and their ^{37}Cl satellite ions at 2 mass units higher. The base peak fragment ion depicted in Fig. 2.1, may be generated by associative resonance capture to form the negative molecular ion radical, followed by neutral loss of the silyl alcohol. The observation of a proton transfer ion for TBDMS derivatized 1′-OH MDZ was in contrast to the electron capture molecular ion observed by Rubio et al. for the TMS derivative. The mass spectrum of the TBDMS D_2-1′-OH MDZ internal standard was similar to that of the unlabelled compound with the exception of the 2 mass unit difference (eg. base peak fragment ion m/z

325) because of deuterium incorporation. This spectrum showed no contribution of non-deuterium incorprated 1′-OH MDZ at m/z 323. The mass spectrum of TBDMS 4-OH MDZ consisted solely of the base peak fragment ion (m/z 323, Fig. 2.2), and its ^{37}Cl satellite. Both ions are also consistent with neutral loss of the TBDMS alcohol from the associative resonance capture generated molecular ion. Signal abundances indicating an electron capture molecular ion (m/z 455) or proton transfer ion (m/z 454) were not observed for derivatized 4-OH MDZ.

The signal-to-noise ratio of a 2 μL injection of a mixture of non-extracted, derivatized standards was measured before every analytical run to ensure optimal run conditions. This mixture mirrored an extracted standard containing 10 ng/mL D_2-1′-OH MDZ, 1 ng/mL 1′-OH MDZ, and 0.2 ng/mL 4-OH MDZ. Thus, the injection contained 0.25 ng D_2-1′-OH MDZ, 0.025 ng 1′-OH MDZ, and 0.005 ng 4-OH MDZ derivatives. The mixture typically gave similar signal-to-noise ratios (>20) for the two metabolites and a higher signal to noise ratio (>100) for the internal standard.

Calibration Curves

Calibration curves were obtained by plotting the SIM (single ion monitoring) chromatogram peak area ratios (metabolite/internal standard) of the corresponding metabolites versus the known concentrations of 1′-OH MDZ and 4-OH MDZ. The ion channel monitored for the metabolites was m/z 323 while m/z 327 was monitored for the internal standard (the ^{37}Cl isotopic species of the D_2-1′-OH MDZ). Straight lines ($r^2 = 1.000$) were observed over the concentration range of 0.3 to 45 ng/mL for 1′-OH MDZ

and of 0.06 to 9 ng/mL for 4-OH MDZ as shown in Figs. 2.3 and 2.4. All calibration curves demonstrated good fit to regression lines. The curves shown represent the mean area ratios at each concentration point from 3 successive calibration curves. Calibration standards of human liver microsomes that contained no added midazolam metabolites did not have signals at the metabolite retention times. Extraction and derivatization of human liver microsomes containing added midazolam, but not metabolites, gave metabolite peak area ratios that were essentially zero. No interferences were observed that would falsely suggest a significant metabolite level.

Precision and Accuracy

The assay intra-day and inter-day accuracy and precision were determined by analysis of the duplicate determinations of 5 successive calibration curves. The results for 1′-OH MDZ and 4-OH MDZ are shown in tables 2.1 and 2.2, respectively. The LOQ for 1′-OH MDZ and 4-OH MDZ were 0.3 ng/mL as established by analytical methods validation standards which suggest < 20% deviation from the nominal value for both accuracy and precision at the LOQ [Shah, 1991]. To the best of our knowledge, this is the most sensitive quantitative assay for midazolam metabolites that has been developed.

Kinetic Parameters of Midazolam Metabolism

Once developed, the assay was utilized for the determination of the steady-state kinetic parameters of metabolite formation in the S-13,000 × g subcellular supernate from a human liver biopsy sample. Midazolam

product formation was linear with time for up to 5 minutes, but reactions were limited to 4 minutes to accurately determine initial rates. Estimates of K_m and V_{max} parameters for both metabolites were calculated by Eadie-Hofstee plots which gave straight lines for both metabolites ($r^2 \geq 0.95$, Figs. 2.5 and 2.6). Formation rates for 1′-OH MDZ gave a K_m value of 1.52 μM and a V_{max} value of 110.5 pmol/min/mg protein. Formation rates for 4-OH MDZ gave a K_m value of 19.4 μM and a V_{max} value of 209.7 pmol/min/mg protein. Kinetic parameters for both metabolites are similar to the range of values observed previously (vide supra). Assuming 1′-OH MDZ and 4-OH MDZ formation account for all significant midazolam consumption, <1% of the substrate was depleted at the lowest concentration (0.2 μM). A typical chromatogram representing assay of a 0.2 μM incubation of midazolam with this biopsy sample shows symmetrical, base-line separated peaks with no interfering peaks and significant signal-to-noise ratios for the metabolites at sub-ng/mL levels (Fig. 2.7).

2.4 Discussion

Further development of the GC/NCIMS assay reported by Rubio gave a highly sensitive, selective, reproducible assay for midazolam metabolites from human liver microsomal preparations. A number of changes were introduced into the assay procedure as outlined in the direct comparisons below. The extraction solvent system and evaporation temperature were changed to avoid air oxidation of midazolam during work-up. An alternative derivatization procedure gave differences in the

fragmentation patterns of the silylated metabolites. Fortunately, the complete fragmentation observed in the mass spectrum of TBDMS 4-OH MDZ worked in favor of high sensitivity for the minor metabolite. Changes in the SIM detection resulted in a less complicated procedure for the calculation of the unknowns from the calibration curves that is less prone to error. The refinements above resulted in a more sensitive assay that included simultaneous detection of 4-OH MDZ. The possible advantages of this assay are discussed at the end.

Extraction and Derivatization

The sample work-up was changed over the course of several months as preliminary studies were conducted on the extraction procedure. Firstly, although Rubio silanized all assay glassware before use, we found no difference in assay performance when non-silanized glassware was used and thus did not silanize the assay glassware. Secondly, because metabolites were observed in extracts of midazolam spiked control microsomes, but not in non-extracted, derivatized samples of midazolam, air oxidation during work-up was inferred. The original assay used a one time extraction by 6 mL of a 4:1 mixture of benzene and methylene chloride and had been changed to a 5:1 mixture of toluene and isopentyl alcohol in our studies to mimic the polarity while increasing the safety of the extraction procedure. Both systems are relatively high boiling and the extracts had been evaporated under a stream of nitrogen at the 60°C temperature used by Rubio. Therefore, several low boiling solvent systems were screened and evaporated at ≤ 40°C to slow air oxidation during the work-up. Using low-boiling extraction solvent systems (including 100%

ether, 100% ethyl acetate, and 100% methylene chloride) and evaporating at a lower temperature decreased the contribution of air-oxidized midazolam metabolites in the blanks. Although a poor extraction effeciency (~80%) was observed from the relatively polar ethyl acetate metabolite extraction, no interfering peaks were observed in the metabolite chromatograms. Therefore, the samples were extracted with 2 aliquots of ethyl acetate (2 mL each) to maximize the extraction efficiency. Ethyl acetate extraction of midazolam spiked, control microsomes followed by evaporation at ≤ 40°C and subsequent derivatization gave peak area ratios for the metabolites that were essentially zero.

Once the samples were evaporated, derivatization with 20% MTBSTFA/acetonitrile was driven to completion in sealed vials at 80°C. This is in contrast to the original assay in which the organic residues were vacuum dried before derivatization for 20 min at room temperature in 25% bis-(trimethylsilyl)acetamide/acetonitrile. The TBDMS ether derivatization was employed herein to promote dissociative resonance capture to a $[M^{\cdot-} - t\text{-butyl}^{\cdot}]^-$ ion exclusively, rather than relying on the mixture of parent and fragment ions observed by Rubio. Complete fragmentation to a single ion would be expected to confer greater sensitivity for quantitative analysis in SIM mode for the metabolites by concentrating all ion intensity into a single mass spectral peak and its ^{37}Cl satellite. However, loss of the *t*-butyl radical via dissociative resonance capture was not observed and instead a spectrum consistent with neutral loss of the entire TBDMS alcohol from the associative resonance capture molecular ion radical was observed. The mass spectrum of TBDMS 1′-OH MDZ provided a high abundance fragment ion (m/z 323), no molecular ion

radical (in contrast to Rubio's TMS derivatives), and the proton transfer ion (m/z 454). In summary, changes in the extraction procedure eliminated significant contamination of the assay from air-oxidized midazolam metabolites while the alternative derivatization procedure seems to have given rise to different fragmentation patterns than those observed previously.

4-OH MDZ

While the mass spectrum of TBDMS 1′-OH MDZ contained both a proton transfer ion and the base peak fragment ion, the mass spectrum of TBDMS 4-OH MDZ consisted solely of the m/z 323 fragment ion. The differences in the mass spectra of the two metabolites suggests that the proton affinity of the 4-OH MDZ metabolite is higher than that of the 1′-OH MDZ metabolite and thus no proton transfer ion is observed for 4-OH MDZ. If the ion abundance observed for TBDMS 4-OH MDZ is concentrated into the m/z 323 ion channel, and thus enhanced relative to that of the 1′-OH MDZ derivative, then SIM of m/z 323 for both metabolites may confer greater sensitivity for the 4-OH MDZ, minor metabolite. Indeed, the signal-to-noise data suggests greater sensitivity for the 4-OH MDZ metabolite should be observed. When 0.025 ng TBDMS 1′-OH MDZ and 0.005 ng TBDMS 4-OH MDZ were co-injected, the signal-to-noise was similar for both metabolites and always >20. Although the LOQ for 4-OH MDZ was expected to be 5-fold lower than that for 1′-OH MDZ (based on the signal-to-noise data), statistics did not allow the assignment of a lower LOQ. The inter- and intra-day accuracies are < 10% for a nominal concentration of 0.06 ng/mL 4-OH MDZ, but inter- and intra-

day precisions were both >20% (Table 2.2). Therefore, the LOQ for the 4-OH MDZ metabolite was 0.3 ng/mL, the same as that for 1′-OH MDZ, although 3- or 4-fold greater sensitivity may yet be achieved for the 4-OH metabolite without changing the assay. One explanation for the lack of precision at low concentrations may be differential extraction characteristics for the 4-OH MDZ versus the D_2-1′-OH MDZ internal standard. However, the advantage of high abundace ion currents for the minor metabolite was not lost in light of calculating the same LOQ for both metabolites.

Calibration Curves

Although the two assays utilized the same stable-labelled internal standard molecule, ions for SIM of the metabolites and internal standard were fundamentally different between the two assays. Previously, spectra of the TMS derivatives of 1′-OH MDZ and D_2-1-OH MDZ gave base peak $M^{\cdot -}$ ions at m/z 413 and m/z 415, respectively. By selecting the ^{35}Cl, m/z 415 peak for SIM of the internal standard, Rubio's curvilinear calibration curves were complicated by the contribution of the ^{37}Cl isotopic species of the 1′-OH MDZ metabolite derivative into the m/z 415 ion channel as predicted by the significant theoretical natural abundance of ^{37}Cl, at 32.5% of all chlorine atoms. Thus, a computer program was used to analyze the curves and unknown concentrations were calculated by using an equation which incorporated 3 parameters generated by the computer program. Greater errors in determination of metabolite concentration would be generated as the ratio of 1′-OH MDZ/D_2-1′-OH MDZ increases because small differences in metabolite/internal standard ratios give rise to large

differences in amounts of 1′-OH MDZ.

In contrast to the original assay, the ^{37}Cl isotopic species of the base-peak fragment ion of the TBDMS D_2-1-OH MDZ internal standard, m/z 327, was employed for SIM in our studies to avoid isotopic dilution complications. The contribution of TBDMS 1′-OH MDZ into the M + 4, m/z 327, ion channel was < 0.8% of the total ion current observed during SIM of 5 consecutive ions, m/z 323 through 327, after injection of the derivatized metabolite standard. The contribution of TBDMS D_2-1′-OH MDZ into the M-2, m/z 323, ion channel was <0.076% of the total ion current observed in the same SIM window, m/z 323 through 327, after injection of the derivatized stable-labelled metabolite internal standard. Therefore, calibration curves generated by monitoring the ratio of metabolite/internal standard (m/z 323/m/z 327) over several metabolite concentrations were not complicated by overlapping ion abundances. Straight lines were observed by simple linear regression analysis (Figs. 2.3 and 2.4). Unknown concentrations are calculated by dividing the experimental peak area ratios (metabolite/internal standard) by the slope of the regression line. The ease of this analysis obviates the use of computer programs for the determination of metabolite amounts and allows visual inspection of the calibration curve data for initial validation of a sample set.

In summary, the revised GC/NCIMS assay was successfully adapted to give greater sensitivity with simultaneous determination of the 4-OH MDZ metabolite. A LOQ that was >3-fold lower than the most sensitive published assay for 1′-OH MDZ and >16-fold lower than the most sensitive published assay for 4-OH MDZ was achieved.

Application of this assay to the determination of steady-state kinetic constants from incubations employing at least one midazolam concentration that is identical to those typically achieved *in vivo* demonstrated its utility. A full product formation kinetic analysis was conducted in the S-13,000 × g subcellular fraction of a human liver biopsy tissue sample that initially weighed <20 mg. The sensitivity of the assay allowed kinetic analysis in the presence of immunochemically-quantitated CYP3A4 protein at the femtomole level, or <10% of the microsomal protein used in previous *in vitro* studies of midazolam metabolism [Kronbach, 1989; Fabre, 1988; Gorski, 1994; Gascon, 1991]. Accurate estimates of K_m and V_{max} from experiments conducted with biopsy tissue may allow the *in vitro* calculation of intrinsic clearance, V_{max}/K_m, in a population of individuals for whom the *in vivo* clearance parameters are known. This presents the unique opportunity of being able to study and compare *in vitro* and *in vivo* clearances of midazolam and evaluate variables that might lead to differences between these two parameters.

Before attempting to predict midazolam metabolism behavior *in vivo* from simple mass-balance derived kinetic equations, the *in vitro* system must be completely understood. The next two chapters diverge from the goal of predicting *in vivo* metabolism to address the relatively limited time-dependent formation of midazolam metabolites within the current *in vitro* system.

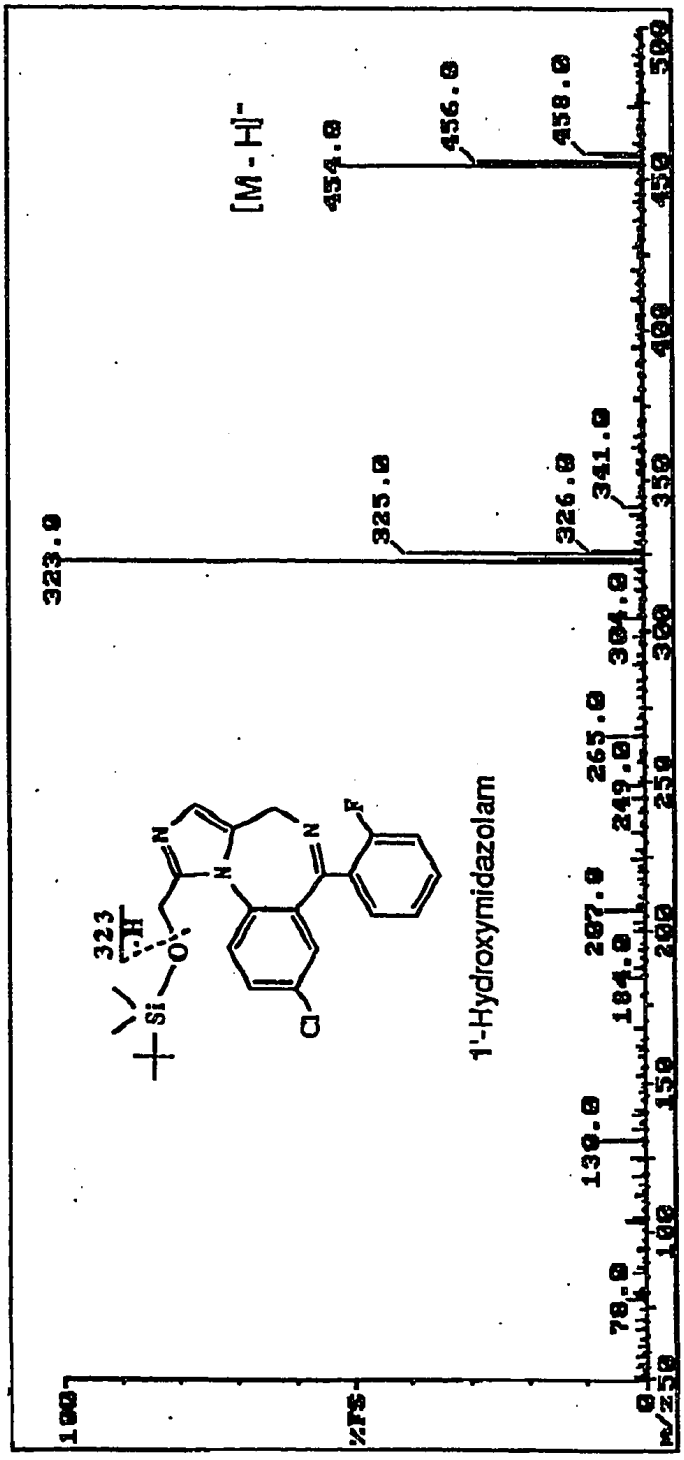

Figure 2.1. Methane negative chemical ionization mass spectrum of the TBDMS derivative of 1'-OH MDZ.

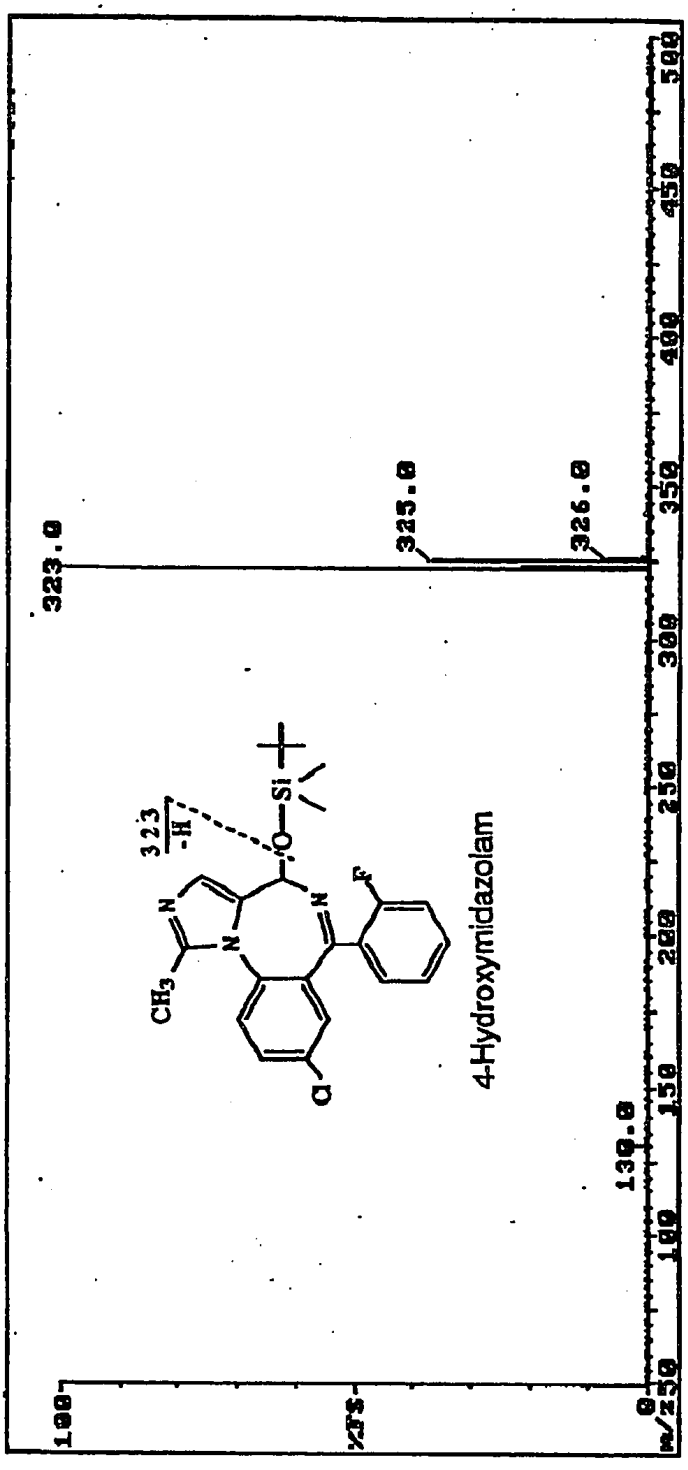

Figure 2.2. Methane negative chemical ionization spectrum of the TBDMS derivative of 4-OH MDZ.

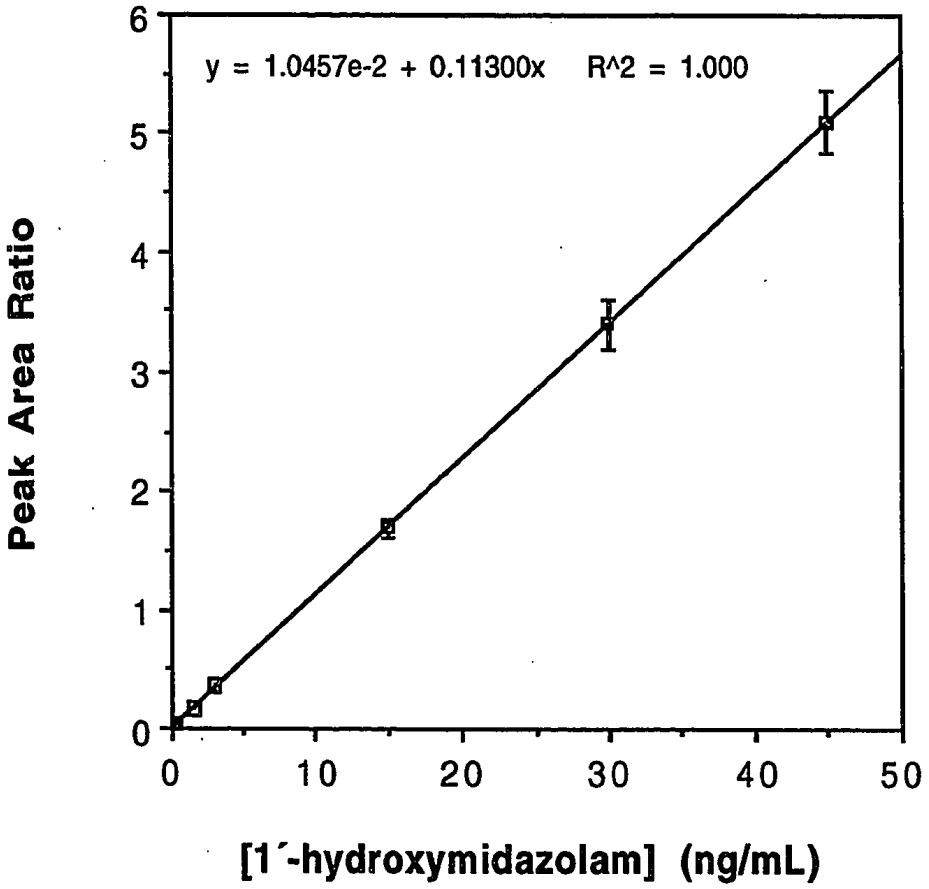

Figure 2.3. Mean of three successive calibration curves for the determination of 1´-OH MDZ in human liver microsomes. The error bars represent the standard deviation at each concentration.

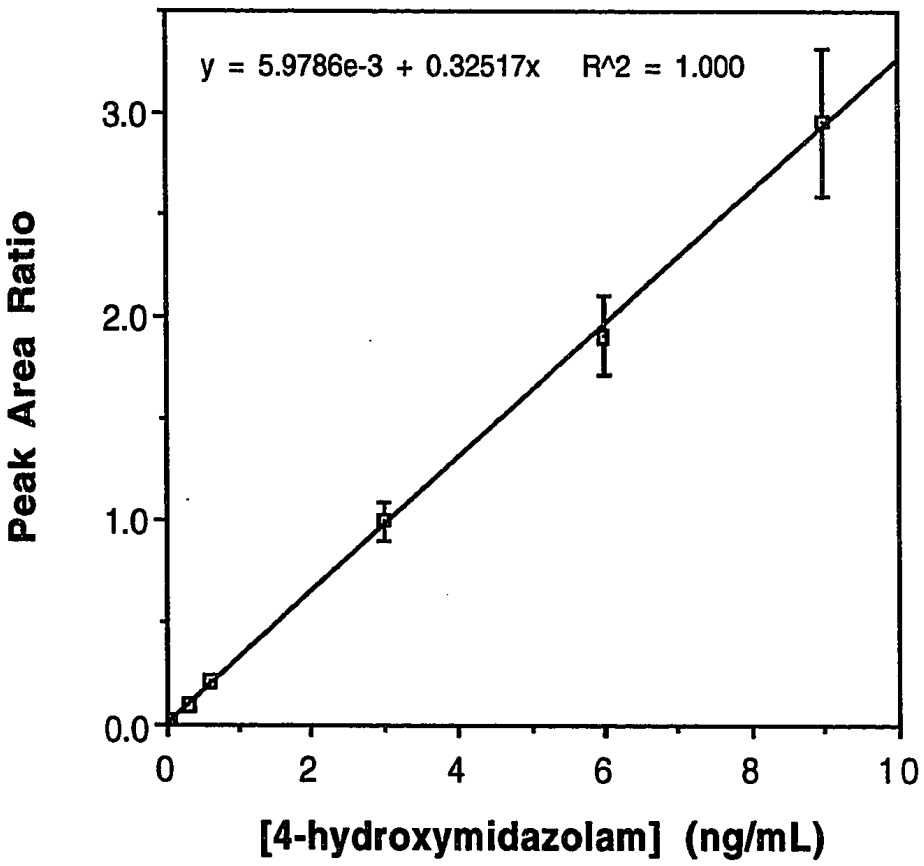

Figure 2.4. Mean of three successive calibration curves for the determination of 4-OH MDZ in human liver microsomes. The error bars represent the standard deviation at each concentration.

Table 2.1. Intra-day and inter-day accuracy and precision (n = 5) for the determination of 1′-OH MDZ in human liver microsomes

	Intra-day		Inter-day	
Nominal Concentration (ng/ml)	Accuracy (%Found/Nominal)	Precision (%CV)	Accuracy (%Found/Nominal)	Precision (%CV)
0.3*	108.0	5.1	119.3	14.1
1.5	105.3	5.1	106.7	3.0
3	100.4	4.4	106.4	6.1
15	102.3	1.6	101.1	2.7
30	98.1	1.2	100.0	1.4
45*	100.8	2.1	100.4	0.4

*n = 4

Table 2.2. Intra-day and inter-day accuracy and precision (n = 5) for the determination of 4-OH MDZ in human liver microsomes

Nominal Concentration (ng/ml)	Intra-day		Inter-day	
	Accuracy (%Found/Nominal)	Precision (%CV)	Accuracy (%Found/Nominal)	Precision (%CV)
0.06*	106.7	20.3	103.3	28.3
0.3	101.7	7.4	108.7	5.5
0.6	106.3	3.7	112.5	5.2
3	102.1	2.0	105.1	2.6
6	100.0	3.8	100.2	0.2
9*	104.8	5.0	101.9	3.3

*n = 4

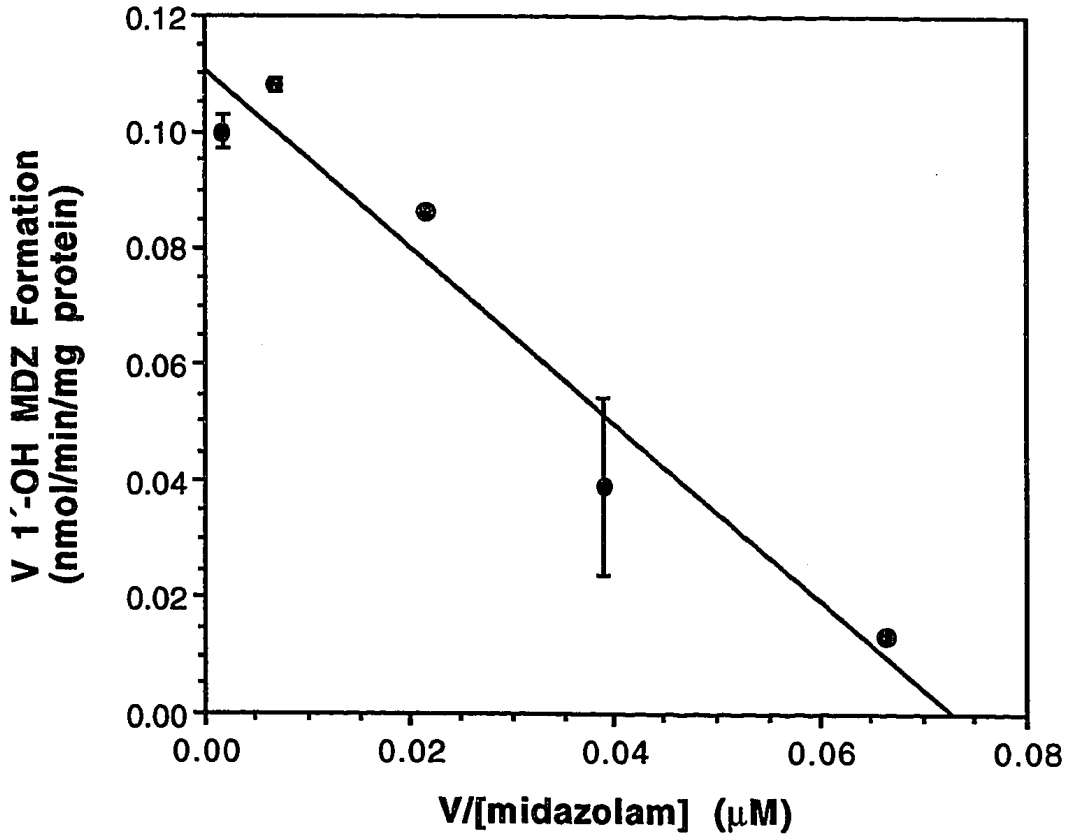

Figure 2.5. Eadie-Hofstee plot for the formation of 1´-OH MDZ from a human liver biopsy S-13,000 × g subcellular fraction at 0.2 to 64 μM midazolam. Error bars represent standard deviations of duplicate determinations at each concentration.

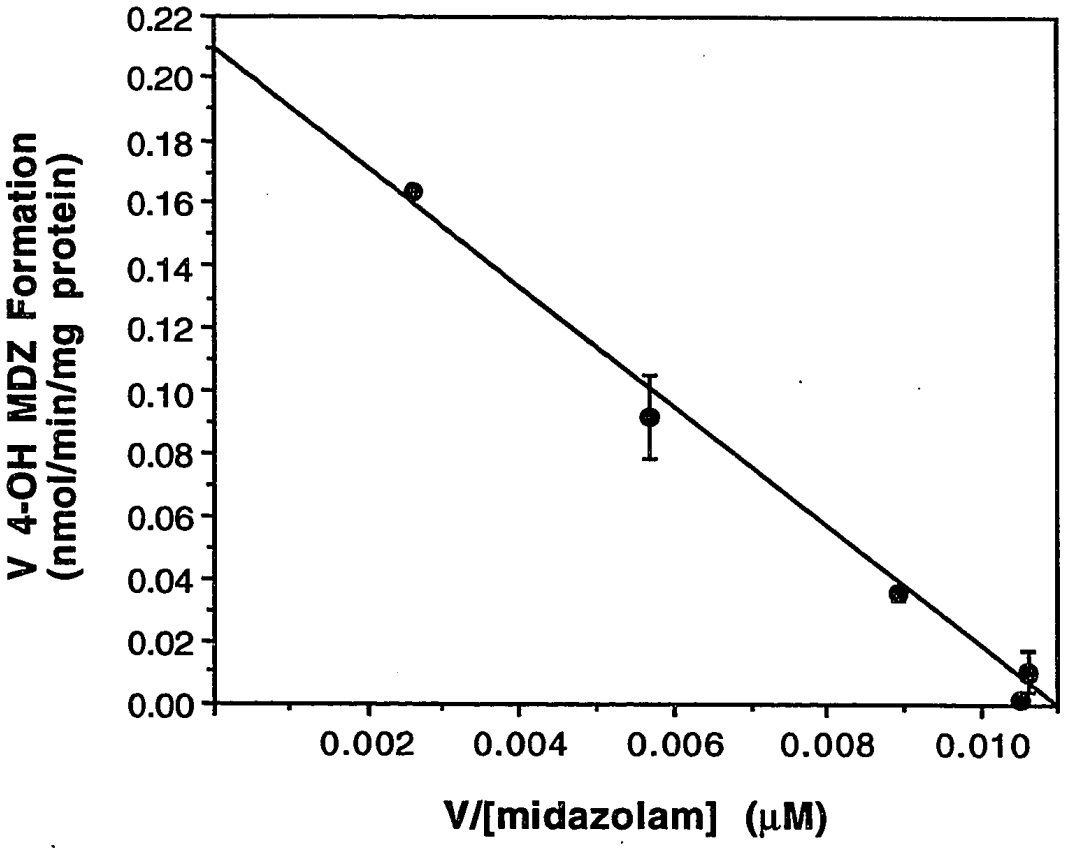

Figure 2.6. Eadie-Hofstee plot for the formation of 4-OH MDZ.

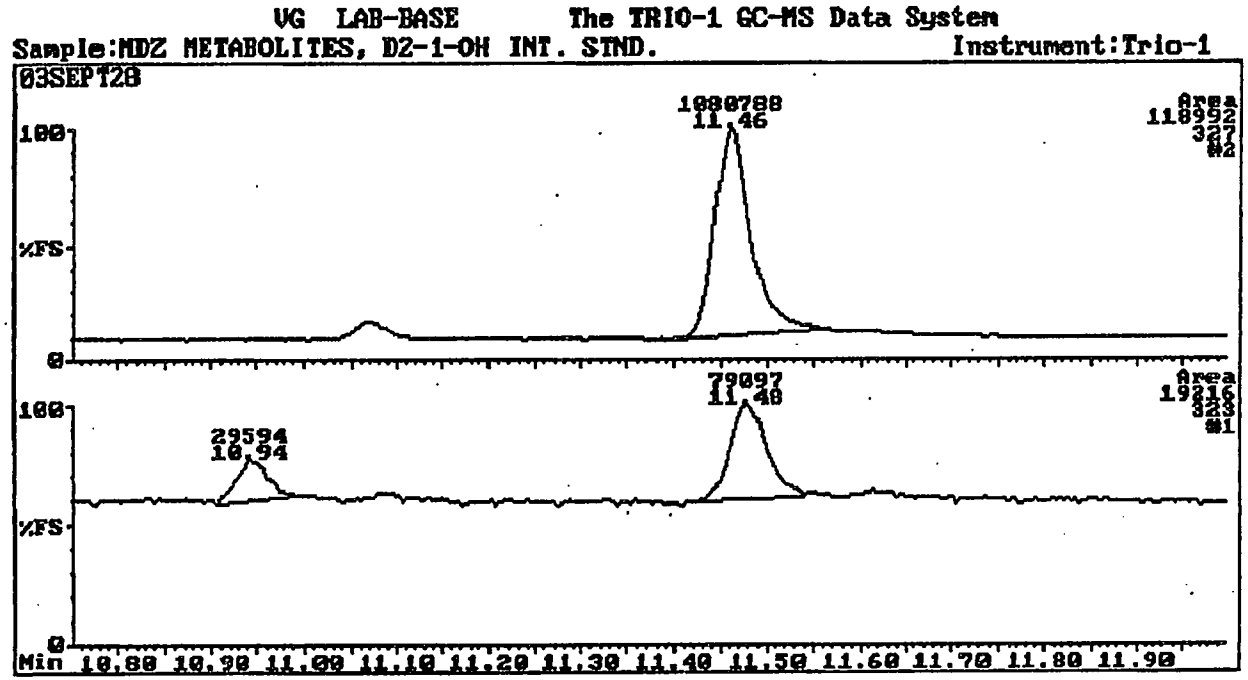

Figure 2.7. SIM chromatogram of midazolam metabolites (m/z 323, bottom) and D_2-1′-OH MDZ internal standard (m/z 327, top) extracted from a human liver microsomal incubation containing 250 pM CYP3A4 and 200 nM midazolam.

CHAPTER THREE

INACTIVATION OF CYTOCHROME P450 3A4 BY MIDAZOLAM: KINETIC MECHANISM

3.1 Time Dependence of Midazolam Metabolite Formation

Incubating midazolam with human liver microsomes and NADPH gave apparent linear time dependent product formation for only 5 minutes. Product formation rates beyond the initial 5 minutes decreased significantly through the next 15 minutes then slowly approached zero from 20 to 45 minutes. These observations are consistent with those previously reported by Fabre et al. [Fabre et al., 1988]. Thus, accurate determination of the Michaelis constants for 1′-hydroxymidazolam formation required the measurement of product formation rates at time periods that did not exceed 4 minutes. Product rate measurements beyond 4 minutes would have resulted in the calculation of erroneous kinetic constants. The studies described in this chapter explore possible reasons for the observation of the time dependent change in product formation rates from midazolam as indicated above.

Factors that might be responsible for non-linear product formation include substrate depletion, cofactor (NADPH) depletion, product depletion, product inhibition, and enzyme inactivation. Initial exploratory studies conducted in our laboratory to examine each of these various possibilities gave the following results. Substrate depletion, estimated from the sum of products formed after a 10 minute incubation

with 4 μM midazolam, indicated that less than 5% of the midazolam had been consumed. Since the steady-state assumption is still valid with less than 5% depletion of substrate, product formation rates would be expected to remain constant for at least 10 minutes. The observation that product formation rates decreased before the end of a 10 minute incubation eliminates substrate depletion as the cause of the non-linearity. Utilization of an NADPH generating system, which constantly regenerates the cofactor during the course of the reaction, did not significantly alter the time course of the reaction (Fig. 3.1). Product depletion was eliminated by demonstrating that incubating 0.23 μM 1′-OHMDZ (equal to three times the maximum amount generated during a typical incubation of midazolam) with NADPH and P450, proceeded without loss of 1′-OHMDZ while co-incubation of 0.21 μM 1′-OHMDZ with 4 μM midazolam and cytochrome P450 did not lead to product inhibition. In summary, the observed decrease in rate of midazolam product formation after a 5 minute incubation could not be explained by substrate depletion, cofactor depletion, product depletion or product inhibition. By default, this left enzyme inactivation of CYP3A4 by midazolam as the most likely reason for the non-linear time dependent formation of midazolam metabolites.

One possible source of enzyme inactivation is mechanism-based inactivation, the kinetics of which can be described by the following scheme:

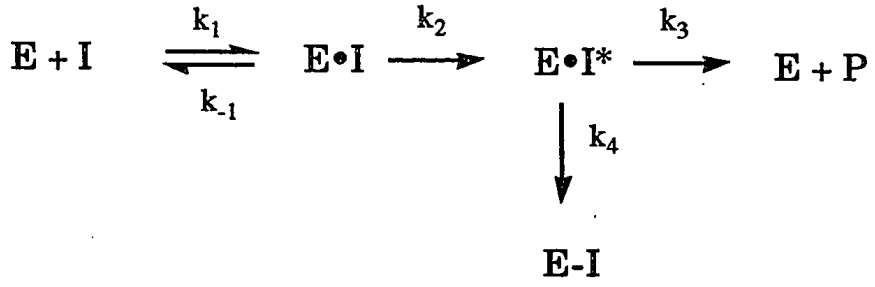

Scheme 1

where E, I, and P are enzyme, inactivator, and product, respectively, [Walsh et al., 1978]. A caveat of applying this simplified scheme to cytochrome P450 monooxygenase activity is that other factors, besides substrate activation, can lead to the destruction of the enzyme and these variables must be accounted for before mechanism-based inactivation can be established. For example, P450 heme can be destroyed in the presence of NADPH, NADPH-P450 reductase, and O_2 alone, without the presence of substrate [Schaefer et al., 1985]. Schaefer et al. show that hydrogen peroxide (H_2O_2) is at least partially responsible for this loss of heme. In the presence of substrate, catalytic turnover may further confound experimental observations by increasing the inactivation of P450 via generation of H_2O_2 and other highly reactive oxygen intermediates. Decomposition of oxycytochrome P450 leads to release of superoxide anion ($O_2^{\cdot-}$) and subsequent, spontaneous production of H_2O_2 from $O_2^{\cdot-}$ with a stoichiometry of 1:2, respectively [Estabrook et al., 1979; Kuthan et al., 1982]. Superoxide anion and hydrogen peroxide may also participate in the Haber-Weiss reaction:

$$O_2^{\cdot-} + Fe^{3+} \rightarrow O_2 + Fe^{2+}$$

$$Fe^{2+} + H_2O_2 \rightarrow (FeOH)^{2+} + HO\cdot$$

generating a highly reactive hydroxyl radical [McClune et al., 1977]. P450 can also be destroyed during lipid peroxidation, a process which may occur in microsomal preparations of P450 [Levin et al., 1973]. Another possibile complicating factor is the release of a substrate derived reactive electrophile from the active site and its nonselective inactivation of P450. Fortunately, all of the complicating factors outlined above can be inhibited or even eliminated by the addition of iron chelators and reactive intermediate traps. Since the addition of glutathione, EDTA, superoxide dismutase, or catalase to midazolam incubations did not significantly change the product formation time profile (Figs. 3.1 - 3.3), it was concluded that the rapid loss of CYP3A4 activity during midazolam turnover was not a consequence of a reactive event extraneous to the active site of the P450 system. Experiments were then undertaken to further probe the possibility that midazolam is a mechanism-based inactivator of CYP3A4.

Recently, mechanism-based inactivation studies have demonstrated that oxidative processing of a methyl-imidazole group by P450 can lead to inactivation. Furafylline is an isoform-selective inactivator of CYP1A2 [Kunze et al, 1991] that contains a methyl-imidazole moiety similar to that found in midazolam (Fig. 3.4). Kunze et al have established that inactivation of CYP1A2 by furafylline is dependent upon catalytic processing of the imidazole C-8 methyl group by demonstrating that replacing the C-8 protons with deuterium leads to an intermolecular deuterium-isotope effect, $k_H/k_D \approx 2.0$, on k_{inact}. Furthermore, hydroxylation of the imidazole C-8 methyl group results in formation of the major product of furafylline metabolism in human liver

microsomes. These results are consistent with P450 oxidation at the methyl carbon of a methyl-imidazole group generating a reactive intermediate that branches to either formation of the hydroxylated metabolite or enzyme inactivation (Scheme 1). The major site of midazolam hydroxylation is at the C-1′ methyl group, giving 1′-OH MDZ. Thus, a direct analogy between CYP1A2 oxidation of furafylline and CYP3A4 oxidation of midazolam appears reasonable and supports the notion that midazolam may be a mechanism-based inactivator of CYP3A4.

3.2 Mechanism-Based Inactivation Kinetics

There are seven accepted criteria used to establish mechanism-based inactivation [Silverman, 1988]. The criteria are:

1) Time dependent inhibition.
2) Saturable inactivation kinetics.
3) Catalysis dependent inactivation.
4) Lack of supression of inactivation by reactive-intermediate scavengers.
5) Inhibition of inactivation by a competing substrate.
6) Irreversibility.
7) A 1:1 stoichiometry between inactivated enzyme and enzyme-bound inactivator.

Experiments described in this chapter will address the criteria numbered 1 through 5 as presented above. Chapter 4 will address criteria numbered 6 and 7. The kinetics of mechanism-based inactivation can be followed experimentally in several alternate ways.

These include inactivator loss, product formation, or enzyme loss [Tatsunami et al., 1981]. The experiments reported in this thesis utilize remaining activity as a reporter of enzyme loss. The data are presented as fractions of the activity observed in the absence of inactivator, and are termed "% remaining activity". This section of the chapter (3.2) provides a general description of the procedures used to determine the kinetic parameters, and demonstrate catalysis dependence and substrate protection. Section 3.3 describes the method and the substrate utilized for determining % remaining activity.

Initial evidence for a branched reaction pathway that leads to either product formation (P) or enzyme destruction (E-I), as represented above in scheme 1, can be provided by an active site titration experiment. In such an experiment the partition ratio, or the ratio of product forming events relative to enzyme inactivating events, k_3/k_4, is determined. The endpoint of fractional activity remaining, i.e. the activity level after treatment with the inactivator relative to the activity level observed with no inactivator, is measured at several inactivator concentrations in the presence of a constant level of enzyme. If the fractional activity remaining when inactivation has ceased (either due to inactivator depletion or enzyme inactivation), is proportional to the molar ratio of inactivator to enzyme, then the partition ratio can be determined from the slope of the line as - $(1/(1+ k_3/k_4))$ [Waley, 1980; Tatsunami et al., 1981; Waley, 1985]. The constancy of the partition ratio when the substrate concentrations are varied, as reflected by a linear result, is a useful preliminary test of the mechanism. Observation of active-site titration as

described above justifies testing whether or not a proposed inactivator displays time-dependent and saturable inactivation kinetics.

The kinetic parameters for inactivation of enzymes exhibiting Michaelis-Menten kinetics can be determined by methods analogous to those for substrate turnover. The reversible binding affinity constant, K_I, and maximal rate of inactivation, k_{inact}, are determined via graphical analysis of initial inactivation-rate data similar to the determinations of K_m and V_{max}, respectively. If time-dependent inactivation is observed, then the initial rate of inactivation can be measured at several inactivator concentrations. An inverse plot of inactivation rates vs. inactivator concentration, a Kitz and Wilson plot, gives the K_I and k_{inact} via calculations completely analogous to those based on the Lineweaver-Burke plot for K_m and V_{max}, assuming saturable inactivation kinetics are observed [Kitz et al., 1962]. Additionally, the half-lives of inactivation at several inactivator concentrations can be used to determine K_I and k_{inact} with *a priori* knowledge of the partition ratio [Waley, 1985]. Both the inverse-plot and half-life plot method are used to demonstrate saturable inactivation kinetics for the inactivation of CYP3A4 by midazolam.

The requirement of catalytic turnover for inactivation is definitively established when the rate of inactivation can be shown to be subject to an isotope effect as in the case of furafylline [Kunze, 1991]. In the absence of an inactivator analog that contains deuterium at the metabolic site, the necessity of catalytic turnover for inactivation can be inferred by the lack of inactivation that is observed when a co-factor is removed from the reaction. In the case of cytochrome P450, inactivation should not be observed in the absence of NADPH or the co-substrate, O_2.

Because a mechanism-based inactivator is by definition a substrate for the enzyme, any substrate or competetive inhibitor of the enzyme should decrease the rate of inactivation by competing for the active site and reducing the formation of the E·I complex. If increasing amounts of another CYP3A4 substrate give decreasing rates of CYP3A4 inactivation, then inactivation of CYP3A4 by midazolam is unambiguously tied to an active site phenomenon presuming the presence of the competing substrate in the active site.

3.3 Testosterone and Alfentanil as CYP3A Probes

The measurement of specific loss of CYP3A4 enzyme activity in human liver microsomes requires a selective substrate for CYP3A4. Additionally, the measurement of enzyme inactivation rate by a remaining activity assay requires the ability to stop the inactivation process, then begin the measurement of remaining activity at specific time points as near simultaneously as possible. This can be accomplished by a two-phase incubation in which a primary, inactivation incubation is conducted with the inactivator which is then diluted into a secondary, remaining activity incubation using a marker substrate for the enzyme. Not only must the marker substrate be specific for the enzyme, but it should also have high affinity with a high turnover rate. A high-affinity marker substrate would most effectively protect the enzyme from further inactivation by residual traces of inactivator during the secondary incubation. Ideally, a marker substrate which displays a high turnover rate would provide measurable amounts of metabolite under conditions in which the enzyme was >90% inactivated in the

primary incubation and subsequently diluted 10-fold. The suitability of using testosterone as a selective, high-affinity high turnover rate probe of CYP3A4 and alfentanil as a selective substrate for CYP3A4 is discussed below.

Testosterone

The most extensive characterization of the selectivity of testosterone 6ß-hydroxylase activity for CYP3A proteins has been carried out by Waxman et al. [Waxman et al., 1988]. The initial studies utilized indirect approaches, including antibody inhibition, chemical inhibition and correlative analyses, to show that P450 enzymes belonging to the CYP3A subfamily are major contributors to testosterone 6ß-hydroxylation. In a later study utilizing a more direct approach, Waxman et al. suggested that CYP3A4 has the highest affinity and fastest 6ß-hydroxylation turnover rate for testosterone of any P450 present in human liver microsomes [Waxman et al., 1991]. After screening eleven human P450s which had been cloned and expressed in human hepatoma Hep G2 cells to produce a single-enzyme preparation of each P450, they found that the only human liver enzymes that oxidized testosterone in the 6ß position were members of the CYP3A subfamily. CYP4B1, a lung specific enzyme, also demonstrated this activity. The rate of 6ß-hydroxylation from the CYP3A4 preparation was 5-fold higher than in the CYP3A5 preparation at a testosterone concentration of 50 μM. CYP3A4 was also shown to give an 8-fold lower K_m value for testosterone 6ß-hydroxylation relative to CYP3A5. CYP3A5 is expressed polymorphically in adult human livers, with about 25% of individuals

producing this protein. When CYP3A5 is expressed, the level is usually ~30% that of CYP3A4 [Wrighton et al., 1989; Wrighton et al., 1990]. In light of these results, livers which have been shown to express CYP3A4, and not CYP3A5, by western blot analysis, were carefully selected from a bank of human livers and labelled HL #113, HL #122, HL #124, and HL #135 for use in the inactivation experiments in our laboratory. Testosterone 6ß-hydroxylation is used as a selective reporter of CYP3A4 remaining activity measured in microsomes of the selected livers based on the absence of CYP3A5.

Alfentanil

Alfentanil was selected as a probe to demonstrate that CYP3A4 inactivation can be slowed by the presence of another substrate that is selectively metabolized by CYP3A4. As in the case of testosterone, initial studies designed to determine the specific cytochrome P450 isoform that catalyzes alfentanil metabolism utilized indirect approaches, including antibody and chemical inhibition experiments and correlative analyses. The P450 enzymes belonging to the CYP3A subfamily were found to be major contributors to the oxidative N-dealkylation of alfentanil in human liver microsomes [Kharasch et al., 1993; Yun et al., 1992]. Later studies confirmed these results and, utilizing a more direct approach, showed that only CYP3A4 exhibited significant catalytic activity toward alfentanil dealkylation of six human P450 isoforms that had been expressed in single-enzyme preparations [Labroo et al., 1995]. CYP3A5 was not screened and the contribution of this enzyme to alfentanil metabolism is not yet known. The reported K_m and V_{max} for piperidine

nitrogen dealkylation of alfentanil in human liver microsomes are approximately 25 μM and 3 nmol/min/mg protein respectively [Lavrijsen et al., 1988]. Testosterone and alfentanil were used as selective probes of CYP3A4 to fully characterize the kinetic mechanism of inactivation of CYP3A4 by midazolam.

3.4 Materials and Methods

Materials

Midazolam was a gift kindly provided by Drs. William Garland and Bruce Mico, Roche Laboratories (Nutley, NJ). Alfentanil was a gift kindly provided by Dr. Evan D. Kharasch, University of Washington. Testosterone and 6ß-hydroxytestosterone (6ß-OHT) were purchased from Steraloids (Wilton, NH) and testosterone was recrystalized 4 succesive times from acetone/H_2O. Cell microsomes containing cDNA-expressed human cytochrome P450 3A4 and P450 reductase (M107r, lots 19 and 22) were purchased from Gentest (Woburn, MA). Human liver microsomes were prepared as outlined previously [Rettie et al., 1992]. 11α-Hydroxy-progesterone (11α-OHP), NADPH (reduced form, tetrasodium salt), glucose-6-phosphate, glucose-6-phosphate dehydrogenase, and antirabbit IgG alkaline phosphatase conjugate were purchased from Sigma Chemical Co. (St. Louis, MO). HPLC solvents were purchased from Fischer Scientific (Fair Lawn, NJ). Nitrocellulose was purchased from Schleicher and Schuell (Keene, NH); alkaline phosphatase substrates, 5-bromo-4-chloro-3-indoyl phosphate and nitroblue tetrazolium, were

purchased from Kirkegaard & Perry Laboratories (Gaithersburg, MD). All other reagents were of the highest purity commercially available.

Western Blot Analysis of CYP3A4 in Human Liver Microsomes

The spectral content of P450 in microsomes was determined by the method of Omura and Sato [Omura, 1962]. Briefly, human liver microsomes were diluted 50-fold into a 1:1 mixture of 100 mM potassium phosphate buffer containing 1 mM EDTA (pH 7.4) and 100 mM potassium phosphate buffer containing 40% glycerol and 1% emulgen (ph 7.4). The sample was reduced with a small amount of sodium dithionite, a baseline spectrum was acquired, carbon monoxide was gently bubbled into the sample for approximately 45 seconds, and the concentration was calculated from differential absorbance (450 nm - 490 nm). Purified human CYP3A4 protein and specific rabbit polyclonal anti-CYP3A4 IgG were gifts kindly provided by Dr. Kenneth Thummel (University of Washington) and had been characterized as reported previously [Kharasch et al., 1993]. Western blot analyses of individual liver samples were performed in duplicate as described previously [Favreau et al., 1987]. Briefly, each sample well was loaded with approximately 2 pmol microsomal CYP3A4 (based on earlier immunochemical quantitation of different microsomal preparations of the individual livers). A standard curve was generated by loading 0.5, 1, 2, and 3 pmol of pure CYP3A4 protein standard in duplicate. At the end of the electrophoretic run, partially resolved protein bands were transferred to nitrocellulose and incubated 2 h with 1 μg/mL specific

rabbit polyclonal anti-CYP3A4 IgG for primary immunodetection. The nitrocellulose was then washed and incubated 1 h with 1 μg/mL antirabbit IgG alkaline phosphatase conjugate for secondary detection. After washing, immunopositive bands were visualized with the addition of 5-bromo-4-chloro-3-indoyl phosphate/nitroblue tetrazolium substrate and immediately washed with H_2O to avoid over-exposure. The bands were detected and quantified by densitometry with a Millipore Bioimage scanner. Amounts were determined by relating sample optical density to a standard curve of optical density vs. pmol CYP3A4.

Incubation Assay

For determination of inactivation kinetic constants, preincubations contained 0, 5, 10, 20, and 40 μM midazolam, 1 mM NADPH, and 70 nM P450 in a 2 mL volume of 100 mM potassium phosphate buffer containing 1 mM EDTA. After equilibrating 1.8 mL of the complete incubation mixture minus NADPH at 37° C for 3 min, the primary incubation was initiated by adding 200 μL of 10 mM NADPH and vortexing the sample for 3 seconds. Each concentration of midazolam used for the primary incubation was initially set-up in a single incubation tube. Three 100 μL aliquots from each midazolam primary incubation tube were immediately transferred to three individual secondary incubation sample tubes to represent zero-time for the primary incubation in triplicate. Subsequent transfers were also made in triplicate at 1, 2, 3, and 4 minutes giving a total of 15 secondary incubation tubes for each concentration of midazolam. The secondary incubation sample tubes contained 400 μM testosterone, and 1 mM

NADPH in potassium phosphate, EDTA buffer, in a total volume of 1 mL after transfer. Testosterone metabolism was started at the time of transfer, carried out for 12 min, then terminated by the addition of 2 mL ethyl acetate, followed by 3 seconds of vortexing, then placement of the tube on ice. Before extraction, 11α-hydroxyprogesterone (0.5 μg/100 μL) was added to each sample as the internal standard. For HL #124, the half-life method for the determination of the inactivation kinetic constants was employed [Waley, 1985]. The incubation assays were identical with the following exceptions. Preincubations contained 0, 10, 20, 40, and 80 μM midazolam and 10, 10, 20, 40, 80 nM P450, respectively, to maintain a constant enzyme/inactivator ratio. For cDNA-expressed CYP3A4 incubations, 28 nM P450, according to the manufacturer's stated concentration, was included in the primary incubations (total volume of 1.6 mL). Substrate protection was measured against 40 μM midazolam primary incubations including 0, 100, 200, or 400 μM alfentanil in HL #124 microsomes in a manner consistent with determination of the kinetic constants.

For determination of the partition ratio in human liver microsomes, preincubations contained 0, 1, 2, 4, 8, 12, 16, 20, 24, 28, and 32 μM midazolam and 0.5 μM P450 spectral content in HL #124. The primary incubations were started by addition of 100 μL of an NADPH generating system consisting of 10mM NADPH, 137 mM glucose-6-phosphate, and 28 IU of glucose-6-phosphate dehydrogenase. Transfers to the secondary incubation were made in duplicate after 30 min. Remaining activity was measured as above. For determination of the partition ratio in cDNA-expressed CYP3A4 cell microsomes,

preincubations contained 0, 4, 8, 12, 16, 20, 28, 32, 36, and 40 μM midazolam and 0.225 μM CYP3A4. Transfers to the secondary incubation were made in duplicate after 40 min. Remaining activity was assayed as above.

Assay of 6ß-hydroxytestosterone

Standard and Sample Preparation: Stock solutions at a concentration of 0.1 mg/mL of 6ß-OHT and 11α- hydroxyprogesterone were prepared in methanol and stored in a dessicator at -20°C. For each standard curve, an appropriate volume of the 6ß-hydroxytestosterone stock was diluted into 1 mL of distilled, deionized water and subsequent dilutions were made in water. The concentrations of the analytes used to generate a standard curve for 6ß-OHT were 0.01, 0.04, 0.16, 0.64, and 2.56 μg/mL. Microsomal standards were prepared by the addition of known amounts of 6ß-OHT standard in water (100 μL) and 10 μL of 40 mM testosterone in methanol to 890 μL control human liver microsomes diluted to 7 nM P450 in potassium phosphate buffer (100 mM, pH = 7.4) containing 1 mM EDTA. For each sample set 11α-hydroxyprogesterone internal standard stock solution was diluted into water and 100 μL was added to each microsomal standard to give a final concentration of 0.5 μg/mL.

Extraction Procedure: The samples were extracted with 2 x 2 mL volumes of ethyl acetate by vortex mixing (approximately 10 seconds), centrifugation (2500 rpm), and separation of the upper, organic phase via disposable pasteur pipets. After extraction and separation of the organic phase, the samples were dried over sodium sulfate, decanted and placed

in a heated water bath where the solvent was removed under a steam of dry nitrogen. The concentrated extracts were dissolved in 50 µL of 50:40:10 water/methanol/acetonitrile and the samples were transferred to autoinjector vials equipped with 200 µL limited volume inserts. A 20µL aliquot was injected for analysis.

HPLC / UV Analysis: Separation and quantitation was achieved by a modification of the procedure of Darbyshire et al. [Darbyshire et al., 1994]. A Hewlett Packard 1050 solvent delivery system was equipped with a 250 mm Hewlett Packard Spherisorb ODS-2, 4 mm i.d., 5 µm pore size reverse-phase cartridge column and operated at 0.9 mL/min at 30° C. The column was equilibrated with 50:40:10 water/methanol/acetonitrile and a linear sovent gradient developed between 44/46/10, 40/48/12, 36/49/15, 15/65/20 over 15, 8, 4, and 2 min respectively and eluted for 5 min before returning to the equilibrium conditions over 10 min. Metabolites were detected with a Hewlett Packard multiwavelength UV detector operating at 242 nm. Peaks were integrated with a Hewlet Packard 3396 Series II integrator. Amounts were determined by relating peak area ratios of the metabolite to internal standard to standard curves generated with authentic standards. 6ß-OHT, 11α-OHP, and testosterone were eluted over 8.6, 18.0, and 24.8 min, respectively. The limit of quantitation for 6ß-hydroxytestosterone was 0.01 µg/mL by this method based on <15% inter- and intra-day coeffecient of variation (% CV) at this concentration (n = 5).

3.5 Results

Testosterone 6ß-hydroxylation kinetics were characterized in our laboratory. Time dependent formation of 6ß-hydroxytestosterone in human liver microsomes was observed over the 15 minutes tested. Initial rates of formation were measured in HL #122 microsomes to determine the K_m and V_{max} values from the slope and intercept of Eadie-Hofstee plots over the concentration range 6.25 μM to 400 μM. A straight line was observed ($r^2 > 0.99$), indicative of single-enzyme kinetics, and gave K_m = 25 μM, and V_{max} = 24 nmol product/min/nmol enzyme (data not shown). Although previous authors did not explicitly state the kinetic parameters, the rates per unit enzyme, at similar concentrations, are in general agreement with those given by Waxman et al. [Waxman et al., 1988; Waxman et al., 1991].

Active-Site Titration

Experiments were conducted to determine whether or not loss of enzyme activity was proportional to the molar ratio of midazolam to CYP3A4. The quantity of CYP3A4 in HL #124 microsomes was determined by Western blot analysis as described in the Materials and Methods. The anti-CYP3A4 polyclonal antibody detected a single protein in all of the liver microsomal samples examined that co-migrated with the CYP3A4 standards. The concentration of CYP3A4 measured in HL #124 was compared to the spectral content of P450 to give 45% CYP3A4 relative to total P450 content.

Microsomes from HL #124 were then incubated with variable concentrations of midazolam in the presence of an NADPH regenerating system and the reaction was allowed to proceed to approximate completion before determination of remaining CYP3A4 activity. Because long incubation times, such as those employed, were expected to generate significant levels of midazolam metabolites, a control experiment was performed to evaluate the ability of 1′-OH MDZ and 4-OH MDZ to inhibit testosterone metabolism. Co-incubation of 5 μM 1′-OH MDZ or 5 μM 4-OH MDZ with 400 μM testosterone did not inhibit testosterone 6ß-hydroxylation (data not shown). The fractional remaining activity was found to be proportional to the molar ratio of midazolam to CYP3A4 (Fig. 3.5). The kinetics predicted by Scheme 1 give the slope of the line in Fig. 3.5 as - $1/(1+ k_3/k_4)$, which yields a partition ratio of $k_3/k_4 = 199$. The partition ratio was similarly measured in the cDNA expressed CYP3A4 preparation. The slope of the line in Fig. 3.6 gives $k_3/k_4 = 213$.

Time Dependence, Saturability, and Kinetic Parameters

The kinetics of inactivation of CYP3A4 by midazolam were determined in three human liver microsomal preparations and a commercially available, cDNA-expressed CYP3A4 preparation. For HL #122, HL #113, and the cDNA-expressed preparation, primary (inactivation) incubations contained 0, 5, 10, 20, and 40 μM midazolam. The primary incubations were diluted into a secondary incubation containing 400 μM testosterone at 0, 1, 2, 3, and 4 minute time points as described in the materials and methods. Time-dependent inactivation of

testosterone 6ß-hydroxylation was observed in all enzyme preparations tested. Data is shown for HL #122 and the cDNA-expressed enzyme (Figs. 3.7 and 3.9). As shown, plotting natural log (% remaining activity) vs. time gave a linear result at each concentration of midazolam indicating pseudo-first-order inactivation kinetics. The rates of inactivation were determined by linear regression analysis of the data at each concentration of midazolam. Transformation of the rate data into a double-reciprocal plot of inactivation rate vs. midazolam concentration gives a line with a positive intercept on the ordinate, demonstrating saturation (Figs. 3.8 and 3.10). Each enzyme preparation displayed saturation kinetics. The K_Is and k_{inact}s were calculated from the double-reciprocal plots as described previously [Kitz et al., 1962], and are shown in Table 3.1.

The K_I and k_{inact} shown in Table 3.1 for HL #124 were determined by the half-life of inactivation method. In this experiment 0, 10, 20, 40, and 80 μM midazolam were used to inactivate the enzyme and the midazolam to CYP3A4 ratio was kept constant at ~2000:1. The remaining activity was determined as described above. The % inactivation vs. time was plotted for each midazolam concentration. Values ranging from 10 to 70 % inactivation from 0 to 4 minutes, respectively, were observed at each concentration and the half-life of inactivation was determined by interpolation at 50% inactivation. The half-life data was transformed into a plot of [midazolam] $\times t_{1/2}$ vs. [midazolam] (Fig. 3.11) and the values of K_I and k_{inact} determined as described previously [Waley, 1985].

Requirement of Catalysis

Experiments designed to determine if inactivation requires catalysis and if the inactivation can be inhibited by trapping reagents were conducted in HL #124 microsomes. Remaining activities measured from parallel experiments of microsomes alone, or microsomes containing 1 mM NADPH were nearly identical and considered maximal (100%, Table 3.2). When microsomes which contained no NADPH, but included 40 μM midazolam, were used, 90% remaining acitivity was observed relative to no midazolam. When both midazolam and NADPH were present in the primary incubation, 30% remaining activity was observed.

Inactivation Not Inhibited by Reactive Intermediate Traps

When, in individual experiments, 100 units of superoxide dismutase, 400 units of catalase, 1 mM glutathione, or 1 mM N-acetyl-L-cysteine was added to the 40 μM midazolam + NADPH inactivation assay, no change in the level of inactivation was observed (Table 3.2).

Substrate Protection

The effect of a competing substrate on the inactivation rate was measured in HL #124 at 40 μM midazolam in a manner consistent with the determination of the kinetic constants. Non-time-dependent, competetive inhibition of testosterone by alfentanil in the secondary incubation was estimated by measuring the remaining activity at time = 0 minutes at each concentration of alfentanil. The inhibition observed at time = 0 minutes was then subtracted from each time point for each

corresponding alfentanil concentration. The remaining activity data, minus the time 0 level of inhibition, was then used to plot the rate of midazolam inactivation in the presence of varying amounts of alfentanil relative to no added alfentanil (Fig. 3.12). As shown, increasing amounts of alfentanil resulted in decreasing pseudo-first-order rates of inactivation.

3.6 Discussion

The results of these studies support the hypothesis that non-linear, time-dependent formation of midazolam metabolites is due to mechanism-based inactivation of CYP3A4 by midazolam. Testosterone 6ß-hydroxylation was successfully utilized as a high affinity, high-turnover rate, probe of remaining CYP3A4 activity. If testosterone, based on its affinity for CYP3A4, had not effectively protected CYP3A4 from further inactivation during the secondary incubation, then pseudo-first-order rates of inactivation would not have been observed (Figs. 3.7 and 3.9). The high turnover rate consistently provided amounts of 6ß-OHT $\geq$ 0.1 µg/mL, 10-fold higher than the limit of quantitation, even under conditions resulting in 70 - 80% inactivation of 2.8 nM cDNA-expressed CYP3A4. The discussion that follows focuses primarily on the meaning of the results as they address the first 5 criteria for mechanism-based inactivation listed above.

Active-Site Titration

Active-site titration revealed a branched reaction pathway with a high commitment to product formation relative to inactivation. Accurate determination of the partition ratio required knowledge of the initial enzyme concentration used in the study. Selective quantitation of CYP3A4 from the mixture of proteins in HL #124 microsomes was desired and thus Western blot analysis was employed. The antibody used in these studies has been shown to detect both CYP3A4 and a protein of slightly higher molecular weight than CYP3A4 which is presumed to be CYP3A5 [Thummel et al., 1994; Wrighton et al., 1989]. Because only one protein was observed, it was concluded that HL #124 does not contain CYP3A5. In addition to the immunochemically-quantitated microsomes, a known amount of expressed CYP3A4, based on the manufacturer's reported amount (measured by differential UV absorbance), was used in the active-site titration experiments. The partition ratio values observed in these preparations were very similar (Figs. 3.5 and 3.6), and indicate that each molecule of the enzyme completes approximately 200 catalytic cycles before the inactivation event. Therefore, midazolam is not a particularly efficient inactivator, yet 80% inactivation can be observed within four minutes at 40 μM midazolam (Figs. 3.7 and 3.9) because the rate of turnover is very high.

Time-Dependence and Saturability

The criterion of time-dependent inhibition of CYP3A4 by midazolam was satisfied as shown in Figs. 3.7 and 3.9. Furthermore, the observed natural log (% remaining activity) vs. time data gave

straight lines which allowed direct calculation of the pseudo-first-order inactivation rates by determination of the slope using linear regression analysis. The criterion of saturable inactivation kinetics was satisfied as evidenced by the observation of a positive y-intercept in the Kitz and Wilson plots (Figs. 3.8 and 3.10). K_I and k_{inact} values were calculated from the intercept data. By definition, K_I and k_{inact} consist of individual rate constants for the transformations shown in Scheme 1, and are independent of the initial enzyme concentration. Theoretically, under steady-state conditions, the values for each constant should not change with the enzyme preparation, ie. each CYP3A4 preparation, including individual human liver microsomes, should give the same K_I value, and the same k_{inact} value. Experimentally, the K_I and k_{inact} values for HL #113, HL #122, and the expressed system shown in Table 3.1 are found to be variable. The standard deviation of each parameter is ± 25% of the mean value. The error in these values on first analysis seems to be inordinately large, however, simulated experiments have shown that errors in K_I and k_{inact} values calculated by the method described above can be expected to be large [Waley, 1985]. The simulations demonstrate that the error can be as high as 20% of the mean values, even if errors in the determination of % remaining activity remain as low as ± 0.25%. The high level of error results from compounding due to multiple-linear regression. First, linear regression analysis is used to determine the inactivation rates. Then, each rate becomes a point on the regression line from which K_I and k_{inact} are determined. Small errors in rate have a profound effect on the error in the regression line of the Kitz and Wilson plot and the K_I and k_{inact} values calculated from this line. The %

remaining activity data measured in the experiments above, by testosterone 6ß-hydroxylation, varied by as much as ± 2% of the mean value - an error nearly 10-fold higher than the error of the % remaining activity data in Waley's simulated experiment which translated into a ± 20% error in K_I and k_{inact}. Therefore, the error in the set of K_I and k_{inact} values calculated from HL #113, HL #122, and expressed CYP3A4 preparations, at ± 25% of the mean, is low, relative to the error one might have expected in light of Waley's experiments. The values obtained can be considered as identical within experimental error.

As a possible solution to the compounding error problem, Waley suggested a half-life of inactivation method for the determination of steady-state inactivation kinetic constants that would result in less variability; ± 2% in K_I and k_{inact}. This method was used to obtain a more accurate estimate of the parameters, and the results are shown for HL #124 in Table 3.1. The resulting K_I was very near the average of the K_Is measured previously, while the k_{inact} was higher than all previously measured values. Although there is now reasonable certainty that the K_I value of 14 μM is a close approximation of the concentration at which the half-maximal inactivation rate is achieved, further studies are necessary to determine whether the apparent k_{inact} value is closer to 0.2 or 0.5 min^{-1}.

Requirement of Catalysis

The requirement for catalysis was demonstrated by omitting a critical co-factor, NADPH, from the incubation. When NADPH was excluded from the 4 minute primary incubation, 10% inhibition was

observed. This level of inhibition is consistent with that observed in time-zero primary incubations, indicating the lack of enzyme inactivation in the absence of NADPH. Conversely, NADPH-dependent inactivation was extensive, at 70% inactivation (Table 3.2). The non-time-dependent inhibition of testosterone turnover in the secondary incubation is due to the midazolam transferred to the secondary incubation. The expected level of inhibition can be estimated by comparing the rates, with and without inhibitor, predicted by the model for competetive inhibition:

$$v = \frac{V_{max} * [S]}{[S] + K_m (1 + \frac{[I]}{K_i})}$$

where v is the predicted rate of 6ß-hydroxylation; V_{max} is the maximal rate of testosterone turnover; [S] is testosterone concentration; K_m is the affinity constant for testosterone; [I] is midazolam concentration; and K_i is assumed to be equal to the K_m for midazolam (1.5 μM, Chapter 2). This model estimates a 13% level of inhibition of testosterone 6ß-hydroxylation by the 4 μM midazolam that is transferred to the secondary incubation and is similar to the 10% level of inhibition observed in the absence of NADPH. Therefore, all of the observed inhibition can be accounted for, the majority of which is dependent on P450 catalysis, by the mechanism-based inactivation hypothesis.

Inactivation Not Inhibited by Reactive Intermediate Traps

When agents that consume reactive oxygen intermediates, or trap electrophilic species, were included in the preliminary incubation, the level of inactivation was not attenuated (Table 3.2). These results suggest

that midazolam inactivation of CYP3A4 is an active-site process that does not involve build-up of reactive intermediates outside the active site. Superoxide dismutase and catalase, which utilize $O_2^{\cdot -}$ and H_2O_2, respectively, as substrates, do not have access to these reactive oxygen intermediates within the P450 active site where they would be generated. Therefore, reactive oxygen intermediates may be involved in the inactivation of CYP3A4 and, if so, would not constitute mechanism-based inactivation. For example, it is possible that midazolam potentiates decoupling of reduced oxygen intermediates from the CYP3A4 heme-iron atom during catalysis which irreversibly damage the enzyme before being released from the active site. If a midazolam derived reactive intermediate is responsible for the inactivation, it is unlikely that it escapes the active site before reacting with the enzyme, which is consistent with mechanism-based inactivation.

Substrate Protection

To demonstrate involvement of the active site directly, another substrate of CYP3A4, alfentanil, was co-incubated with midazolam in the primary incubation of HL #124 microsomes. Relatively high concentrations of alfentanil were necessary to compete with midazolam for the active site and protect the enzyme from inactivation. Thus, significant amounts of alfentanil were transferred to the remaining activity assay and inhibition of testosterone 6ß-hydroxylation was observed. By measuring the remaining activity at time = 0 minutes at each concentration of alfentanil, an estimate of non-time-dependent inhibition of testosterone can be subtracted from each time point of the

corresponding alfentanil concentration. After correcting for the non-time dependent inhibition of testosterone 6ß-hydroxylation by alfentanil, a trend is revealed in the data shown in Figure 3.12. As the alfentanil concentration increases, the slopes of the regression lines approach zero, indicating decreasing rates of inactivation. Alfentanil, a selective substrate for CYP3A4, protects the enzyme from midazolam turnover-mediated inactivation by competing for the active site.

Five criteria for mechanism-based inactivation of CYP3A4 by midazolam have been demonstrated. Consistent, time-dependent, saturable inactivation kinetics were observed from three individual human liver microsomal preparations as well as a cDNA expressed CYP3A4 preparation. The requirement of catalytic turnover for inactivation was inferred from the observation that inactivation requires NADPH. Inactivation of CYP3A4 by electrophiles released from the active site is unlikely because the levels of inactivation observed were unaffected by modifiers that trap various types of reactive species. Decreasing pseudo-first-order rates of inactivation were observed in the presence of increasing concentrations of alfentanil, a competing substrate. These five observations, considered together, constitute convincing evidence that midazolam is a mechanism-based inactivator of CYP3A4. Chapter 4 will focus on demonstrating the remaining two criteria, irreversibility, and stoichiometric binding of midazolam to the inactivated enzyme. In Chapter 6, the analogy between furafylline and midazolam is reconsidered, and the impact of enzyme inactivation on *in vitro* midazolam metabolism studies is addressed.

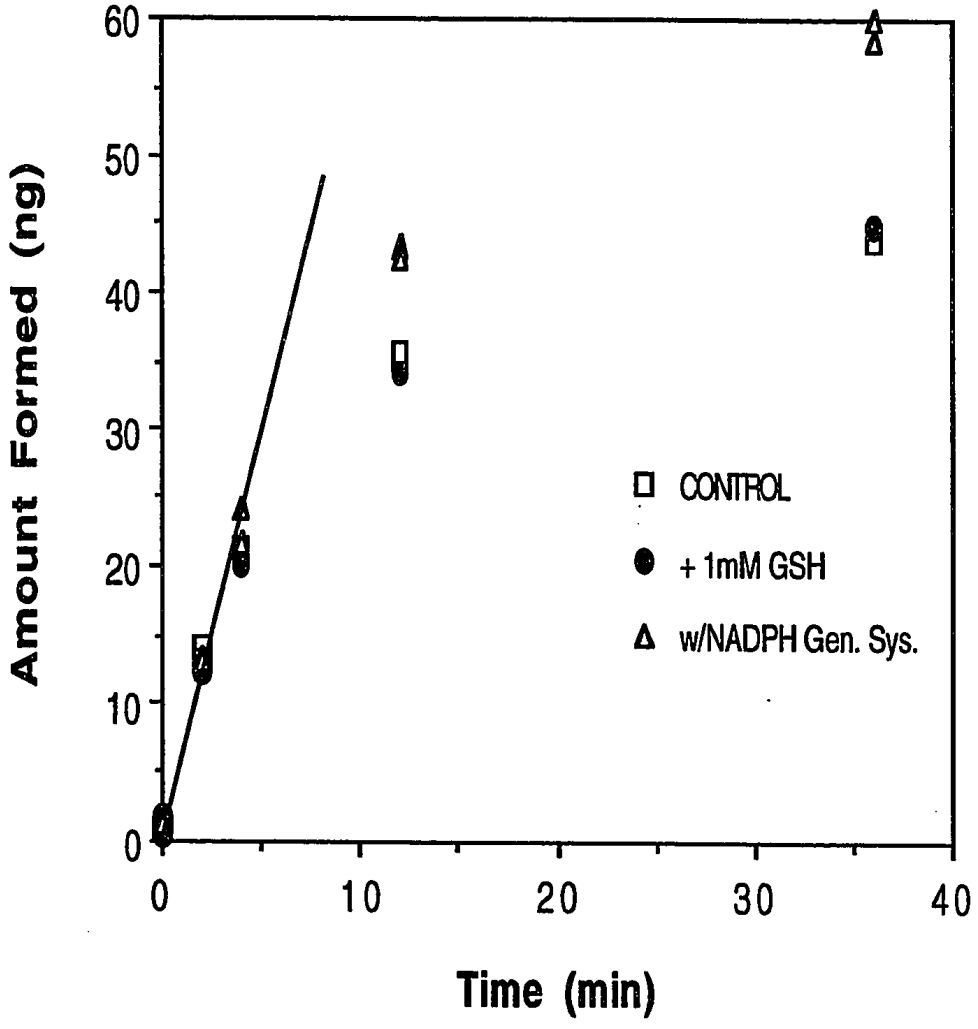

Figure 3.1. Effect of glutathione and and an NADPH regenerating system on 1´-OHMDZ formation over time.

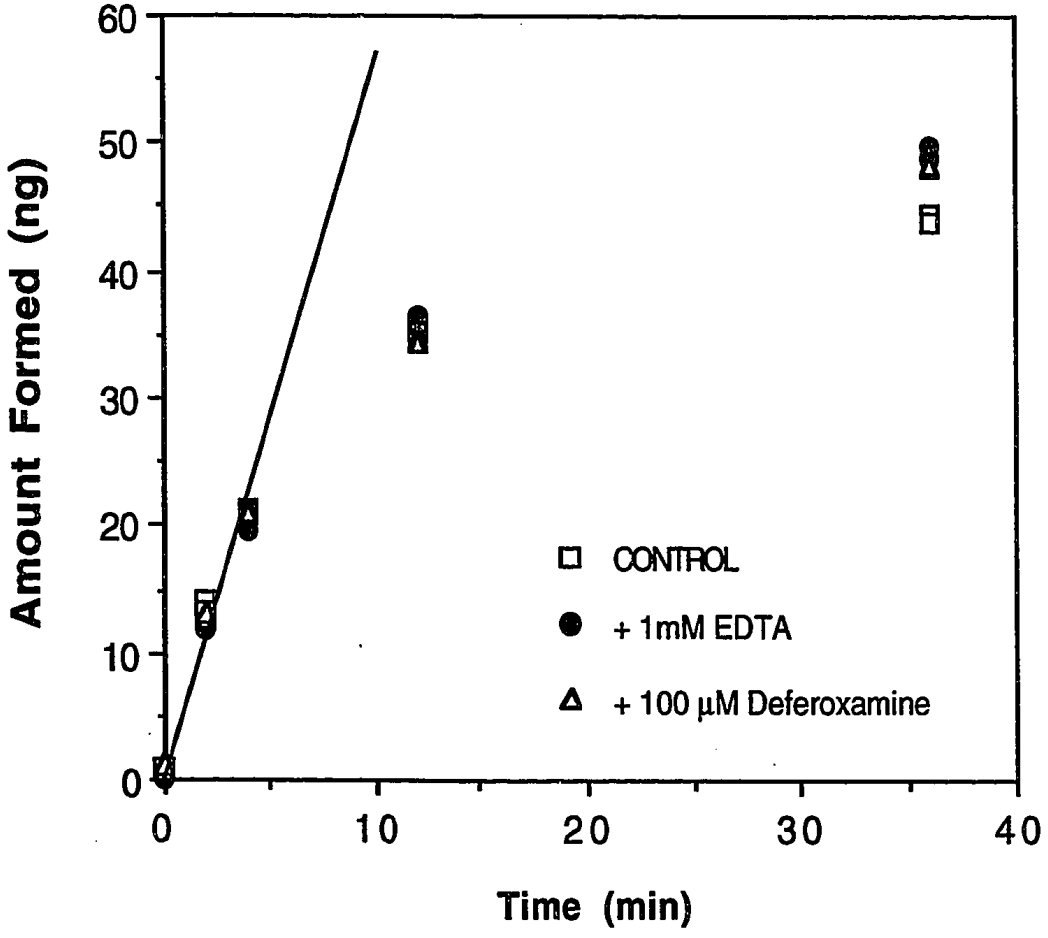

Figure 3.2. The effect of EDTA and deferoxamine on 1´-OHMDZ formation over time.

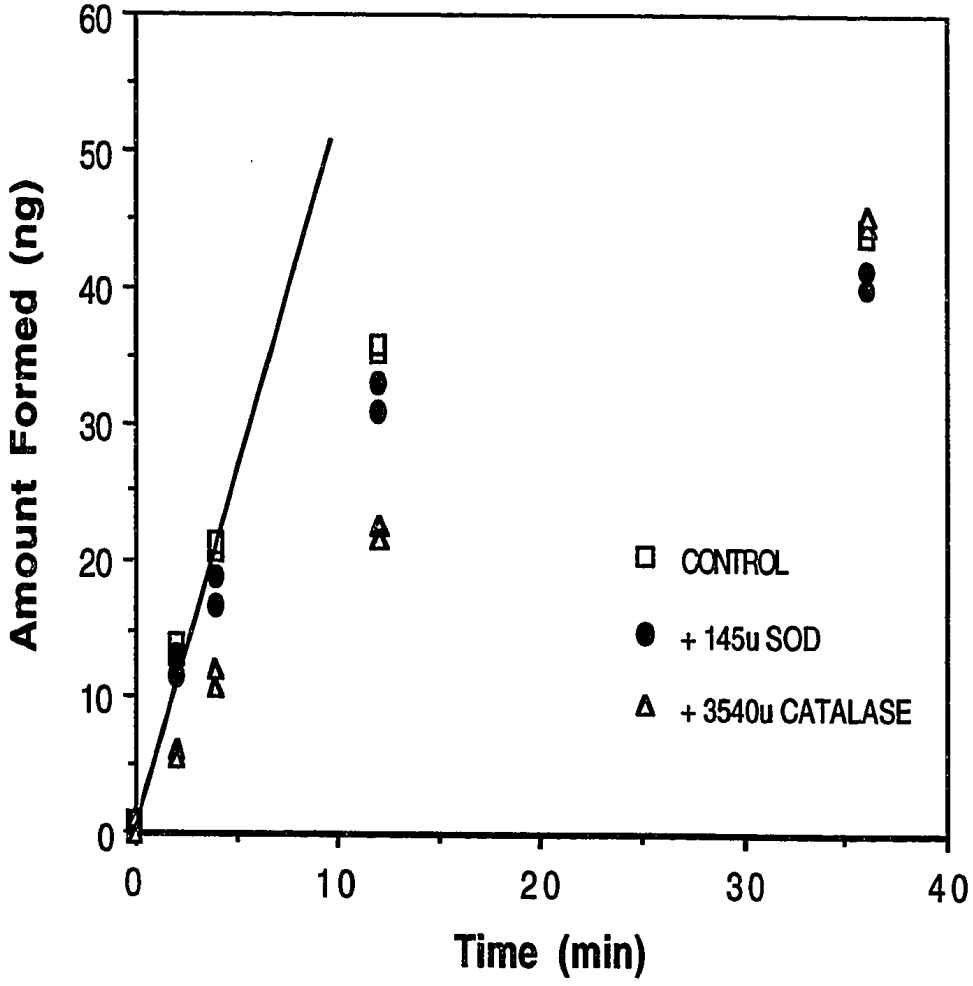

Figure 3.3. The effect of superoxide dismutase and catalase on 1′-OHMDZ formation over time.

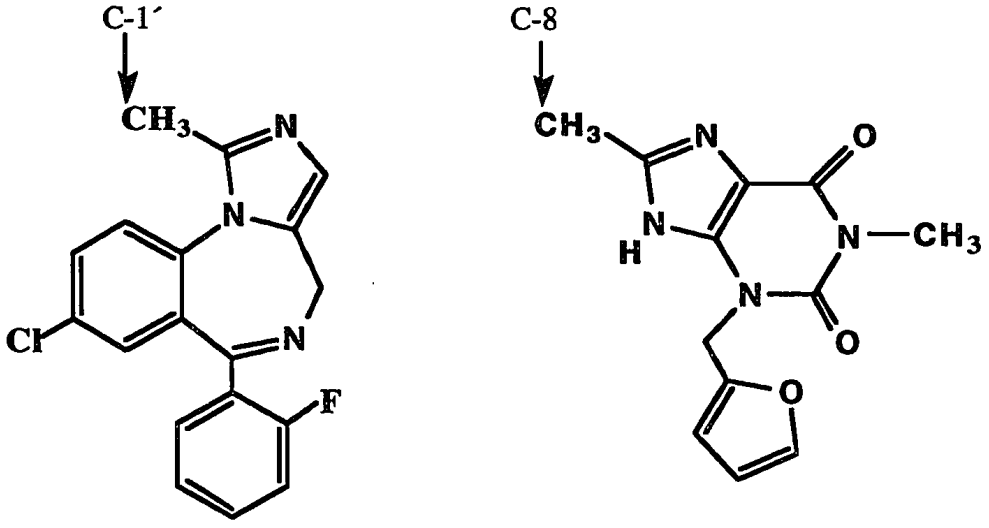

MIDAZOLAM FURAFYLLINE

Figure 3.4. Structures of midazolam and furafylline. Furafylline is a known CYP1A2 inactivator which inactivates the enzyme during catalytic processing of the C-8 carbon atom.

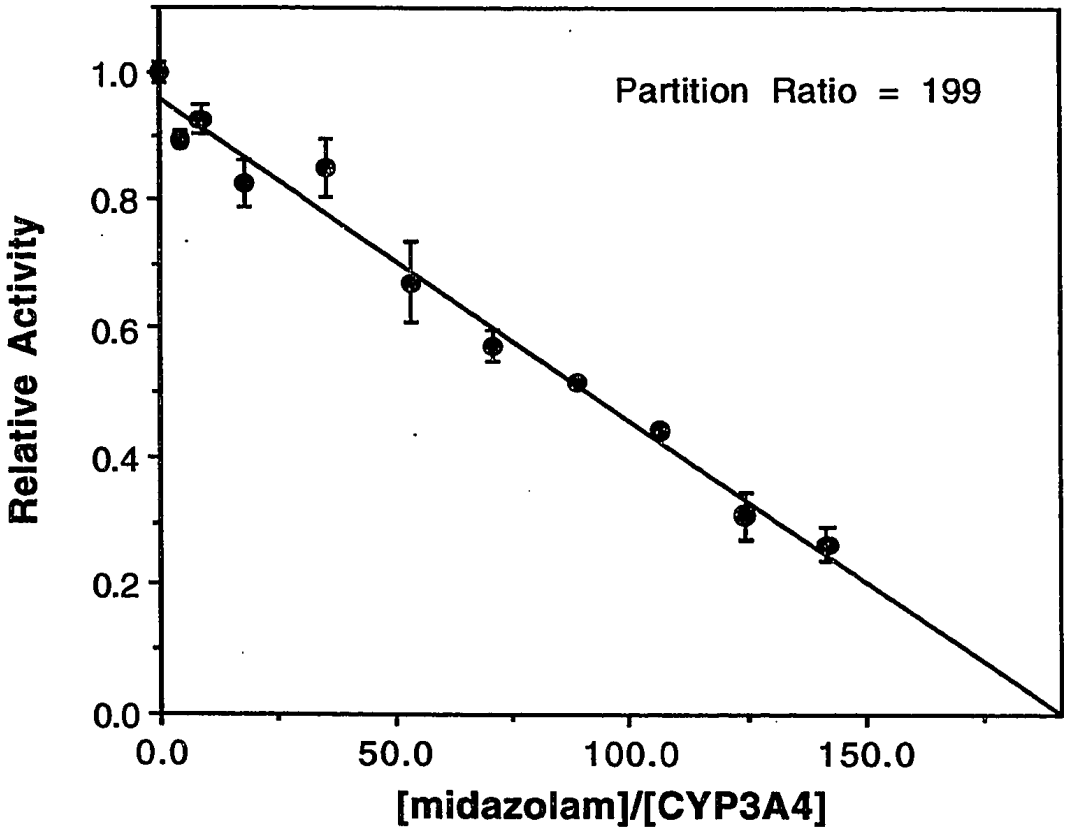

Figure 3.5. Active site titration of immunochemically quantitated CYP3A4 in HL #124 microsomes. Error bars represent the standard deviation of duplicate determinations at each midazolam concentration.

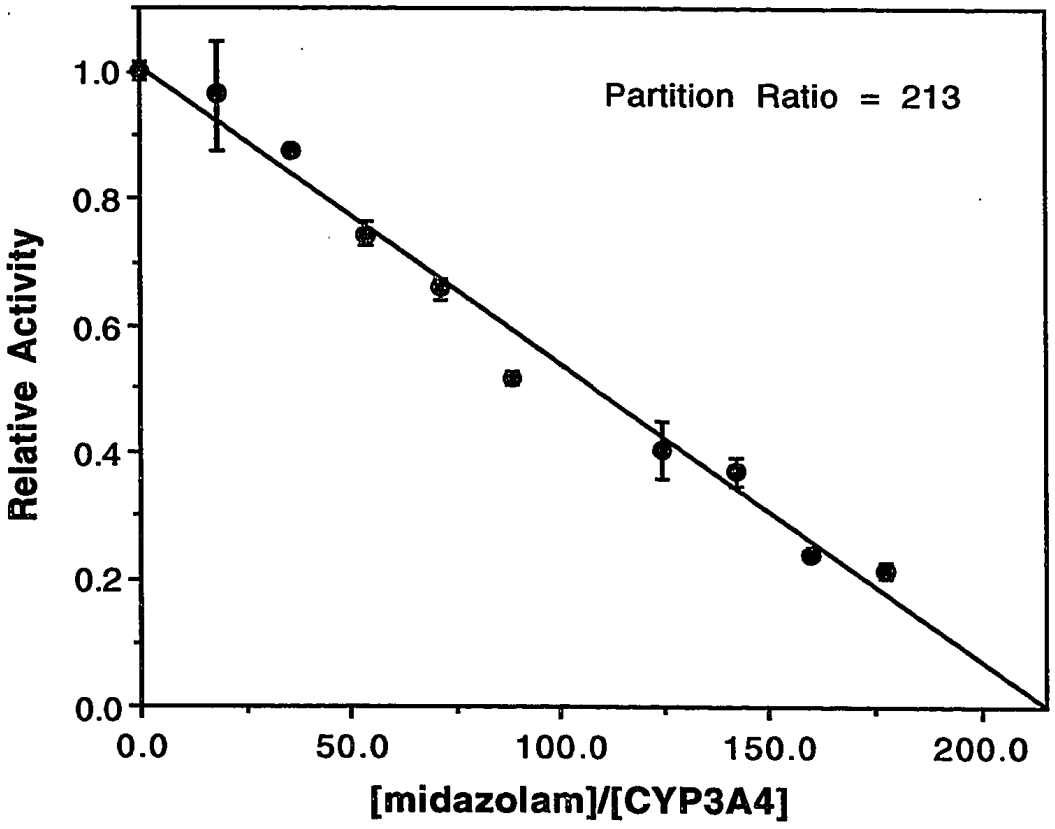

Figure 3.6. Active site titration of cDNA-expressed CYP3A4 in lymphoblastoid cell microsomes. Error bars represent the standard deviation of duplicate determinations at each midazolam concentration.

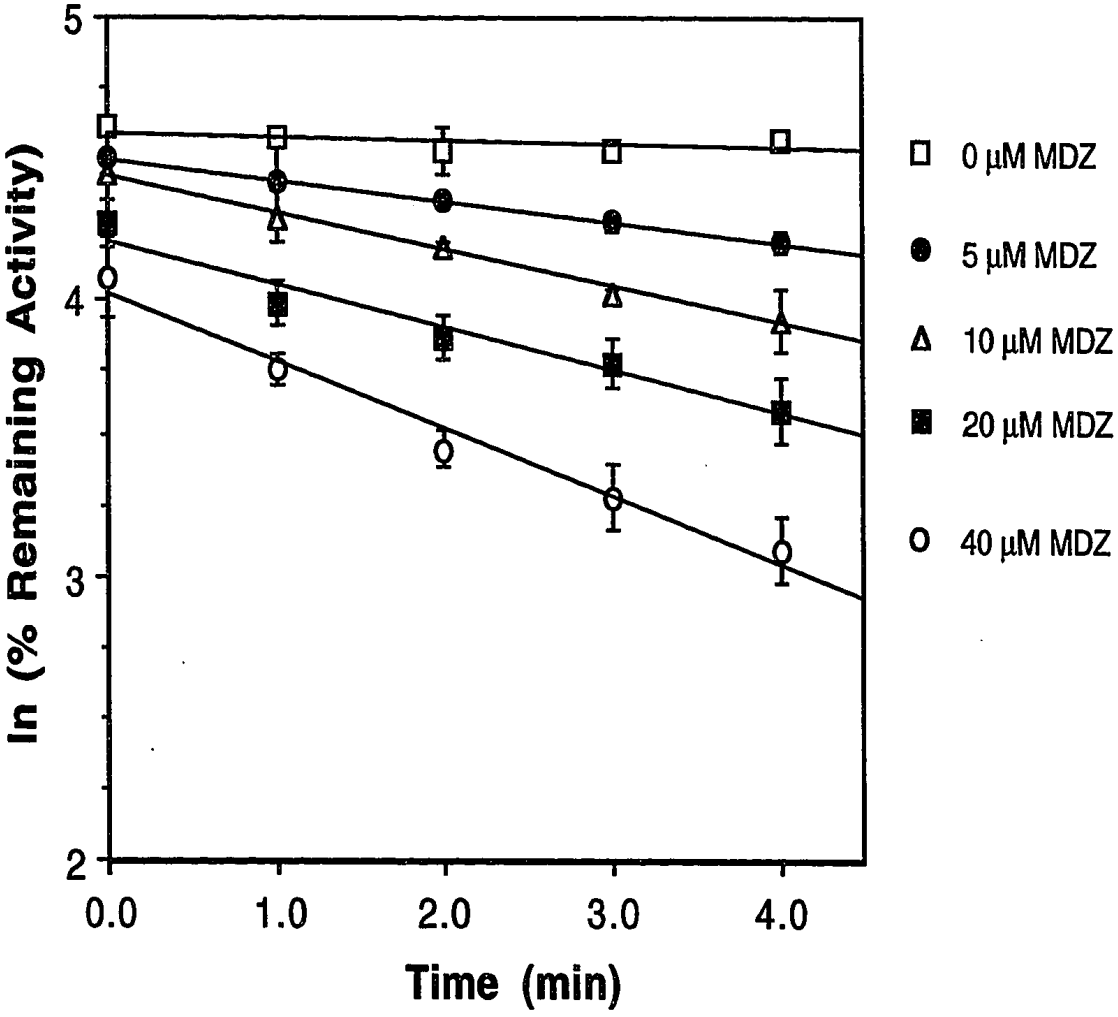

Figure 3.7. Time-dependent loss of HL #122 microsomal CYP3A4 activity by midazolam. Error bars represent the standard deviation of triplicate determinations at each time point.

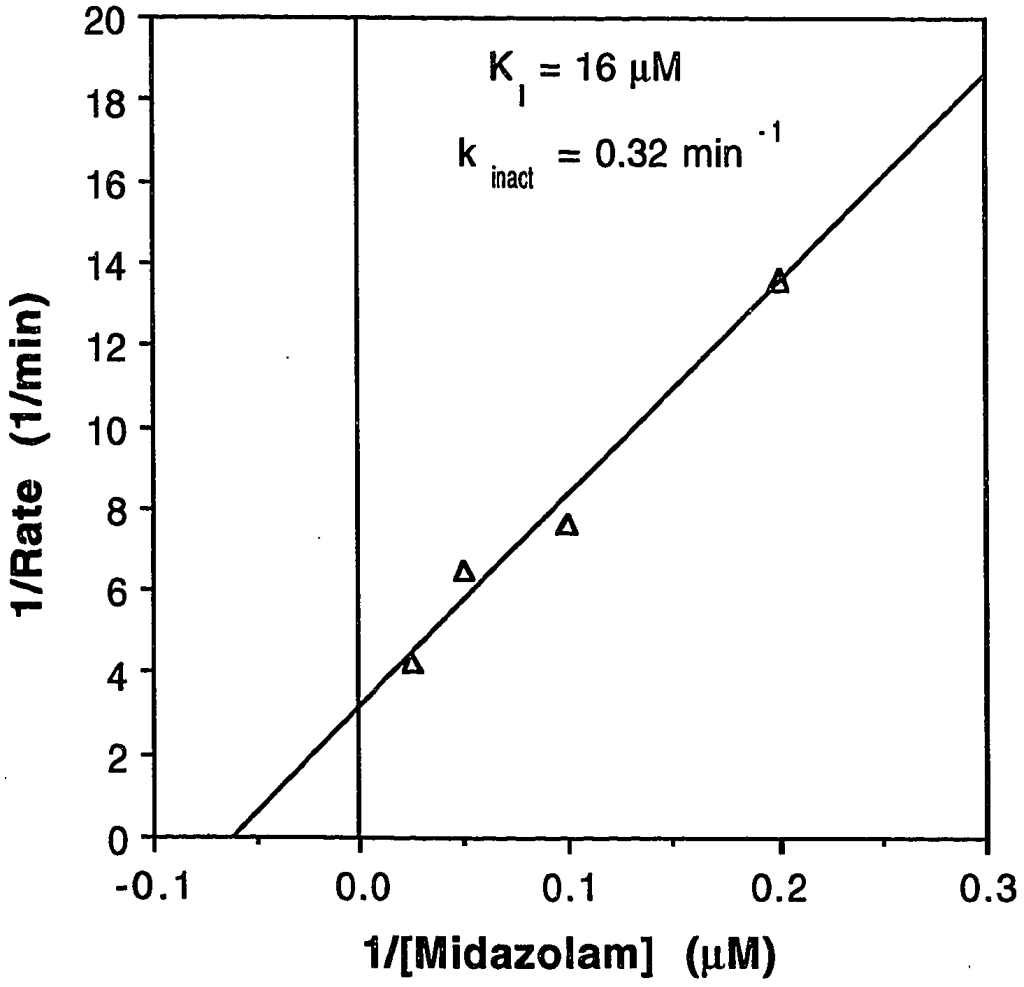

Figure 3.8. Kitz and Wilson, double-reciplocal plot of inactivation rate vs. midazolam concentration showing saturable inactivation kinetics in HL #122 microsomes.

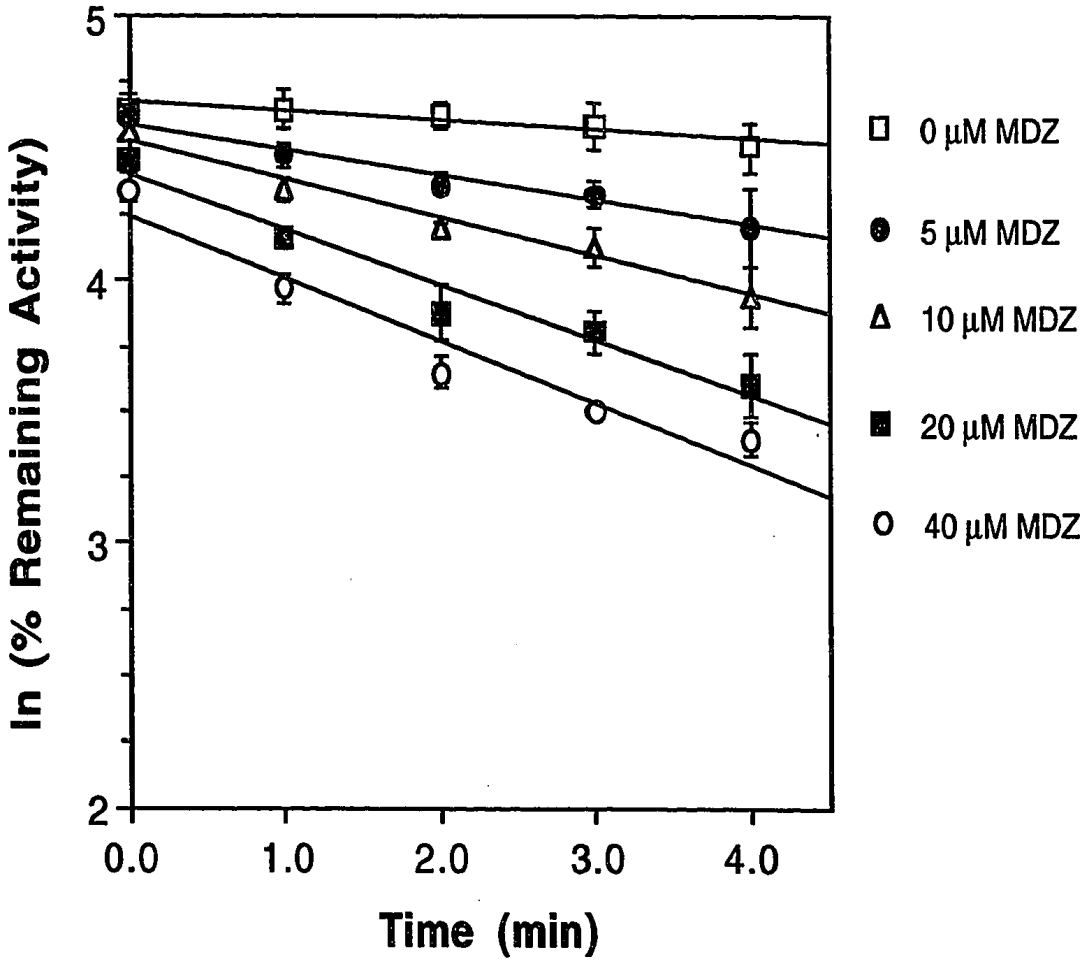

Figure 3.9. Time-dependent loss of cDNA-expressed CYP3A4 activity by midazolam. Error bars represent the standard deviation of triplicate determinations at each time point.

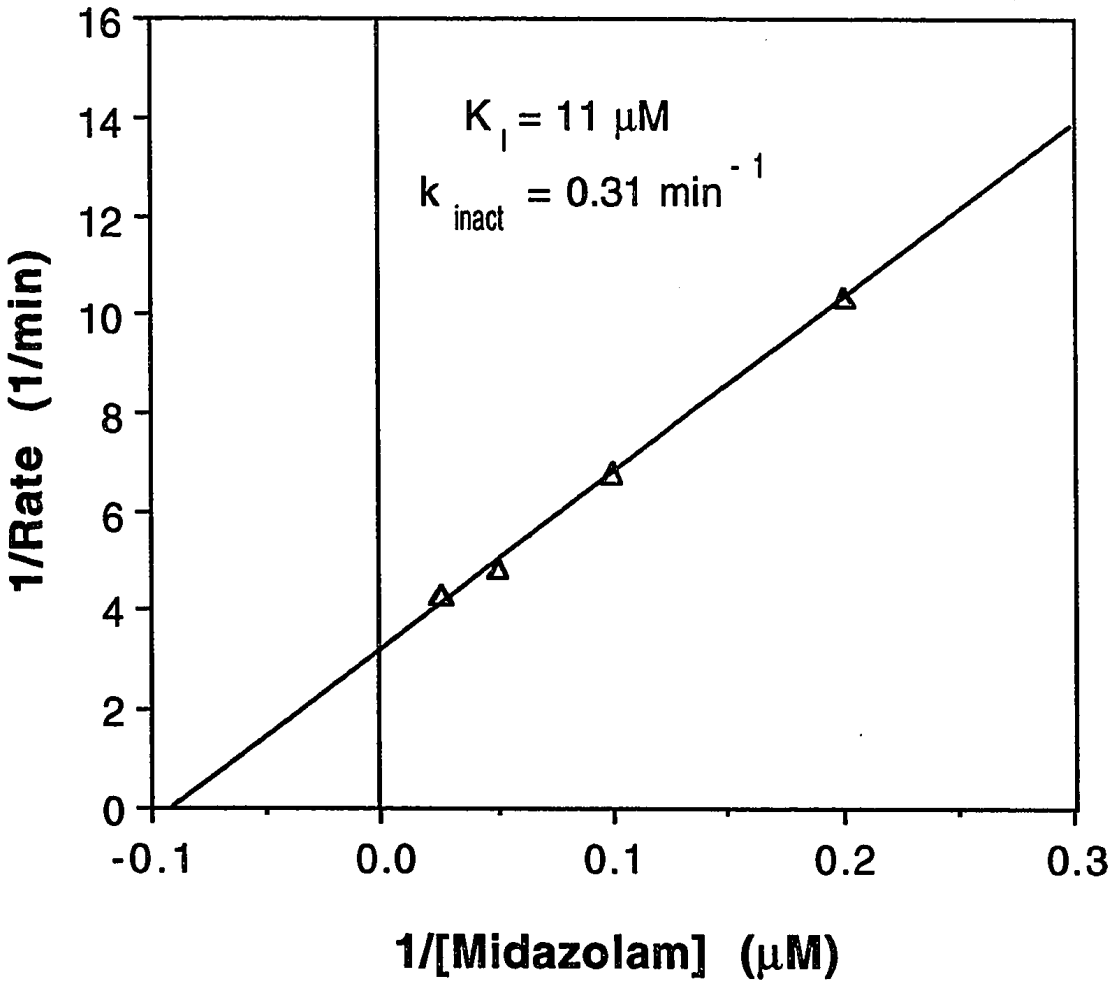

Figure 3.10. Kitz and Wilson plot showing saturable inactivation kinetics in cDNA-expressed CYP3A4.

Table 3.1. Kinetic constants calculated for the inactivation of CYP3A4 activity by midazolam in various microsomal suspensions.

Enzyme Source	K_I (μM)	k_{inact} (min^{-1})
HL #122	16	0.319
HL #124*	14	0.524
HL #113	19	0.201
expressed CYP3A4	11	0.309

*half-life method

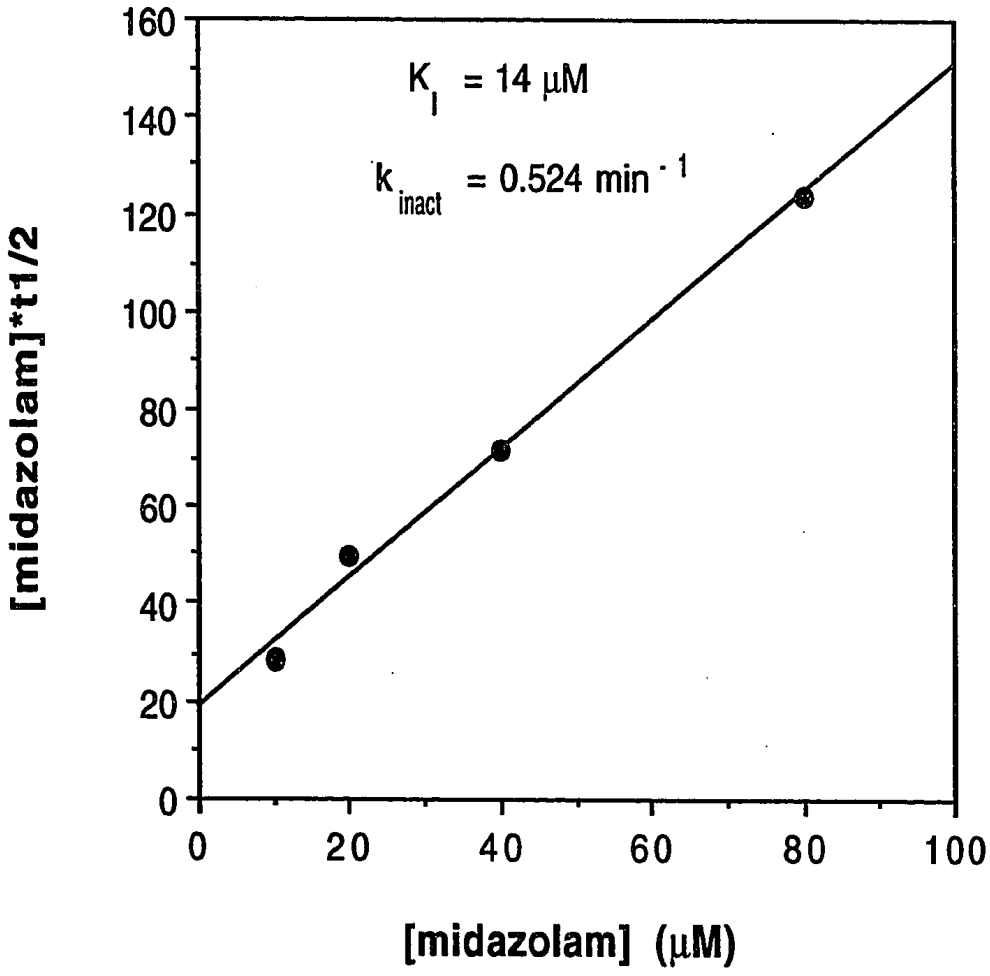

Figure 3.11. Inactivation half-life plot for the determination of inactivation kinetic constants in HL #124 microsomes.

Table 3.2. Effect of NADPH and trapping agents on the inhibition of CYP3A4 activity by midazolam.

Inactivation Assay Components t = 4 min	Relative Remaining Activity, %
no NADPH (control)	100
NADPH (1 mM)	100
midazolam (40 μM)	90
NADPH, midazolam (40 μM)	30
NADPH, midazolam (40 μM), superoxide dismutase (100 units)	30
NADPH, midazolam (40 μM), catalase (400 units)	28
NADPH, midazolam (40 μM), glutathione (1 mM)	30
NADPH, midazolam (40 μM), N-acetyl-L-cysteine (1 mM)	28

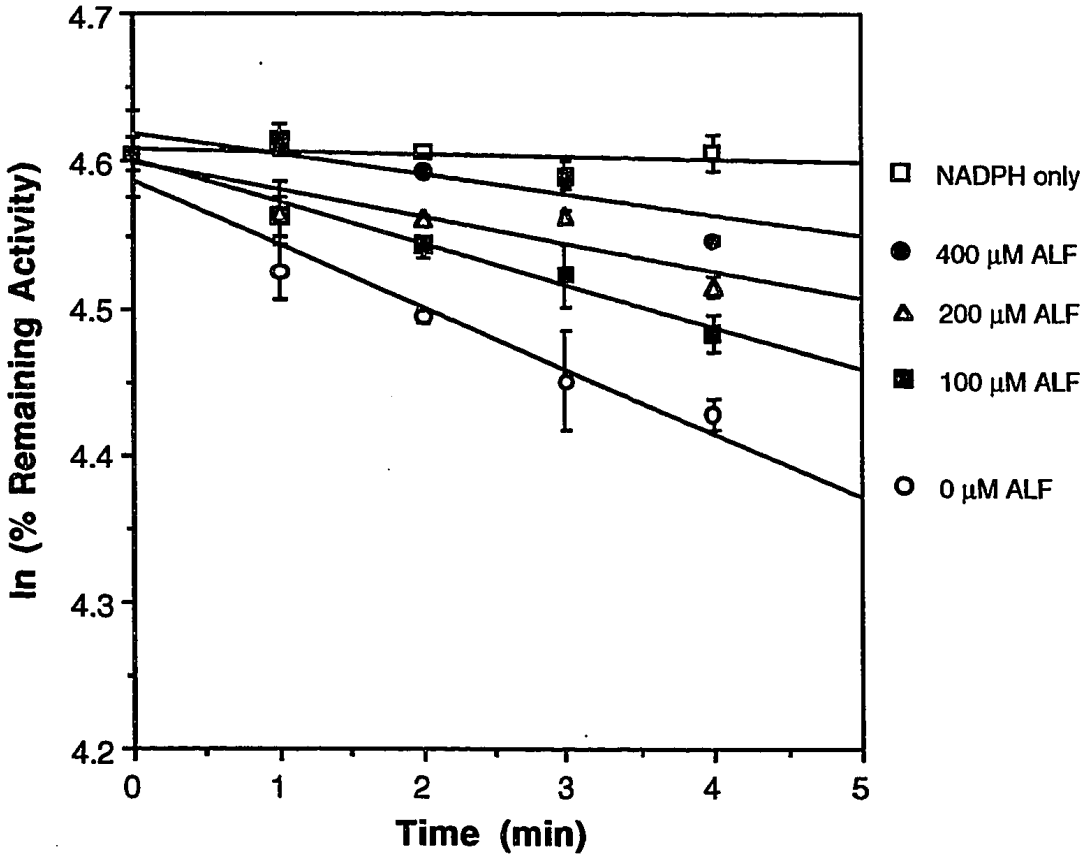

Figure 3.12. Concentration dependent substrate protection from midazolam mediated inactivation of CYP3A4 activity in HL #124 microsomes by alfentanil (ALF). Error bars represent the standard deviation of triplicate determinations at each time point.

CHAPTER FOUR

INACTIVATION OF CYTOCHROME P450 3A4 BY MIDAZOLAM: IRREVERSIBLE BINDING AND UV/VIS CHARACTERISTICS

4.1. Binding of Known CYP3A4 Inactivators

Mechanism-based inactivation of an enzyme (Scheme 1, p 42) results in the irreversible binding of the inactivator to the enzyme. Three modes of irreversible binding have been observed for cytochrome P450 enzymes which can result in destruction of the enzyme:

1) covalent binding of the inactivator to the apoprotein
2) covalent binding of the inactivator to the heme prosthetic group
3) inactivator mediated covalent binding of the heme prosthetic group to apoprotein [Osawa et al., 1989].

Only the first two modes of binding can strictly meet the criterion of stoichiometric, 1:1, binding of the inactivator to inactivated enzyme. The studies described in this chapter address the possibility of midazolam becoming irreversibly bound to CYP3A4 resulting in 1 mol of bound midazolam per mol of inactivated CYP3A4. The criterion of irreversibility is therefore suggested by the characterization of binding to the enzyme. Also, effects of midazolam metabolism-dependent inhibition of CYP3A4 on the UV/VIS characteristics of microsomal P450 are demonstrated.

Although mechanism-based inactivation has been well characterized for several cytochrome P450 enzymes, the number of studies conducted with human members of the CYP3A subfamily remain limited.

To date, only 2 mechanism-based inactivators have been described for CYP3A4, 17α-ethynylestradiol [Guengerich, 1988] and gestodene [Guengerich, 1990]. Both of these inhibitors remain only partially characterized with respect to the accepted criteria listed above (p 44). The data supporting inactivation of CYP3A4 by these compounds, including the caveats associated with characterizing their binding to CYP3A4, are reviewed below. A third selective inhibitor of CYP3A4, troleandomycin (TAO), forms a tight-binding, metabolic-intermediate complex with the enzyme [Watkins et al., 1985]. The UV/VIS characteristics of this complex are given in the final section of this introduction.

17α-Ethynylestradiol

Inhibition of CYP3A4 by 17α-ethynylestradiol (EE2, Fig. 4.1) was suggested in an article which had the objective of demonstrating that CYP3A4 is the major catalyst involved in the oxidation of this compound in human liver tissue [Guengerich, 1988]. Evidence for the selectivity of CYP3A4 for the catalysis of 17α-ethynylestradiol 2-hydroxylation was provided by indirect approaches, including antibody inhibition, chemical inhibition and correlative analyses. In addition, the author suggested that EE2 appears to be a mechanism-based inactivator of P450. The loss of CYP3A4 activity was demonstrated by incubating 100 μM EE2 with microsomes and NADPH for 30 minutes, diluting the incubation mixture 50-fold with the addition of nifedipine (final concentration 200 μM), and measuring nifedipine oxidase activity. Nifedipine oxidation was inhibited 40% relative to a control that excluded EE2 in the primary incubation.

Further evidence for inactivation included: (1) time-dependent loss of spectrally detectable P450 in microsomes treated with 100 μM EE2, and (2) lack of time-dependent loss of the P450 Soret in the absence of NADPH. Lastly, an experiment was performed to explore the nature of the reactive intermediate responsible for the loss of P450 as described below.

If EE2 is a mechanism-based inactivator of CYP3A4, then irreversible binding of radiolabelled EE2 should result in 1 mol bound adduct per mol inacitvated CYP3A4. However, associating the loss of spectrally detectable P450 to a single, EE2 metabolic process can be complicated by the occurrence of non-selective protein binding by EE2. For example, it is possible that a reactive intermediate could be formed outside the active site of an enzyme before becoming covalently bound. The major product of human liver microsomal oxidation of EE2 is 2-hydroxy-17α-ethynylestradiol. It has been shown that the *o*-catechol formed by 2-hydroxylation of EE2 can be readily oxidized to the corresponding *o*-quinone in human liver microsomes, a product which is capable of binding irreversibly to microsomal proteins [Bolt et al., 1977]. Binding of the *o*-quinone can be reduced by the presence of ascorbate in the incubate [Purba et al., 1987] suggesting that at least some of the reactive intermediate is either generated outside the active site of the enzyme where it is formed or is formed by reactive oxygen intermediates in the medium. When Guengerich included 1 mM ascorbate in the EE2 incubation mixture, the loss of spectrally detectable P450 was the same as that observed without ascorbate. Based on this result he suggested that if inactivation was mediated by a quinone intermediate, loss of the P450

Soret should have been attenuated by the presence of ascorbate. It therefore is more likely that, as shown in animal models [White et al., 1977], catalytic processing of the acetylene group of EE2 results in the formation of a reactive intermediate which destroys the enzyme by binding to the prosthetic heme of CYP3A4 and results in a spectral loss of P450. Several acetylenic compounds have been shown to bind irreversibly to P450 prosthetic heme during catalytic processing of the acetylene group [Ortiz de Montellano, 1988]. If EE2, upon catalytic processing in microsomes, irreversibly binds to CYP3A4 via both the *o*-quinone and the oxidized acetylene group, then the quantitation of EE2 binding could result in >1 mol bound adduct per mol inactivated CYP3A4. Further studies are necessary to establish the stoichiometry of EE2 binding relative to CYP3A4 inactivation.

Gestodene

Inhibition of CYP3A4 by gestodene (Fig. 4.1) was characterized in detail [Guengerich, 1990]. Time-dependent inhibition was demonstrated by loss of spectrally detectable P450 and loss of nifedipine oxidase activity in human liver microsomes. A Kitz and Wilson plot of the inactivation rate data, generated by the loss of nifedipine oxidation, revealed a saturable inactivation process, K_I = 46 μM and k_{inact} = 0.39 min^{-1}. A partition ratio of 9 was estimated by dividing initial rate of substrate loss at 20 μM gestodene by the initial rate of the loss of nifedipine activity at the same concentration of gestodene. The inactivation process was dependent on cofactor (NADPH), and the loss of spectrally detectable P450 was

attenuated in the presence of other CYP3A4 substrates (quinidine and nifedipine). Inactivation by gestodene seemed to be limited to CYP3A4. CYP2D6, CYP1A2, CYP2E1, and CYP2C19 activities in microsomes were unaffected by gestodene treatment under conditions which reduced nifedipine oxidase activity by >90%. Therefore, the criteria of time-dependence, saturability, catalysis dependence, and substrate protection were explicitly demonstrated. No attempt was made to demonstrate that the inactivation process was limited to the active site by including reactive intermediate trapping reagents in the inactivation assay. In contrast, three attempts were made to characterize irreversible binding of radiolabelled gestodene to CYP3A4.

Initial experiments attempted to characterize the binding of ^{3}H-gestodene to CYP3A4 in human liver microsomes. First, after treating microsomes with ^{3}H-gestodene and NADPH, the protein was pelleted and washed several times in warm (70° C) ethanol. The proteins were then separated by electrophoresis and individual slices of the gel were monitored for radioactivity. Since no radioacitivity was observed in the gel segments, a second study was conducted. This time, after treating the microsomes with ^{3}H-gestodene and NADPH, CYP3A4 was isolated from the microsomes and purified to electrophoretic homogeneity. The radioactivity was measured and indicated 0.12 nmol of bound ^{3}H-gestodene adduct per nmol CYP3A4. When the purified protein was subjected to tryptic digestion and the peptides separated by HPLC, several peptides indicated measurable levels of radioactivity which cumulatively accounted for 0.01 nmol of bound adduct per nmol CYP3A4. The third

study was conducted with CYP3A4 that had been expressed in yeast, partially purified, and reconstituted. After the inactivation incubation assay, the work-up was extensive. First, the contents of the incubation were extensively dialyzed against buffer. Then, reductase was removed by ion-exchange chromatography. Finally, any remaining unbound ^{3}H-gestodene was removed by gel-filtration chromatography. Only 53% of the CYP3A4 was recovered and contained radioactivity which indicated only 0.06 nmol ^{3}H-gestodene per nmol CYP3A4.

In summary, although the results of Guengerich's study argue strongly for the hypothesis that gestodene is a mechanism-based inactivator of CYP3A4, experiments with radiolabelled gestodene consistently indicated sub-stoichiometric binding to the enzyme. These results, according to the author, suggest that the mechanism of CYP3A4 inactivation by gestodene involves gestodene binding to the prosthetic heme. As mentioned above, acetylenic steroids have been shown to bind to the prosthetic heme of P450 enzymes in animal models, but no search was made for such adducts in the case of gestodene.

The results presented in Chapter 3 argue strongly that midazolam is a mechanism-based inactivator of CYP3A4. If so, irreversible binding of radiolabelled midazolam should occur with a 1:1 stoichiometry with the level of inactivated CYP3A4. However, as suggested above for EE2, events that may not be related to inactivation can contribute to greater than stoichiometric levels of adduct formation. In contrast, as shown for gestodene, less than stoichiometric levels of adduct formation may be observed when quantitation of bound adducts is restricted to the

apoprotein portion of the enzyme. Our initial studies paralleled one of the methods used by Guengerich to determine whether labelled inactivator was binding to the enzyme. However, for quantitative determination of binding, we employed a strategy differing from Guengerich's in that it (a) excluded extensive work-up of the enzyme preparation, (b) utilized gentle conditions for the removal of excess radioactivity, and (c) monitored the extent of loss of enzyme activity. A simple work-up procedure utilizing mild conditions was employed in an attempt to avoid excising the prosthetic heme group from the enzyme active site during work-up. If the heme prosthetic group remains associated to the enzyme, then stoichiometric binding can be expected whether radiolabelled midazolam binds to either heme or apoprotein. The level of inactivation was measured by the remaining activity assay so that the expected level of binding was known, and the stoichiometry of amount bound per inactivated enzyme could be calculated.

Metabolite-Intermediate Complexes of CYP3A4

The third selective inhibitor of CYP3A4, troleandomycin (TAO), is N-dealkylated and oxidized to a nitroso metabolite which forms a ferrous-nitrene-like complex which exhibits a characteristic Soret band at 455 nm [Franklin, 1977; Pessayre et al., 1981; Wrighton et al., 1985]. Complex formation also prevents the binding of CO and therefore decreases the absorbance of dithionite-reduced microsomes at 450 nm [Franklin, 1977]. The activity and CO-binding capacity are restored upon oxidation of the iron to the ferric state by potassium ferricyanide, which destabilizes the

complex resulting in release of the metabolite [Franklin, 1977]. Cytochrome P450 3A enzymes seem to have a characteristic ability to N-dealkylate many secondary and tertiary amines which, following further oxidation, form the 455 nm-absorbing complex [Bensoussan et al., 1995]. Furthermore, CYP3A4, as well as other human cytochrome P450 enzymes, have been shown to form the 455 nm-absorbing complex upon treatment with N-hydroxy-didesmethylimipramine and NADPH [Bensoussan et al., 1995]. Therefore, complex formation does not seem to be limited to substrates undergoing N-dealkylation reactions as the initial oxidation step.

Midazolam does not contain a 1° or 2° amine funtionality and enzyme catalyzed N-oxidation of this compound has not been reported. However, it is possible that the ring-opened form of midazolam (Fig. 1.2, p 11), which does contain a 1° amino group, could be oxidized to a nitroso metabolite which forms an inhibitory complex with CYP3A4. If such a complex is formed as a result of N-oxidation of ring-opened midazolam, then midazolam inactivated microsomes should display the characteristic Soret band at 455 nm.

4.2. Materials and Methods

Materials

^{3}H-Midazolam (labelled at the C-3 position of the imidazole ring) was kindly provided by Dr. A. A. Liebman, Roche Laboratories (Nutley, NJ). Testosterone and 6ß-hydroxytestosterone (6ß-OHT) were purchased

from Steraloids (Wilton, NH) and testosterone was recrystalized 4 succesive times from acetone/H_2O. (R)-Warfarin and (S)-warfarin were gifts kindly provided by Dr. Kent Kunze (University of Washington). Chlorzoxazone was a gift kindly provided by Dr. Raimund Peter (University of Washington). Cell microsomes containing cDNA-expressed human cytochrome P450 3A4 and P450 reductase (M107r, lot 30) were purchased from Gentest Corporation (Woburn, MA). Human liver microsomes were prepared as described previously [Rettie et al., 1992] and the P450 concentrations were determined as described above (Ch. 3, p 51). The content of CYP3A4 in HL #124 was determined by western blot analysis as described above (pp 51-52). Potassium ferricyanide, sodium dithionite, 11α-hydroxyprogesterone (11α-OHP), NADPH (reduced form, tetrasodium salt), glucose-6-phosphate, glucose-6-phosphate dehydrogenase (EC 1.1.1.49, Type VII from Bakers Yeast), and catalase (EC 1.11.1.6, from Bovine Liver) were purchased from Sigma Chemical Co. (St. Louis, MO). Durapore hydrophobic membrane filters (polyvinylidene fluoride, 25 mm diameter, 45 μm pour size) were purchased from Millipore Corporation (Bedford, MA). EcoLume™ liquid scintillation cocktail was purchased from ICN Biomedicals (Costa Mesa, CA). To detect radioactivity in HPLC effluent, Flow-Scint™ II liquid scintillation cocktail was purchased from Packard Instruments Co. (Meriden, CT). HPLC solvents were purchased from Fischer Scientific (Fair Lawn, NJ). Methylene chloride and triethylamine was purchased from Aldrich Chemical Co. (Wilwaukee, WI), further purified by

distillation over P_2O_5, and stored over dessicant. All other reagents were of the highest purity commercially available.

Radioelectrophoretic Analysis

An ethanol:toluene solution containing 1.0 mCi ^{3}H-midazolam (26.9 Ci/mmol) was obtained from Hoffman-LaRoche, Inc. (Nutley, NJ). Before being used for radioelectrophoretic analysis, the specific radioactivity was diluted to approximately 0.5 Ci/mmol by adding 0.076 mg (233 nmol) of non-labelled midazolam to 330 µL of this solution. ^{3}H-midazolam (final concentration 100 µM) was incubated with HL #124 microsomes (final concentration 1 µM P450) with and without an NADPH-regenerating system (final concentrations of 13.7 mM glucose-6-phosphate, 2.8 IU/mL glucose-6-phosphate dehydrogenase, and 1 mM NADPH) for 45 minutes at 37° C in a total volume of 0.1 mL. First, 13.9 µL ^{3}H-midazolam/ethanol:toluene was individually aliquoted into two 1.5 mL conical polypropylene vials and the ethanol:toluene was removed by a stream of nitrogen. Second, a 90 µL aliquot containing 0.1 nmol P450, 100 mM potassium phosphate buffer, and 1 mM EDTA (pH 7.4) was added to each vial and gently mixed at 37° C for 5 min. Then, a 10 µL aliquot of the NADPH-regenerating system in potassium phosphate-EDTA buffer was added to start the reaction. Buffer alone was added to the control (no NADPH). The reaction was stopped after 45 min upon the addition of 1 mL ethanol. The precipitated protein was pelleted by centrifugation at 3000 rpm for 10 min and the supernatant was removed. The protein was then washed in this way, by vortexing with 1 mL warm (60° C) ethanol

and repelleting the protein, until only background radioactivity remained in the supernatant (after 6 cycles of washing and centrifugation). The samples were dried under a gentle stream of nitrogen before being prepared for gel electrophoresis.

The microsomal proteins were separated by sodium dodecyl sulfate-polyacrylamide gel electrophoresis (SDS-PAGE) using the method of Laemmli [Laemmli, 1970]. In short, the protein was solubilized in 20 μL Tris-HCl buffer (31.25 mM, pH 6.8) containing 2% SDS, 5% 2-mercaptoethanol, and 0.0025% bromophenol blue. Prior to electrophoresis, the samples were heated in a bath of boiling water for 3 min. Purified human CYP3A4 protein (60 μg, a gift kindly provided by Dr. Kenneth Thummel, University of Washington) was similarly prepared for electrophoresis and loaded into sample wells on each side of the wells containing the microsomal protein. The separating gel contained 9% acrylamide and was 1 mm thick and 12 cm long. After the electrophoretic run, the proteins were visualized by coomasie blue staining and the gel was fixed to Whatman filter paper. The gel was photographed before each lane was isolated by cutting with a scissors. Continual wetting with distilled water was necessary to keep the gel from curling away from the filter paper. Each lane was cut into 23 individual segments ~5 mm long (an attempt was made to include only one major protein-staining band per slice). Each section was transferred to a scintilation counting vial and solubilized in 0.5 mL of a 19:1 mixture (v/v) of 30% H_2O_2 and concentrated NH_4OH by heating 3 h at 60° C. Each solubilized gel segment was neutralized with 30 μL glacial acetic acid, and 14 mL scintillation cocktail

was added. Radioactivity was counted in a Packard Tri-Carb model 2000CA liquid scintilation counter (Packard Instruments Co., Downers Grove, IL).

Purification and radiochemical dilution of ^{3}H-MDZ

The radiochemical purity of the ^{3}H-midazolam solution obtained from Hoffman-LaRoche, Inc. was assesed by HPLC coupled to a radiochemical detector. A Hewlett Packard 1050 solvent delivery system was equipped with a 150 mm Hewlett Packard Spherisorb ODS-2, 4mm i.d., 5 µm pore size reverse-phase cartridge column and operated at 1.0 mL/min at 30° C. The column was equilibrated with 70/30 potassium phosphate buffer (10 mM, pH 7.4) /methanol:acetonitrile (1:1) and a linear sovent gradient developed to 30/70 over 25 min and returned to the equilibrium conditions over 10 min. Radioactivity was detected with a Radiomatic A-100 Flo-One®\Beta radioactive flow detector. UV absorbance was detected with a Hewlett Packard multiwavelength UV detector operating at 220 nm. A 50 µL aliquot of the sample was concentrated under a stream of nitrogen and solubilized in 50 uL of of the solvent system used to equilibrate the HPLC column. A 20 µL aliquot was injected into the HPLC system. The % radiochemical purity was calculated by comparing the amount of radioactivity (CPM) observed for ^{3}H-midazolam as a % of the total radioactivity detected during the run.

^{3}H-Midazolam was purified by column chromatography. A miniature column was prepared by placing a plug of silanized glass wool

in the end of a pasteur pipet and charging the pipet with a slurry of activated silica gel (60 Å, 200-300 mesh) in 96/3/1 (CH_2Cl_2/CH_3OH/$(CH_3CH_2)_3N$) to a length of ~5 cm. A 0.7 mL aliquot of the ^{3}H-MDZ solution was dried under a stream of nitrogen, solubilized in 0.1 mL 96/3/1 (CH_2Cl_2/CH_3OH/$(CH_3CH_2)_3N$), and applied to the top of the column. The column was eluted under gravity with 5 mL 96/3/1 (CH_2Cl_2/CH_3OH/$(CH_3CH_2)_3N$) and ~200 µL fractions were collected. The fractions were analyzed by thin-layer chromatography (TLC) and fraction #5 indicated a faint spot under UV irradiation of the TLC plate. This fraction was dried under a stream of nitrogen, and transferred to a 1 mL reactivial with 4 × 50 µL aliquots of methanol. A 5 µL aliquot was injected into the HPLC system and radiochemical purity was assesed as above.

The methanolic solution of purified ^{3}H-midazolam was concentrated under a stream of nitrogen, 0.744 mg non-labelled MDZ was added, and the contents were dissolved in 231.4 mg (231.4 µL) H_2O to give a 9.87 mM solution of ^{3}H-MDZ. A 5 µL aliquot was counted in 14 mL of scintilation cocktail and found to contain 1.685 µCi radioactivity giving a specific activity of 0.03415 Ci/mmol. This sample, at > 98% radiochemical purity, was used in all of the studies utilizing radioactivity described below and is referred to as "^{3}H-MDZ".

Stoichiometry of inactivated CYP3A4 to irreversibly bound ^{3}H-MDZ

Incubations: ^{3}H-MDZ (final concentration 100 µM) was incubated in triplicate with HL #124 microsomes (final concentration 0.5 µM P450) with and without an NADPH-regenerating system (final concentrations of

13.7 mM glucose-6-phosphate, 2.8 IU/mL glucose-6-phosphate dehydrogenase, and 1 mM NADPH) at 37° C for 40 min in a total volume of 0.5 mL. First, the microsomes were diluted into ice cold 100 mM potassium phosphate buffer (pH 7.4) containing 1 mM EDTA and 445 µL (0.25 nmol P450) aliquots were dispensed into 6, 16 × 125 mm culture tubes. Then, 5 µL (50 nmol) ^{3}H-MDZ was added to each tube and the samples were allowed to equilibrate at 37° C for 3 min. During equilibration, 50 µL potassium phosphate, EDTA buffer was added to three of the sample tubes (minus NADPH controls). To the other three sample tubes a 50 µL aliquot of the NADPH-regenerating system in potassium phosphate-EDTA buffer was added to start the reaction. After 40 min, duplicate 20 µL transfers of each of the 6 incubation mixtures were aliquotted into secondary incubation tubes containing 400 µM testosterone and 1 mM NADPH in potassium phosphate, EDTA buffer at 37° C to give a total volume of 1 mL. The testosterone activities were determined as described in Ch. 3 (pp 54-56). Then, ~3 mL ice cold methanol was added to the remaining 0.46 mL in each sample tube and the microsomal proteins were allowed to precipitate at 0° C for 2 h.

For the determination of inactivation and binding in cell microsomes containing expressed CYP3A4, incubations were conducted essentially as described for HL #124 with the following changes. The P450 concentration (0.6 µM P450) was based on the manufacturer's stated concentration. The total volume was 0.3 mL, and the volumes of the individual components of the incubations were adjusted accordingly.

Work-up: Work-up of the radiolabelled protein essentially followed the method of Lillibridge et al. [Lillibridge et al., 1996]. The precipitated proteins were vortexed and poured onto a filtration manifold equipped with hydrophobic filters (25 mm diameter, 45 μm pour size). The filtrate was aspirated and 5 mL methanol was placed on each filter and allowed to stand for 2 min before being re-aspirated. The proteins were washed in this way until 10 × 5 mL methanol washes were completed. The filters were then removed from the manifold and the protein was solubilized by soaking the filters in 1.2 mL 1.0 N NaOH for 24 h. The samples were vortexed and 0.8 mL of the solubilized protein was aliquoted into 0.895 mL 1.0 N HCl and radioactivity was counted in 14 mL scintillation cocktail.

UV/VIS Analysis: Time Study

Incubations: The CO-binding characteristics of midazolam-treated microsomes were measured after incubating 0 and 200 μM midazolam (MDZ) with HL #124 microsomes (0.5 μM P450), an NADPH-regenerating system (final concentrations of 13.7 mM glucose-6-phosphate, 2.8 IU/mL glucose-6-phosphate dehydrogenase, and 1 mM NADPH), and 200 units/mL catalase at 37° C for 0, 3, 10, and 30 min in a total volume of 5 mL. First, the microsomes were diluted into ice cold 100 mM potassium phosphate buffer (pH 7.4) containing 1 mM EDTA and 250 units/mL catalase. Then, 4.0 mL aliquots (2.5 nmol P450, 1000 units catalase) were dispensed into 2, 20 mL scintilation vials. Next, 0.5 mL of the NADPH-regenerating system in potassium phosphate-EDTA buffer was added to

each vial and the samples were allowed to equilibrate at 37° C for 3 min. During equilibration, 0.5 mL distilled H_2O was added to one of the vials (minus MDZ control). To the other vial a 0.5 mL aliquot (1 µmol) of MDZ/H_2O was added to start the reaction. The samples were vortexed and a portion of each reaction mixture was immediately quenched by transferring 1 mL of each incubation into an equal volume of ice cold, 100 mM potassium phosphate buffer (pH 7.4) containing 1 mM EDTA, 40% (v/v) glycerol, and 1% (v/v) emulgen 911. The quenched samples represented the 0 min incubations. Identical transfers were made at 3, 10, and 30 min and the quenched samples were held on ice until P450 measurements were made.

P450 Measurements: The P450 spectra were acquired on a dual beam UV-Visible spectrophotometer (Cary 3-E) by the method of Omura and Sato [Omura et al, 1962]. Briefly, the quenched HL #124 samples were reduced with a small amount of sodium dithionite, vortexed, equally divided between a reference and a sample cuvette, and a baseline spectrum was recorded from 390 to 500 nm. Carbon monoxide was gently bubbled into the sample cuvette for approximately 45 seconds, and the P450 spectrum was acquired. Each spectrum was normalized to 0 absorbance at 490 nm, and electronically stored so that the spectra could be superimposed on the same chart.

UV/VIS Analysis: Difference Spectrum

Incubations: A study was conducted in HL #135 microsomes that was parallel to the time-study experiment in HL #124 microsomes. Only

slight modifications were made beyond the fact that different liver tissue was used: the total volume was 2.5 mL and the reactions were quenched after 0 and 30 min.

P450 Measurements: For HL #135 microsomes, the P450 spectra of both 0 min samples (+MDZ and -MDZ) and the one 30 min sample which did not contain MDZ were acquired essentially as described above for HL #124 microsomes. Precautions were taken to ensure each sample was spectroscopically identical (aside from the differences due to enzyme content) by pre-weighing 2 mg portions of sodium dithionite for reducing each of the samples.

In addition to these experiments, the measurements outlined below were made to ascertain whether MDZ metabolism induced the formation of a reduced cytochrome P450-metabolic intermediate complex which absorbs at ~455 nm [Franklin, 1991]. Before measuring the CO-bound spectrum of the microsomes that had been inactivated 30 min with MDZ + NADPH, a spectrum of the sample was acquired with oxidized P450 as the reference. Control microsomes, which had been diluted, but not incubated with MDZ nor NADPH, were added to an equal volume of ice cold, 100 mM potassium phosphate buffer (pH 7.4) containing 1 mM EDTA, 40% (v/v) glycerol, and 1% (v/v) emulgen 911. The sample was equally divided between reference and sample cuvettes and a baseline spectrum of the oxidized P450 was recorded from 390 to 500 nm. The sample cuvette was emptied, rinsed and recharged with HL #135 microsomes which had been incubated in the presence of midazolam and NADPH for 30 min and quenched as described above. A spectrum was

then acquired. The contents of the sample cuvette were then recombined with the remaining 30 min-inactivated sample, reduced with 2 mg sodium dithionite, equally divided between the reference and sample cuvettes, and the baseline was recorded. A P450 spectrum was obtained as described above. Then, 5 μL of a 15 mM solution of potassium ferricyanide (final concentration 50 μM) was added to the sample cuvette and P450 spectra were acquired over the next 15 min. Each spectrum was normalized to 0 absorbance at 490 nm, and electronically stored so that a difference spectrum could be obtained .

Isoform-Selective Assays for CYP1A2, CYP2E1, and CYP2C9

All preincubations conducted to determine the selectivity of MDZ for CYP3A4 inactivation were performed under identical conditions. The primary incubations contained 0 and 160 μM MDZ, 2.5 μM cytochrome P450, and 1 mM NADPH in a total volume of 1 mL 100 mM potassium phosphate buffer containing 1 mM EDTA and were incubated at 37° C for 20 min. At the end of the 20 min primary incubation, the contents were diluted into differing secondary incubations. For the determination of remaining CYP3A4 activity, 20 μL of the primary incubations were diluted (1:50) into secondary incubation tubes and assayed for testosterone 6ß-hydroxylation as described above (Ch. 3, pp 54-56). For the determination of remaining CYP1A2 activity, 100 μL of the primary incubations were diluted (1:10) into secondary incubation tubes containing 1.5 mM (R)-warfarin and 1 mM NADPH and analyzed for (R)-warfarin 6-hydroxylation. For the determination of remaining CYP2C9 activity, 100

μL of the primary incubations were diluted (1:10) into secondary incubation tubes containing 100 μM (S)-warfarin and 1 mM NADPH and analyzed for (S)-warfarin 7-hydroxylation. (R)-warfarin hydroxylation and (S)-warfarin hydroxylation were measured as described previously by Rettie, et al. [Rettie et al., 1989]. For the determination of remaining CYP2E1 activity, 20 μL of the primary incubations were diluted (1:50) into secondary incubation tubes containing 500 μM chlorzoxazone and 1 mM NADPH and analyzed for chlorzoxazone 6-hydroxylation. Chlorzoxazone hydroxylation was measured by the method of Peter et. al. [Peter et al., 1990].

4.4. Results

Selective Binding of ^{3}H-Midazolam to P450

To determine whether midazolam was binding to microsomal protein, HL #124 microsomes were treated with radioactive MDZ with and without NADPH, and the excess radioactivity was removed. Then the proteins were separated by gel electrophoresis under denaturing conditions, and analyzed for radioactivity. Treating microsomes with ^{3}H-midazolam in the presence of NADPH resulted in only one segment of the separating gel containing a level of radioactivity significantly higher than background levels. This segment contained a protein band and 550 DPM (0.5 pmol) ^{3}H-midazolam which co-migrated with a purified sample of CYP3A4 (Fig. 4.2). Only background radioactivity was observed in the isolated gel segments that contained microsomal protein that had been

treated with ^{3}H-midazolam in the absence of NADPH. The +NADPH microsomes also contained a slightly higher than background level of radioactivity in the segment at the leading edge of the gel, which contained the dye front.

Purification of ^{3}H-MDZ

The radiochemical purity of the ^{3}H-midazolam sample provided by Hoffman-LaRoche Inc. was measured by HPLC coupled with a radioactive flow detector. The sample was injected into the HPLC as described above, and six peaks in the radioactivity chromatogram were observed. The predominant peak (87.2% of total from the six peaks) had a retention time of 18.2 minutes, identical to that of a non-labelled MDZ standard detected by UV absorbance. The sample was then purified by column chromatography and analyzed under identical conditions. The radioactivity chromatogram of the purified sample gave only three peaks. The predominant peak had a retention time of 18.2 minutes and represented 98.3% of the total integrated area of the three peaks. The radioactivity of the purified material was diluted with non-labelled midazolam and a 9.87 μM (0.034 Ci/mmol) stock solution was prepared in distilled H_2O and used in the determination of binding stoichiometry.

The Stoichiometry of Binding

Experiments were conducted to compare the level of irreversibly bound ^{3}H-MDZ to inactivated CYP3A4 following 40 minute incubations of ^{3}H-MDZ (100 μM) and P450 with and without NADPH. The results are

summarized in Table 4.1. For HL #124, 85.1 ± 2.5 % of the testosterone 6ß-hydroxylase activity was abolished. The portion of the incubation mixture that was filtered and washed contained 103.5 pmol total CYP3A4 (based on the immunochemically determined content of CYP3A4, 45%, relative to the spectral content of total P450 in HL #124 microsomes). Because 85% inactivation was observed, the level of inactivated enzyme in the washed sample was 88.1 ± 2.5 pmol CYP3A4. The level of NADPH-dependent binding measured in this sample was 104.1 ± 15.0 pmol ^{3}H-MDZ. For the cell microsomes containing expressed CYP3A4, 84.5 ± 1.2 % of the testosterone 6ß-hydroxylase activity was abolished. The portion of the expressed CYP3A4 incubation mixture that was filtered and washed contained 154.6 pmol total CYP3A4 (based on the manufacturer's reported content of CYP3A4). Because 85% inactivation was observed, the level of inactivated enzyme in the washed sample was 130.2 ± 1.6 pmol CYP3A4. The level of NADPH-dependent binding measured in this sample was 139.9 ± 1.3 pmol ^{3}H-MDZ. The results of the HL #124 and expressed CYP3A4 experiments can be directly compared by calculating the % pmol CYP3A4 inactivated and % pmol ^{3}H-MDZ bound relative to the total CYP3A4 for each experiment (Figure 4.3). There is no statistically significant difference between the % inactivated and % ^{3}H-MDZ binding for either HL #124 or expressed CYP3A4 (paired-sample t test, $n = 3$, $p < 0.01$).

UV Characteristics of CYP3A4 Inactivation

Time-dependent loss of CO-binding capacity was observed in HL #124 microsomes that were incubated with midazolam (200 μM) and NADPH and measured at various times from 0 to 30 minutes (Figure 4.4). No loss of the P450 Soret was observed in control experiments in which microsomes were exposed to only NADPH for various times from 0 to 30 minutes. The loss of P450 spectral content was further characterized in HL #124 by measuring the difference spectrum between the 0 and 30 minute samples, but the spectrum was complicated by differential contribution of the sodium dithionite to the two spectra. This difficulty was overcome when equivalent amounts of sodium dithionite were weighed and used to reduce the samples for P450 spectra from HL #135 microsomes that had been similarly treated with midazolam (200 μM) and NADPH for 0 and 30 minutes. When the difference spectrum was measured (30 minute minus 0 minute) a negative peak was observed at 448 nm and a positive peak was observed at 415 nm (Figure 4.5).

When HL #135 microsomes treated with midazolam and NADPH for 30 minutes were spectroscopically characterized relative to oxidized, control microsomes (reference), an absorbance maximum was observed at 390 nm. After obtaining the P450 spectrum of this sample, potassium ferricyanide was added (final concentration 50 μM) and the absorbance level at 450 nm remained unchanged as spectra were acquired over the next 15 minutes.

Selectivity of Midazolam Inactivation

Selectivity of midazolam inactivation for CYP3A4 was tested in HL #124 microsomes by determining the effect of midazolam primary incubations on P450 activities other than CYP3A4. Testosterone 6ß-hydroxylation (CYP3A4) was inhibited 85%, relative to control activities (0 μM midazolam), after a 20 minute primary incubation in the presence of NADPH and midazolam (160 μM, Figure 4.6). Under identical conditions, chlorzoxazone 6-hydroxylation (CYP2E1) [Peter et al., 1990] and (S)-warfarin 7-hydroxylation (CYP2C9) [Rettie et al., 1992] activities were unaffected. (R)-Warfarin 6-hydroxylation (CYP1A2 and CYP3A4) [Rettie et al., 1992] activity was inhibited 30%, relative to control, under the same conditions.

4.5. Discussion

Selective Binding of ^{3}H-Midazolam to P450

Gel electrophoresis separation of HL #124 microsomal protein treated with radiolabelled midazolam and NADPH provided evidence that the drug is irreversibly bound to CYP3A4 during metabolic turnover. The experimental procedure paralleled that used by Guengerich in the characterization of ^{3}H-gestodene binding [Guengerich, 1990]. In contrast to the results with ^{3}H-gestodene, ^{3}H-midazolam-inactivated microsomes contained significant levels of radioactivity in a single protein band, which co-migrated with a purified standard of CYP3A4 (Fig. 4.2). Although efforts were made to include only one protein band per gel slice,

radioactivity could have been associated with other proteins of similar mass, ie. other isoforms of P450, that co-migrated with the CYP3A4 and therefore these results by themselves do not establish selective, irreversible binding to CYP3A4. These observations are consistent with the results presented in Chapter 3 which argue against the build-up of a reactive intermediate of midazolam that escapes the active site of CYP3A4 before inactivation occurs. If the build-up of a reactive intermediate outside the active site was significant, then non-selective binding of radiolabel to proteins other than P450 would have been observed in the radioelectrophoretogram. The radioactivity observed in the dye front of the gel can be attributed to free (non-protein bound) ^{3}H-midazolam. It is likely that either the excess ^{3}H-midazolam was not completely washed away during work-up or the covalent bond linking midazolam to the protein was labile under the denaturing conditions of the protein sample preparation, and midazolam was released. The amount of radioactivity observed corresponds to 0.01 nmol bound adduct per nmol CYP3A4, therefore, mild conditions were employed for the determination of binding stoichiometry.

The Stoichiometry of Binding

The results presented (Table 4.1, Fig. 4.3) support the conclusion that midazolam is a mechanism-based inactivator of CYP3A4. The level of binding and level of inactivated CYP3A4 were identical within experimental error for both preparations of CYP3A4, ie. both the immunochemically quantitated CYP3A4 in human liver microsomes and

the cDNA-expressed CYP3A4 in lymphoblastoid cell microsomes. These results address both of the remaining criteria for mechanism-based inactivation: irreversibility and 1:1 stoichiometric binding of inactivator to inactivated enzyme. However, the criterion of irreversibility is only partially fulfilled. It is conceivable, under the mild conditions used to filter and wash the samples, that the radioactivity characterized in the protein samples was tightly bound to the active site of CYP3A4 rather than covalently bound to the prosthetic heme or apoprotein of the enzyme. The most likely possibility for this type of tight-binding inhibition involves the formation of a characteristic Soret band at 455 nm. Therefore the UV/VIS characteristics of midazolam inactivated CYP3A4 were measured.

UV/VIS Characteristics of CYP3A4 Inactivation by Midazolam

The UV/VIS characteristics of the inactivation of CYP3A4 by midazolam support the conclusion that midazolam is acting irreversibly at the active site of the enzyme. The CO-binding capacity of microsomal P450 was diminished in a time-dependent manner upon treatment with midazolam and NADPH (Fig. 4.4). Therefore, the active site of the enzyme was altered in a way that prevents the low energy, π - π^* electron transitions observed for the characteristic ferrous, CO-bound heme of cytochrome P450 enzymes which result in a Soret band at 450 nm. One possibility is that the heme-iron atom becomes tightly bound to a metabolic intermediate of midazolam. However, no Soret band at 455 nm, characteristic of an N-oxidized metabolic-intermediate complex, was observed when midazolam +NADPH treated microsomes were analyzed

relative to oxidized microsomal P450. Instead, a typical Type I binding spectrum, a blue-shift resulting from the low spin to high spin transition of the iron, was observed, as reported previously [Fabre et al., 1988]. Additionally, when potassium ferricyanide was added to the reduced, CO-bound microsomes, no increase in the levels of absorption at 450 nm was observed. Therefore, no tight-binding inhibitory metabolic-intermediate complex, typical of the N-oxidation of CYP3A substrates (ie. TAO), had been formed. Instead, a species which displays an absorbance maximum at 415 nm was produced upon treating the microsomes with midazolam and NADPH for 30 minutes (Fig. 4.5).

Selectivity of Midazolam Inactivation

Inactivation of human liver microsomal P450 by midazolam appears to be selective for CYP3A4. CYP2E1 and CYP2C9 activities were unaffected by midazolam treatment which inactivated 85% of the CYP3A4 activity under identical conditions (Fig. 4.6). The 6-hydroxylation of (R)-warfarin was inhibited 30% and has been attributed to both CYP1A2 and CYP3A4 [Rettie et al., 1992]. Therefore, if the contribution of CYP3A4 to (R)-warfarin 6-hydroxylation is as high as 30% at 1.5 mM (R)-warfarin, then no effect by midazolam on CYP1A2 activity has been observed. However, another selective substrate for CYP1A2 activity should be utilized in similar experiments to demonstrate that there is no effect on CYP1A2 activity by midazolam turnover. Furthermore, activities that are selective for other human P450 drug-metabolizing isoforms, such as

CYP2D6 and CYP2C19, should be tested. The data collected thus far suggest that midazolam selectively inactivates CYP3A4.

In summary, the results presented in Chapters 3 and 4 argue strongly that midazolam is a mechanism-based inactivator of CYP3A4. This conclusion is based on the fulfillment of all seven criteria for mechanism-based inactivation. Midazolam is, therefore, the most completely characterized mechanism-based inactivator of CYP3A4 to date. The impact of enzyme inactivation on *in vitro* midazolam metabolism studies is addressed in Chapter 6.

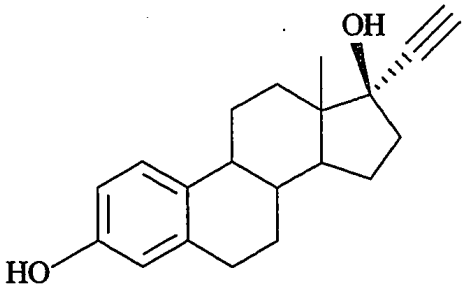

17 α-ethynylestradiol

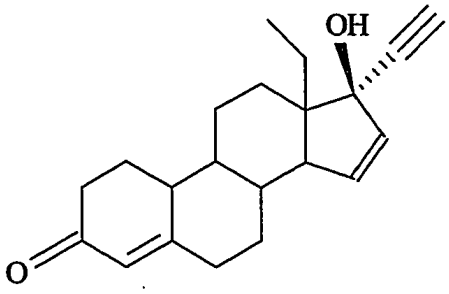

gestodene

Figure 4.1. Structures of suggested mechanism-based inactivators of CYP3A4.

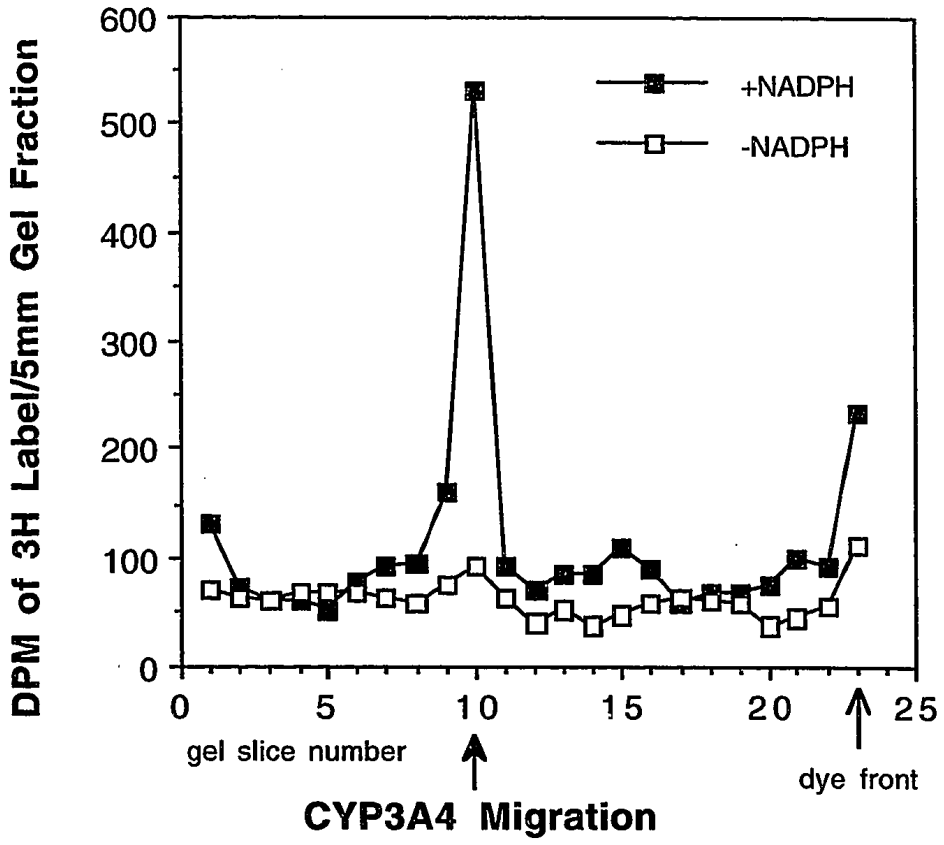

Figure 4.2. SDS-PAGE radioelectrophoretogram of HL #124 microsomal proteins that had been incubated with ^{3}H-MDZ in the presence and absence of NADPH.

Table 4.1. Stoichiometry of inactivated CYP3A4 to ^{3}H-midazolam binding.

Microsomes	% Inactivated	Inactivated CYP3A4 (pmol)	Irreversible Binding (pmol ^{3}H-MDZ)		
			+NADPH	-NADPH	Δ
HL #124	85.1 ± 2.5	88.1 ± 2.5	141.4 ± 9.7	37.2 ± 5.3	104.1 ± 15.0
CYP3A4	84.5 ± 1.2	130.2 ± 1.6	186.4 ± 2.3	46.5 ± 2.2	139.9 ± 1.3

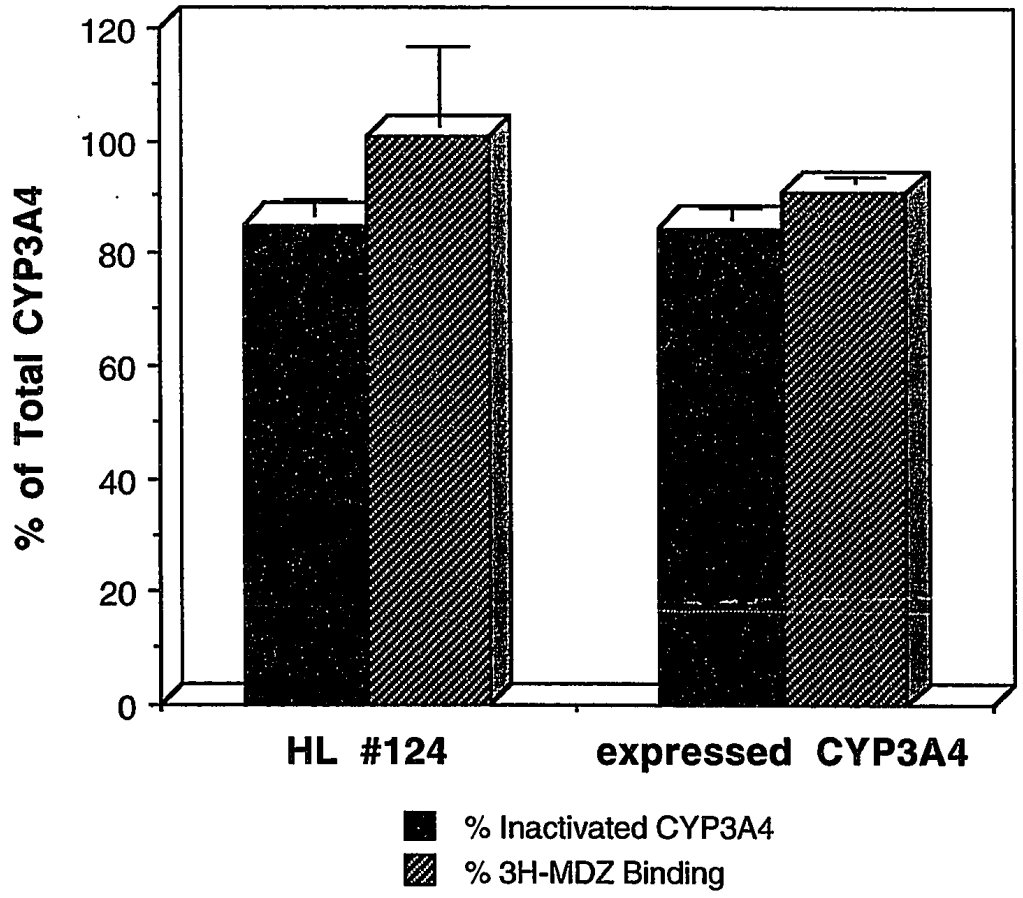

Figure 4.3. Stoichiometry of ^{3}H-MDZ binding to inactivated CYP3A4 as a percent of the total CYP3A4 in the incubations of HL #124 microsomes and commercially available lymphoblastoid cell microsomes.

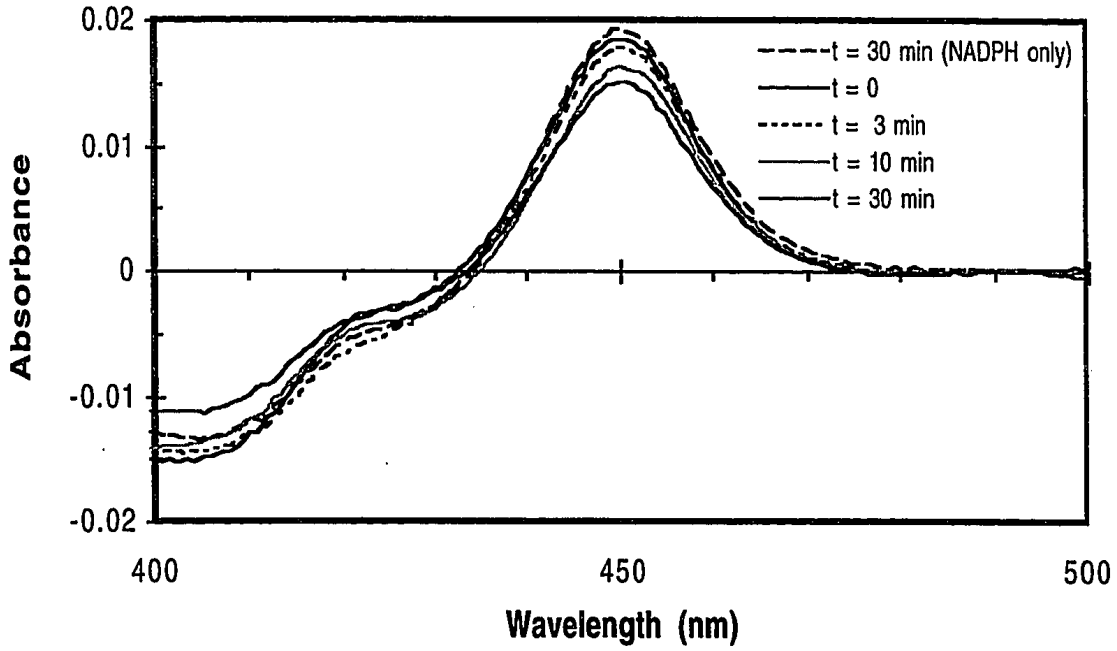

Figure 4.4. Time-dependent loss of HL #124 microsomal P450 spectral content.

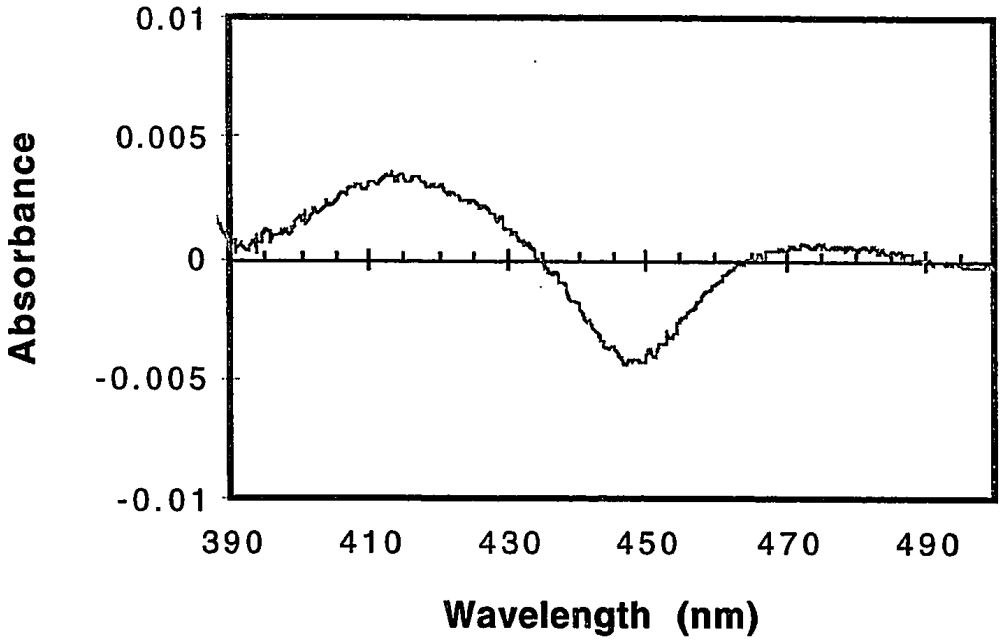

Figure 4.5. Difference spectrum of HL #135 microsomes treated with 200 μM midazolam for 30 minutes minus 0 minutes.

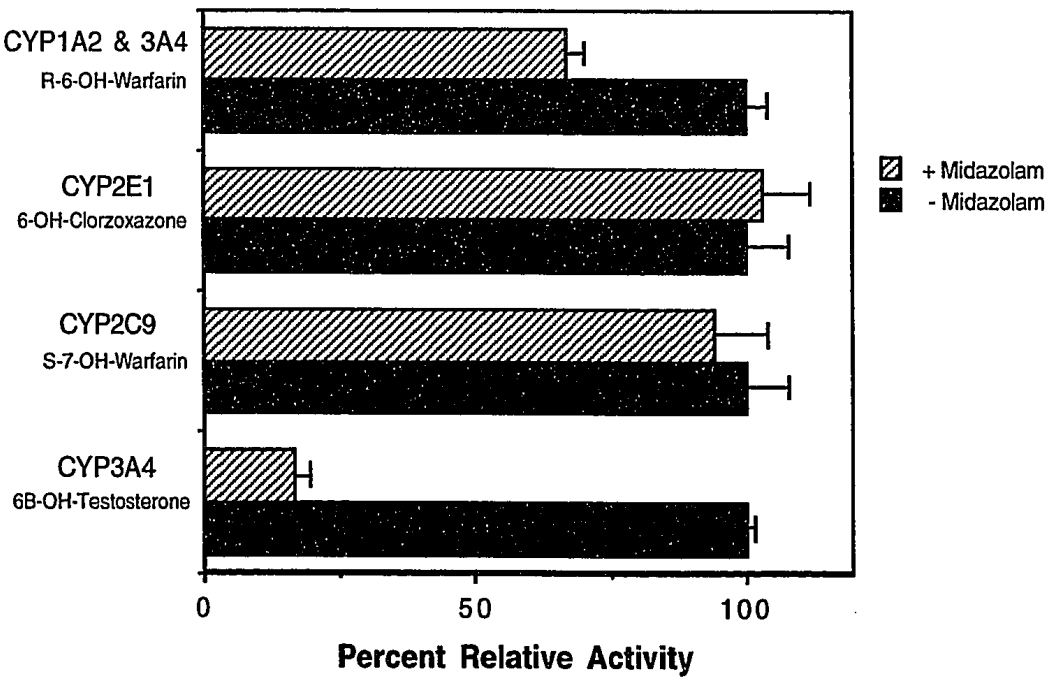

Figure 4.6. Selectivity of midazolam for inactivation of human P450s.

CHAPTER FIVE

THE USE OF MIDAZOLAM AS AN *IN VITRO* PROBE OF CYP3A4: PREDICTING *IN VIVO* METABOLISM

5.1. Introduction

One of the long-term goals of the research presented in this dissertation was to clearly define the *in vitro* metabolism of midazolam in order to test the hypothesis that a reasonable prediction of its *in vivo* metabolism can be obtained from knowledge of its *in vitro* metabolism. One of the primary assumptions of the hypothesis is that the behavior of an enzyme in metabolizing midazolam *in vivo* is identical to its behavior *in vitro*. If true, the *in vivo* and *in vitro* environments can be linked by the enzyme(s) in the two systems. The quantitative parameter that defines the the formation of of a metabolite *in vitro* is the ratio V_{max}/K_m, while the corresponding constant *in vivo* is the intrinsic formation clearance [Gillette, 1971; Winkler et al., 1973]. If each of these parameters can be shown to depend upon enzyme concentration, then the possibility exists of predicting an *in vivo* intrinsic formation clearance by measuring V_{max}/K_m *in vitro*. Substrate concentration is the critical element, as presented in Chapter 2 (Section 2.1), in determining a V_{max}/K_m that is intended to be a predictor of intrinsic formation clearance. Since different enzymes might be the major contributors to the formation of the same midazolam metabolite at different concentrations, it is imperative that the two systems (*in vivo* and *in vitro*) be compared under conditions as similar as possible. If the *in vitro*

system is to reflect *in vivo* metabolism, then midazolam concentrations used *in vitro* should correspond to those found *in vivo* (50 to 100 ng/mL or ~0.15 to 0.3 μM) [Allonen et al., 1981]. Theoretically, accurate measurement of K_m and V_{max} *in vitro* requires the observation of steady-state kinetics which can be approximated experimentally when < 5% of the substrate is consumed and changes in the product concentrations are linear with time. The metabolite assay sensitivity must therefore be ≤ 5 ng/mL to ensure < 5% consumption of this drug at low, *in vivo*-like substrate concentrations in human liver microsomes. Additionally, because changes in the midazolam product concentrations were found to be linear with time for only 4 minutes (Ch. 3, Figs. 3.1 - 3.3), the product formation rates must be measured at time periods that do not exceed 4 minutes. Therefore, a sufficiently sensitive assay for the metabolites was developed (Ch. 2) for the quantitation of the metabolites from 4 minute incubations at 0.2 μM midazolam.

The experiments described in this chapter were conducted primarily for the purpose of establishing that the intrinsic clearance (V_{max}/K_m) of midazolam to 1′-hydroxymidazolam (1′-OH MDZ) in human liver microsomal preparations is determined by the content of CYP3A4 in the same human liver microsomal preparations. The studies were conducted in a population of liver transplant donors and recipients. The liver biopsy samples (referred to as: D-1, D-2, ... etc.) were obtained from fifteen organ donors during liver procurement surgery. This provided a unique opportunity to test hypotheses regarding both the *in vitro* and *in vivo* metabolism of midazolam in an identical population. The initial

determination of the one to one correspondence between 1′-OH MDZ formation and CYP3A4 content in human liver biopsy samples is explicitly described. Once the correspondence between *in vitro* midazolam metabolism and CYP3A4 content had been established in this population, an attempt at corresponding *in vivo* midazolam metabolism to CYP3A4 was made. The *in vivo* data, generated by our collaborators, is referenced in the discussion (Section 5.4).

5.2. Materials and Methods

Materials

Midazolam, 1′-hydroxymidazolam (1′-OH MDZ), 4-hydroxymidazolam (4-OH MDZ), and the deuterated internal standard, 1′-$^{2}H_{2}$-1′-hydroxy-midazolam (D_{2}-1′-OH MDZ) were gifts kindly provided by Drs. William Garland and Bruce Mico, Roche Laboratories (Nutley, NJ). N-methyl-N-*tert*-butyl-dimethylsilyltrifluoroacetamide (MTBSTFA) was purchased from Pierce Chemical (Rockford, IL), NADPH (reduced form, tetrasodium salt) from Sigma Chemical Co. (St. Louis, MO), and ethyl acetate and acetonitrile from Fischer Scientific (Fair Lawn, NJ).

Midazolam Metabolism by Human Hepatic Biopsy Tissue

Biopsy Tissue: Liver biopsy samples (referred to as: D-1, D-2, ...) were obtained from fifteen organ donors during liver procurement surgery [Thummel et al., 1994]. The tissue samples were immediately placed on dry ice and held under these conditions for 1-12 hours while

being transported to our laboratory. Liver tissue was thawed, weighed and homogenized by brief sonication in 100 µL of buffer (50 mM KPi, pH 7.4, 0.25 M sucrose, 0.1 mM phenylmethylsulfonyl fluoride). After centrifugation at 13,000 × g for 10 minutes, at 4°C, the supernatant was removed and stored in air-tight vials at -70°C. The concentration of protein and content of CYP3A4 in the S-13,000 × g fraction were determined as previously described [Thummel et. al., 1991]. The catalytic activity of the 13,000 × g fractions was stable for at least 6 months under these conditions.

Two-Point Estimates of K_m and V_{max}: S-13,000 × g supernatants from the liver biopsy samples were incubated in duplicate with midazolam at 0.2 and 4 µM. The subcellular fraction was thawed and suspended in cold potassium phosphate buffer (0.1 M, pH 7.4) to achieve a final CYP3A4 concentration of 250 fmol/mL. The total reaction volume was 1 mL. Incubation mixtures were gently agitated with midazolam in a Dubnoff metabolic shaking incubator at 37°C for 3 min. The reaction was started with the addition of NADPH (1 mM final concentration) and terminated after 4 min by the addition of 1 mL of 100 mM Na_2CO_3 (final pH 11). The basified incubation samples were spiked with 20 ng of D_2-1′-OH MDZ and extracted, derivatized and analyzed as described above (Ch. 2, Section 2.2). Estimates of K_m and V_{max} parameters were calculated for each liver biopsy sample from an Eadie-Hofstee analysis of the product formation rates for a single-enzyme system as shown below:

$$K_m = \frac{v_2 - v_1}{\left(v_1/c_1 - v_2/c_2\right)}$$

and

$$V_{max} = \frac{v_2(K_m + c_2)}{c_2}$$

where v_1 is the observed velocity (nmol product/min/mg protein) at 0.2 μM midazolam (c_1), and v_2 is the observed velocity at 4 μM midazolam (c_2).

5.3. Results

The kinetic parameters for midazolam 1′-hydroxylation were estimated by rate data generated at two midazolam concentrations (0.2 and 4 μM) for each of fifteen hepatic biopsy samples from a population of organ donors (Table 5.1). The intrinsic clearance values, V_{max}/K_m, and the contents of CYP3A4 in the biopsy samples also appear in Table 5.1. When the V_{max}/K_m values were compared to the contents of CYP3A4 in this population of organ donor tissue, simple linear regression analysis revealed a statistically significant linear relationship ($r^2 = 0.65$, n = 15, $P < 0.001$, Fig. 5.2).

5.5. Discussion

If CYP3A4 activity is responsible for the transformation of midazolam to 1′-OH MDZ in hepatic micrsomes, then the intrinsic clearance values for 1′-OH MDZ formation, V_{max}/K_m, in a population of

human liver biopsy samples should be determined by the content of CYP3A4 in the samples. K_m and V_{max} for 1′-OH MDZ formation were estimated in microsomal hepatic biopsy tissue (S-13,000 × g supernates) obtained from a population of organ donors from rates of formation at two concentrations of midazolam (Table 5.1). More concentrations were not included because most of the biopsy samples did not contain enough protein to allow more than duplicate rate determinations at 2 concentrations. The amounts of 4-OH MDZ produced at the low concentration, 0.2 μM midazolam, were below the limit of quantitation of the assay (Chapter 2), and therefore the kinetic parameters for midazolam 4-hydroxylation were not estimated from this data. When the V_{max}/K_m values were compared to the contents of CYP3A4, only 65% of the varability in intrinsic clearance of midazolam to 1′-OH MDZ could be explained by variablility in the content of CYP3A4 (Fig. 5.2). However, two physiological characteristics of this population of biopsy samples could contribute to the disparity between the content of CYP3A4 and the intrinsic clearance values.

First, the disparity could be due to differences in the induction state of the biopsy samples. The V_{max}/K_m and CYP3A4 content values for five of the samples are obviously far removed from the other ten samples (Fig. 5.2). These five data points correspond to biopsy samples that were obtained from donors that had been exposed to known inducers of CYP3A4 (Table 5.1) [Thummel et al., 1994]. One of the donors, D-5, had been chronically exposed to phenytoin (3 years), while the other four had been exposed to phenytoin, pentobarbital, or phenytoin and

dexamethasone for only three or four days [Thummel et al., 1994]. It is feasible that the induced samples contain varying levels of catalytically active CYP3A4 relative to immunodetectable CYP3A4 apoprotein, depending upon the inducer, the mechanism of induction, and time of exposure. When the five induced samples are removed from the linear regression analysis, the coefficient of determination increases ($r^2 = 0.82$, n = 10).

Second, the disparity between the content of CYP3A4 and the intrinsic clearance values could also be due to contribution of CYP3A5 to the V_{max}/K_m values. The contribution of CYP3A5 to midazolam metabolism has been shown to attenuate the correlation analyses between CYP3A4 content and midazolam turnover [Kronbach et al., 1989; Gorski et al., 1994]. Four of the fifteen biopsy samples used in these studies were shown to express CYP3A5 (Table 5.1) [Thummel et al., 1994]. When the samples containing CYP3A5 are removed from the regression analysis of the ten non-induced samples, the coefficient of determination increases again ($r^2 = 0.97$, n = 6). Therefore, the induction state of the samples and the contribution of CYP3A5 appear to have an attenuating effect on the ability of the content of CYP3A4 to determine the intrinsic clearance of midazolam to 1′-OH MDZ within this population of organ donor samples. However, for these results to be considered statistically significant, similar studies should be conducted in a larger population of human liver microsomal samples.

Therefore, it appears that midazolam can be a useful *in vitro* probe of CYP3A4 activity despite the fact that it is a mechanism-based

inactivator of CYP3A4. However, the functional enzyme concentration was probably diminished in the experiments above. An estimate of the effect of the extent of CYP3A4 inactivation on the V_{max}/K_m values can be provided by a few simple calculations, based on the kinetic parameters for inactivation. The parameters were determined in Ch. 3 and resulted in a mean apparent $K_I = 15.0 \pm 3.4$ μM and a mean $k_{inact} = 0.338 \pm 0.135$ (Table 3.1). These values can now be used to estimate the rate of inactivation of CYP3A4 by midazolam at any midazolam concentration by substituting into an equation completely analogous to the Michaelis-Menten equation (shown in Ch. 6, Section 6.2) [Tudela et al., 1987; equation (10)]. The k_{inact} value is substituted in the place of V_{max} and the K_I value is substituted in the place of K_m. Because the inactivation of CYP3A4 obeys first-order kinetics (Figs. 3.7 and 3.9), the concentration of enzyme (C) present at time (t) can be described by:

$$C = C_o\, e^{-kt}$$

where C_o is initial enzyme concentration and k is the rate of inactivation. By integrating this equation with respect to time one can calculate the time-averaged concentration of active enzyme present, i.e. the area under the enzyme concentration-time curve, during an incubation of midazolam with CYP3A4.

The results of these calculations are shown in Fig. 5.2 where the time-averaged concentration of remaining enzyme is plotted vs time at several midazolam concentrations. As shown in the figure, after a 4

minute exposure to 0.2 μM midazolam, 99% of the CYP3A4 remained, while only 87% remained in the 4 μM incubations. To determine the effect of inactivation on the V_{max}/K_m values, these time-averaged enzyme concentrations were then used to recalculate the rates observed in the biopsy samples on a per nmol CYP3A4 basis. Because identical levels of CYP3A4 were present in the incubations (0.25 pmol/mL, Section 5.2), the rates observed per nmol CYP3A4 should be nearly identical. New V_{max}/K_m values (mL/min) were calculated from the rates for the 6 non-induced biopsy samples which did not contain CYP3A5. The newly calculated values gave a mean V_{max}/K_m value of 9.0 ± 0.6 mL/min. The data reported above, in Table 5.1, was transformed to mL/min for the same 6 samples and the mean V_{max}/K_m value was nearly identical (9.1 ± 0.6 mL/min). Thus, inactivation, as estimated, appears to have had essentially no effect on the V_{max}/K_m values obtained in this small population of liver donors. This result supports the conclusion that midazolam, used at low concentrations can be an effective probe of CYP3A4 despite inactivation. However, the data in Fig. 5.2 suggests that significant enzyme loss occurs at higher concentrations of midazolam. The effect of enzyme inactivation on midazolam product formation rates at high midazolam concentrations is addressed in Ch. 6.

The one to one correspondence between 1′-OH MDZ formation and CYP3A4 content suggests that predicting an *in vivo* intrinsic formation clearance by measuring V_{max}/K_m *in vitro* is at least possible. This conclusion was supported by the *in vivo* results. The formation of 1′-OH

MDZ formation *in vivo* was evaluated in the fifteen organ donors by determining the ratio of 1′-OH MDZ to midazolam in plasma 30 minutes after i.v. injection. This time point corresponds to the peak plasma concentration of 1′-OH MDZ after i.v. injection of midazolam [DeKroon et al., 1989]. Because 1′-OH MDZ clearance is formation rate limited, the intrinsic formation clearance of midazolam to 1′-OH MDZ can be estimated by the ratio of the metabolite to the parent drug [Wilkinson, 1987]. Indeed, when the 1′-OH MDZ/midazolam ratios were compared to the contents of CYP3A4, simple linear regression analysis revealed a statistically significant linear relationship ($r^2 = 0.74$, $n = 15$, $P < 0.001$) [Thummel et al., 1994]. Because both the *in vitro* clearance values and *in vivo* clearance values of midazolam appear to be determined by CYP3A4 content, these studies were repeated in the same population of livers, after having been transplanted to the recipients. The K_m and V_{max} values were determined *in vitro*, as shown above, in biopsy samples obtained 10 days after transplant surgery. Then the *in vitro* V_{max}/K_m values were scaled-up to represent the intrisic clearance of the whole liver. When these *in vitro* values were transformed into the well-stirred model for hepatic clearance [Gibaldi et al., 1982], and compared to the *in vivo* total clearance of an i.v. dose of midazolam in the organ recipients, a quantitatively accurate prediction was obtained [Thummel et al., 1994]. Continuing studies are being conducted to further develop midazolam as a probe of CYP3A4 activity in intestinal tissue [Paine et al., 1995].

Table 5.1. Estimates of K_m and V_{max} and hepatic CYP3A4 contents in subcellular 13,000 × g supernates of human liver biopsy samples from a population of organ donors.

Sample	K_m (μM)	V_{max} (pmol/min/mg)	V_{max}/K_m (mL/min/mg)	CYP3A4 (pmol/mg)
D-1	1.67	0.164	0.0979	11.2
D-2	1.95	0.114	0.0586	6.5
D-3‡	2.38	0.188	0.0791	8.7
D-4‡	2.78	0.149	0.0536	6.3
D-5*	1.57	0.672	0.4282	31.0
D-7	1.85	0.067	0.0364	4.0
D-8	1.80	0.145	0.0804	9.4
D-11	1.99	0.150	0.0754	7.4
D-12‡	2.93	0.125	0.0426	1.1
D-13*	1.91	0.152	0.0793	23.8
D-14*	1.82	0.369	0.2030	22.7
D-16*	2.32	0.404	0.1740	32.8
D-17*	1.79	0.470	0.2628	40.8
D-18‡	3.01	0.197	0.0654	9.1
D-19	2.53	0.072	0.0286	3.1

* Induced Liver

‡ Contains CYP3A5

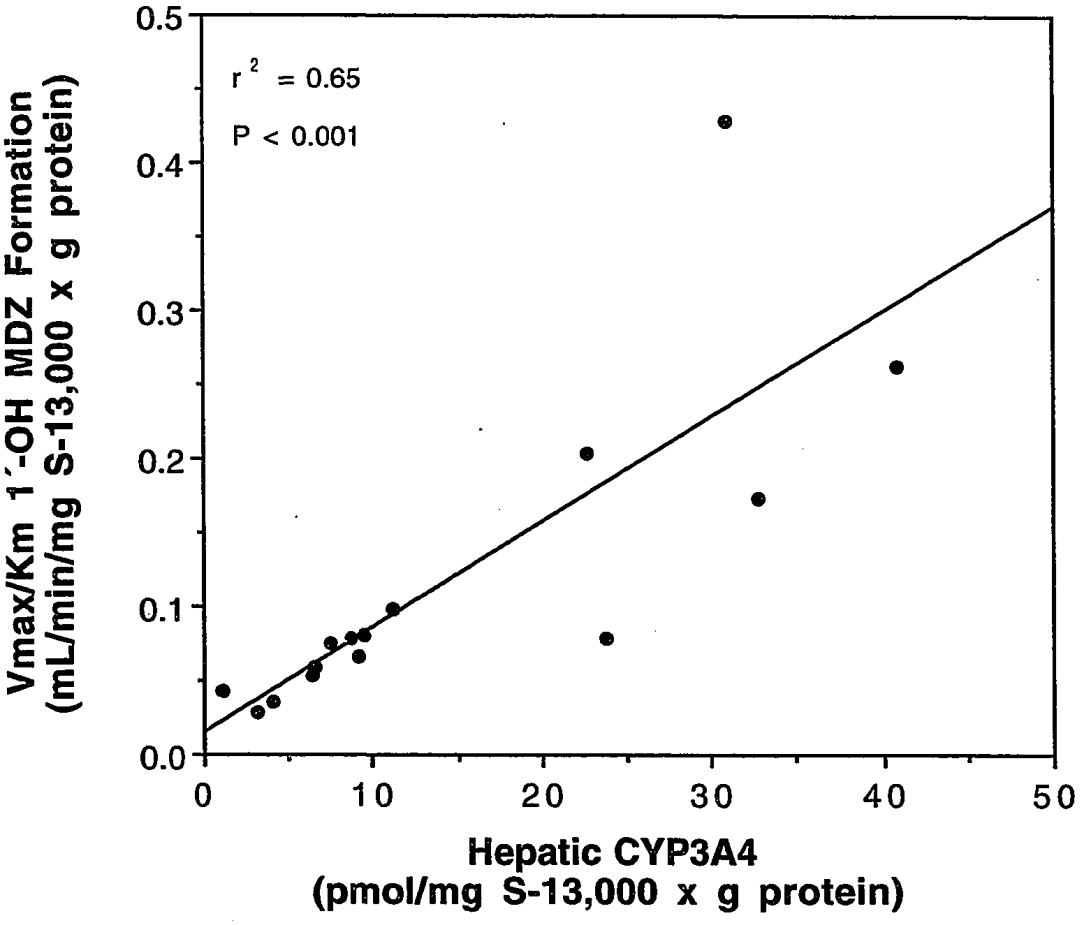

Figure 5.1. Comparison of V_{max}/K_m for the formation of 1´-OH MDZ to hepatic CYP3A4 content in a population of organ donors. The line of best fit and coeffecient of determination (r^2) were calculated by simple regression analysis.

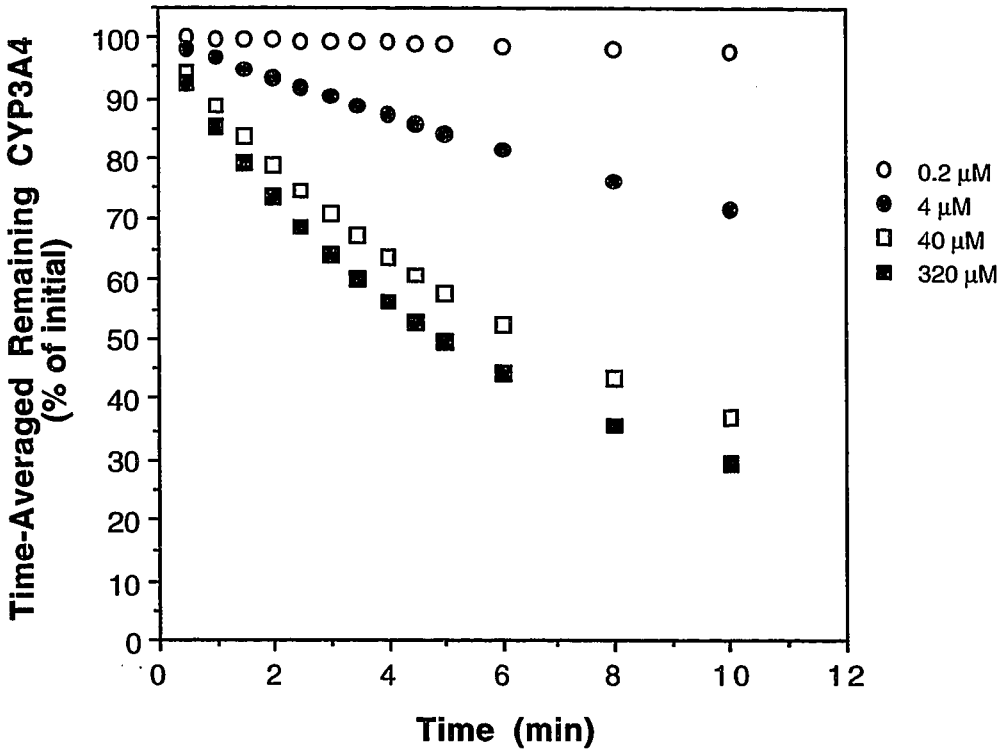

Figure 5.2. The midazolam-concentration dependence of time-averaged concentration of active enzyme remaining, i.e. the area under the enzyme concentration-time curve, calculated at various incubation times.

CHAPTER SIX

THE USE OF MIDAZOLAM AS AN *IN VITRO* PROBE OF CYP3A4: THE UNIQUE KINETIC CHARACTERISTICS OF CYP3A4

6.1. Introduction

At the low plasma concentrations of midazolam prevalent *in vivo*, 1′-OH MDZ is the major metabolite, representing ~70% of the dose excreted into urine [Heizmann et al., 1981]. The minor metabolite, 4-hydroxymidazolam (4-OH MDZ) is responsible for only ~3% of the dose excreted into urine [Heizmann et al., 1981]. Since the 4-hydroxylation pathway does not contribute significantly to the *in vivo* clearance of midazolam it was not considered critical in constructing an *in vitro* predictive model. However, 4-hydroxylation appears to be significant when higher concentrations of midazolam are used in *in vitro* kinetic studies, as discussed below.

The product formation kinetics of midazolam metabolites *in vitro* were first characterized by Kronbach et al., but the results of these studies were not typical of Michaelis-Menten kinetics [Kronbach et al.,1989]. The authors measured the rates of formation of the metabolites after 10 minute incubations and presented the data graphically as a velocity vs. substrate concentration curve (Fig. 6.1). As shown in the figure, the rate of 4-hydroxylation is one-third of the rate of 1′-hydroxylation at 32 μM midazolam, but as substrate concentration increases, the rates of formation of the two metabolites progress differentially until the 4-OH MDZ formation rate exceeds that of 1′-OH

MDZ. Indeed, the most outstanding, gross characteristic of the plotted curves is the rapid decline in the rate of formation of 1′-OH MDZ with increasing concentrations of midazolam > 32 μM. In order to determine the K_m and V_{max} values, and to generate the curves shown, the rate data were fit under the assumption of Michaelis-Menten kinetics with noncompetetive substrate inhibition. The K_m for 1′-hydroxylation was found to be 3.5 μM while the K_m for 4-hydroxylation was found to be 40 μM. Despite the different kinetic parameters, the authors suggest that a single P450 isozyme is primarily responsible for the formation of both 1′-OH MDZ and 4-OH MDZ. In support of this conclusion, a number of experiments produced parallel results between the two metabolites. The experiments included chemical inhibition, antibody inhibition, gross metabolism characteristics in a cDNA-expressed preparation of CYP3A4, correlative analyses of formation velocities to CYP3A content in microsomes of 15 human livers, and correlative analyses between the formation velocities of the two metabolites in the same microsomes. Midazolam metabolism studies reported since the appearance of Kronbach's paper were discussed in detail in Chapter 2 (Section 2.1). These studies also report the determination of two different K_ms for the two metabolites [Gascon et al., 1991; Gorski et al., 1994]. However, a wide range of apparent K_ms were reported in these studies for 1′-OH MDZ formation (from 2.5 to 12.6 μM), and for 4-OH MDZ formation (from 14.7 to 119.0 μM). One possible explanation for the inter-laboratory variability in the K_m of each metabolite is the differing environments of the *in vitro* systems employed. Gorski et al. used a purified, reconstituted system

which gave relatively high K_m values for each metabolite, while microsomes were used by Gascon et al., and gave relatively low K_m values. The K_ms generated in microsomal preparations reported in this chapter are relatively low and closely match the microsomal values observed by Gascon et al. The K_ms generated in our lab with a cDNA-expressed system (alluded to below) are more similar to the reconstituted-system values reported by Gorski et al. The high apparent K_m values observed in the cDNA-expressed system may have been limited by the reductase levels (discussed below), while the high apparent K_m values in the reconstituted system may have been due to a combination of factors, that, when excluded, are known to attenuate CYP3A4 activities in these systems [Shet et al., 1993]. Each individual system consistently gives a higher K_m value for 4-OH MDZ formation.

Simple, Michaelis-Menten kinetics is not consistent with the observation of differing K_ms being associated with the formation of two metabolites from a single substrate by a single enzyme. Assuming steady-state kinetics and irreversible product formation, the properties expected of a one-enzyme, one-substrate, multiple-products system have been stated previously [Branchflower et al., 1977]. They are:

1. The same K_m is observed for all products.
2. The product ratios are constant, and
    a) independent of substrate concentration
    b) independent of enzyme concentration.

Information regarding such a system can be gained by observations of K_m and product ratios. If 1, 2, or both 1 and 2 (above) are not observed

from a one-enzyme, one-substrate system, then the active site of the enzyme or individual rate constants have been altered during the course of rate measurements. Such alterations can be caused by changes in the medium, such as the pH, ionic strength, or temperature. Another possibility is substrate induced alterations in the conformation of the enzyme active site as might occur via an allosteric interaction.

Non-classical product formation kinetics, including allosteric interactions, have been widely reported for substrates of CYP3A4. This appears to be a unique characteristic of this particular cytochrome P450. For example, differences have been observed in K_m between metabolites formed from quinidine by CYP3A4 [Guengerich et al., 1986]. Additionally, allosteric activation of CYP3A4 by α-naphthoflavone has been described [Schwab et al., 1988; Raney et al., 1992]. Studies in the rabbit homolog of CYP3A4, CYP3A6, led investigators to suggest that a non-productive, activator binding site exits on CYP3A isoforms, and that binding of α-naphthoflavone to the activator site alters the conformation of the active site [Johnson et al., 1988]. In contrast, a recent study reported kinetic data on the activation of CYP3A4 by α-naphthoflavone [Shou et al., 1994]. These authors suggested that, rather than a non-productive activator binding site, α-naphthoflavone and a second substrate molecule can bind simultaneously to the active site of CYP3A4, both having access to the iron-bound active oxygen atom. As a final example, effects of differing substrates on the CO-binding kinetics of CYP3A4 have also been utilized as an approach to study the unique characteristics of CYP3A4 [Koley et al., 1995]. These authors describe

different conformers of CYP3A4 which have distinct substrate specificities. While the examples are many, the mechanism by which CYP3A4 is altered to give differing K_ms for 1′-OH MDZ and 4-OH MDZ formation from midaozlam is not understood. Preliminary results were obtained in our laboratory that confirm these unique characteristics of CYP3A4 and suggest additional experiments that could be done to give new insights.

A single enzyme system, i.e. a commercially available cDNA-expressed CYP3A4 preparation (Gentest, Woburn, MA) which was obtained before the company co-expressed NADPH-cytochrome P450 reductase in their cells, was incubated with midazolam at several concentrations ranging from 0.25 to 128 μM in the presence of NADPH. Eadie-Hofstee plots gave linear results for both metabolites ($r^2 \geq 0.96$). The apparent K_m for 1′-OH MDZ was 4.6 μM, while the apparent K_m for 4-OH MDZ was 85 μM (similar to the findings of Gorski et al. as discussed above). When the product ratio, 1′-OH MDZ/4-OH MDZ, was plotted versus midazolam concentration, the product ratio changed drastically from about 10:1 at 0.25 μM midazolam to 1:1 at 128 μM (Fig. 6.2). Because the incubation medium was carefully controlled, effects such as pH or temperature changes are not expected to have contributed to the observed discrepancy in the K_ms or the changes in product ratios. Instead, the only known variables between our individual incubation mixtures were:

1) the amounts of midazolam,
2) the amounts of midazolam metabolites, and

3) the amounts of active CYP3A4 enzyme remaining (see Chapters 3 and 4).

These preliminary results, coupled with the knowledge that CYP3A4 is known to be allosterically modified under certain conditions, suggest that midazolam, or midazolam metabolites may alter the active site of CYP3A4 giving rise to changes in product ratios, and differences in the K_ms. However, before such possibilities can be explored for midazolam, the effects elicited by mechanism-based inactivation of CYP3A4 on the gross kinetic characteristics of the system need to be understood.

As a means of understanding the effect of enzyme inactivation on the gross kinetic differences between 1′- and 4-hydroxylation of midazolam in human liver microsomal preparations, the kinetic parameters of 1′-OH MDZ and 4-OH MDZ formation were measured under the same conditions (lowest possible substrate concentrations, steady-state kinetics) used to measure the *in vitro* intrinsic clearance of midazolam to 1′-OH MDZ. These parameters, along with the kinetic parameters of CYP3A4 inactivation by midazolam presented in Chapter 3 (Table 3.1) were then used to build a model of the gross kinetic characteristics of this complicated system. The purpose of building such a model was to determine if the unusual shape of Kronbach's velocity versus substrate concentration curve (Fig. 6.1) could be accounted for by mechanism-based enzyme inactivation. Finally, the same velocity versus substrate concentration curve features reported by Kronbach were confirmed using human liver microsomes from our laboratory. If the

gross kinetic characteristics of the data presented by Kronbach et al. can be duplicated in microsomes known to be inactivated by midazolam from our laboratory, and both systems can be predicted by the model above, then Kronbach's data can be explained by mechanism-based inactivation of CYP3A4 by midazolam.

6.2. Materials and Methods

Materials

Midazolam, 1´-hydroxymidazolam (1´-OH MDZ), 4-hydroxymidazolam (4-OH MDZ), and the deuterated internal standard, 1´-$^{2}H_{2}$-1´-hydroxy-midazolam (D_{2}-1´-OH MDZ) were gifts kindly provided by Drs. William Garland and Bruce Mico, Roche Laboratories (Nutley, NJ). N-methyl-N-*tert*-butyl-dimethylsilyltrifluoroacetamide (MTBSTFA) was purchased from Pierce Chemical (Rockford, IL), NADPH (reduced form, tetrasodium salt) from Sigma Chemical Co. (St. Louis, MO), and ethyl acetate and acetonitrile from Fischer Scientific (Fair Lawn, NJ).

Midazolam Metabolism by Human Hepatic Biopsy Tissue

Biopsy Tissue: Liver biopsy samples (referred to as: D-1, D-2, ...) were the same as those reported in Ch. 5 (Section 5.2).

Five-Point Estimates of K_m and V_{max}: Studies to determine the K_m and V_{max} parameters were conducted essentially as described above (Section 5.2) with the following modifications. S-13,000 × g supernatant from liver biopsy samples D-8 and D-17 were incubated in duplicate with

midazolam at 0.2, 1, 4, 16, and 64 μM. Estimates of K_m and V_{max} parameters were calculated for each liver biopsy sample from simple linear regression analysis of Eadie-Hofstee plots where: slope = $-K_m$, and y-intercept = V_{max}.

Predicting the Effect of Inactivation on Midazolam Product Formation

The kinetic parameters for the inactivation of CYP3A4 used in the following calculations were the mean K_I and k_{inact} values of those listed in Table 3.1 ($K_I = 15.0 \pm 3.4$ μM and $k_{inact} = 0.338 \pm 0.135$). The mean K_m and mean V_{max} values for the formation of 1′-OH MDZ and 4-OH MDZ were calculated from the set of values obtained from sample R-6 (Section 2.3, Table 5.3), and samples D-8 and D-17 (Section 6.3, Table 6.1). The midazolam concentrations used in the following calculations were 0.2, 1, 2, 4, 10, 20, 40, 80, 160, and 320 μM. The initial concentration of CYP3A4, C_o, was 0.25 pmol/mL. The first two steps below are the same steps used in Section 5.4 to calculate the time-averaged concentration of CYP3A4 during an incubation with midazolam.

1) The rate of enzyme inactivation at each midazolam concentration was estimated by using an equation analogous to the Michaelis-Menten equation [Tudela et al., 1987; equation (10)]:

$$k = \frac{k_{inact} \times [I]}{K_I + [I]}$$

where k is the rate of inactivation at midazolam concentration, [I].

2) The average concentration, C, of enzyme present over t = 4 min and 10 min at each midazolam concentration was determined by solving the definite integral for time-dependent, first-order decay:

$$C = C_o \int_{t_o}^{t} e^{-kt} dt$$

where C_o is the initial enzyme concentration and k is the rate of inactivation from Step 1.

3) The rates of 1′-OH MDZ and 4-OH MDZ formation were estimated by assuming simple Michaelis-Menten enzyme kinetics using the respective kinetic parameters for 1′-OH MDZ and 4-OH MDZ (Table 6.1):

$$v = \frac{V_{max} \times [S]}{K_m + [S]}$$

where v is the rate of product formation at midazolam concentration, [S].

4) To estimate the attenuated amount of product formed at each midazolam concentration, the estimated product formation rate (v, step 3) was multiplied by the time-averaged enzyme concentration (C, step 2):

$$v \times C = \text{nmol product formed min}^{-1}$$

5) To estimate the observed product formation rates, the amount formed (Step 4) at each midazolam concentration was divided by by the initial enzyme concentration (C_o):

(nmol product formed /min)/C_o = rate (nmol product/min/nmol enzyme)

6) The estimated product formation rates for both 1´-OH MDZ and 4-OH MDZ (Step 5, ordinate) were then plotted versus midazolam concentration (abscissa). The lines shown in Figures 6.5 and 6.6 were drawn by the graphics program and are not based on an enzyme kinetic model.

Midazolam Metabolism by HL #124 Microsomes

Experiments performed to determine midazolam product formation rates in HL #124 microsomes were conducted essentially as described above for the biopsy samples (Section 5.2), with the following modifications. The spectral content of P450 was determined by the method of Omura and Sato [Omura et al., 1962] as described above (Section 3.4). Human liver microsomes (HL #124, final concentration 10 nM P450) were incubated in duplicate with midazolam at final concentrations of 0.39, 0.78, 1.56, 3.125, 6.25, 12.5, 25, 50, 100, 200, and 400 μM.

6.3. Results

K_m and V_{max} Determinations: 1′-Hydroxylation and 4-Hydroxylation

Rates determined in biopsy sample D-8 were used to determine K_m and V_{max} parameters for both metabolites by Eadie-Hofstee plots which resulted in straight lines for both metabolites ($r^2 \geq 0.95$, Figs. 6.3 and 6.4). A parallel experiment conducted in biopsy sample D-17 also resulted in straight lines for both metabolites ($r^2 \geq 0.94$, data not shown). The same experiment conducted in biopsy sample R-6 was presented in Chapter 2 (Section 2.3, Figs. 2.5 and 2.6) and had given similar results. The kinetic parameters determined in biopsy samples D-8, D-17 and R-6 were compiled and are shown in Table 6.1. Similar values were obtained for 1′-hydroxylation between the 3 samples. Also, similar values were obtained for 4-hydroxylation between the 3 samples. In contrast, comparing the mean kinetic parameters for 1′-hydroxylation to those for 4-hydroxylation reveals a 12-fold difference between the mean K_ms and a 1.6-fold difference between the mean V_{max}s (Table 6.1).

Predicting the Effect of Inactivation on Midazolam Product Formation

The average concentration of CYP3A4 present after 10 minute incubations and after 4 minute incubations of midazolam with P450 were estimated at each of several midazolam concentrations from 0.2 to 320 μM as described in the materials and methods. The estimated enzyme levels were then used to predict the amounts of 1′-OH MDZ and 4-OH MDZ formed per minute at each midazolam concentration. These

amounts per minute were then transformed into amounts per minute per unit enzyme by dividing by the initial concentration of enzyme. When the 10 minute rates were plotted versus midazolam concentration, 1′-hydroxylation rates increase up to 4 μM midazolam, but then appear to decrease sharply with increasing concentrations of midazolam until a plateau is reached at ~160 μM midazolam (Fig. 6.5). The rates of 4-hydroxylation, however, increase hyperbolically until a plateau is reached at ~160 μM midazolam (Fig. 6.5). When the 4 minute rates were plotted versus midazolam concentration, 1′-hydroxylation rates increase up to 10 μM midazolam, but then appear to decrease gradually with increasing concentrations of midazolam until a plateau is reached at ~160 μM midazolam (Fig. 6.6). The rates of 4-hydroxylation, however, increase hyperbolically until a plateau is reached at ~160 μM midazolam (Fig. 6.6).

Product Formation Rates in HL #124

The product formation rates of midazolam 1′- and 4-hydroxylation were measured in HL #124 microsomes at several midazolam concentrations from 0.39 to 400 μM after 4 minute incubations. The velocity versus substrate concentration curves for each metabolite are presented in Figure 6.7. The 1′-hydroxylation rates increase up to 12.5 μM midazolam, but then decrease gradually with increasing concentrations of midazolam (Fig. 6.7). The rates of 4-hydroxylation, however, increase hyperbolically until a plateau is reached at ~200 μM midazolam (Fig. 6.7).

6.4. Discussion

K_m and V_{max} Determinations: 1′-Hydroxylation and 4-Hydroxylation

Like other substrates of CYP3A4, midazolam turnover appears to be sensitive to changes in the conformation of the active site of CYP3A4 which result in the observation of different K_ms for the two metabolites produced from this single-enzyme, single-substrate sytem. Similar to the findings of other investigators [Kronbach et al., 1989; Gascon et al., 1991], the K_m and V_{max} parameters for 1′- and 4-hydroxylation were consistent among the three biopsy tissue samples utilized and different between the two metabolites (Table 6.1). The mean apparent K_m value for 1′-hydroxylation, 1.66 μM, is similar to the value obtained for the affinity of midazolam for microsomal P450 obtained by differential UV analysis of Type I binding spectra, 3.3 μM [Fabre et al., 1988]. Therefore, it appears that the interaction between CYP3A4 and midazolam can be predominantly characterized by a high-affinity component whether that interaction is measured by turnover rates to the major metabolite, or, in the absence of turnover, by the appearance of a Type I binding spectrum. In contrast, a 12-fold higher apparent K_m value is obtained when 4-hydroxylation rates are used to calculate the affinity of CYP3A4 for midazolam (19.6 ± 2.3 μM, Table 6.1).

This value is similar to the apparent K_I value obtained for the inactivation of CYP3A4 by midazolam (15.0 ± 3.4 μM, Table 3.1). These results suggest that the steady-state, reversible binding of midazolam to

CYP3A4 that initiates the reaction pathway resulting in 4-hydroxylation may also result in the inactivation of the enzyme. If so, then the direct analogy between the inactivation of CYP1A2 by furafylline and the inactivation of CYP3A4 by midazolam, that was suggested in Section 3.1 warrants further investigation (Fig. 3.4). The analogy had been suggested based on the structural similarities between the major site of oxidation on midazolam (localized on the C-1′ methyl group) and the site of oxidation responsible for inactivation by furafylline (also described above as localized on the C-8 methyl group). Now that the C-4 methylene group of midazolam has been implicated in the inactivation of CYP3A4, this direct analogy may not be appropriate. However, the possibility of similar mechanisms cannot be completely discarded. The mechanism of carbon hydroxylation at carbon atoms α to an aromatic ring by P450 involves hydrogen atom abstraction and generation of a carbon centered radical intermediate [Ortiz de Montellano, 1986]. Assuming this mechanism, the radical character of this intermediate, whether on furafylline (C-8) or on midazolam (C-1′ or C-4) carbon atoms, can be delocalized into the imidazole aromatic ring because all of these carbon atoms are in an α-position to the aromatic ring. Stabilization via resonance delocalization may therefore play a role in the inactivation mechanism of both furafylline and midazolam, regardless of which specific, localized site of midazolam metabolism leads to inactivation of CYP3A4.

Predicting the Effect of Inactivation on Midazolam Product Formation

The effect enzyme inactivation has on the gross characteristics of 1′-OH MDZ formation rates can be predicted when the kinetics of midazolam product formation are calculated at midazolam concentrations > 4 μM (Fig. 6.5). This figure matches the gross characteristics of the curves presented by Kronbach et al. (Fig. 6.1). Any effect on the formation of 1′-OH MDZ and 4-OH MDZ by inactivation was assumed to be due to the decrease in catalytically active CYP3A4 during incubation of microsomal P450 with midazolam. CYP3A4 inactivation by midazolam is concentration-dependent, saturable, pseudo-first-order process that can be described by a steady-state kinetic model (Ch. 3) [Tudela et al., 1987]. Therefore, the effect of decreasing CYP3A4 concentration on midazolam product formation rates was estimated by utilizing the kinetic parameters of enzyme inactivation in the calculations outlined in the materials and methods. Because the apparent K_m for 1′-hydroxylation is lower than the apparent K_m of 4-hydroxylation, the rate of formation of 1′-OH MDZ is saturated, and more sensitive to enzyme concentration, at an earlier stage of the incubation than is the rate of formation of 4-OH MDZ. Therefore, as the rates of inactivation increase with increasing midazolam concentration, the time-dependent concentration of active enzyme decreases, and the calculated rates of 1′-hydroxylation start to decrease at a much lower concentration of midazolam than would the rates for 4-hydroxylation. Because the apparent K_m of 4-hydroxylation is similar to the apparent K_I

of inactivation, the two processes approach maximal rates at similar times during the incubation at all midazolam concentrations and the predicted effect of inactivation on the gross characteristics of 4-OH MDZ formation rates are less obvious (Figs. 6.5 and 6.6). These differential effects on 1′ and 4-OH MDZ formation rates were confirmed using human liver microsomes in which midazolam had been shown to inactivate CYP3A4 (HL #124, Chs. 3 and 4).

Product Formation Rates in HL #124

The velocity versus substrate concentration curves for 1′- and 4-OH MDZ formation generated by incubating HL #124 microsomes with midazolam concentrations ranging from 0.39 to 400 μM mirrored the predicted curves (Figs. 6.6 and 6.7). It is likely, then, that the observations of Kronbach et al. (Fig. 6.1) can be explained by mechanism-based inactivation of CYP3A4 by midazolam.

In summary, the kinetics of midazolam turnover change as a function of the concentration of midazolam. When the midazolam concentrations used to measure 1′- OH MDZ formation are ≤ 4 μM, the observed rates can be used to estimate the kinetic parameters of metabolite formation (Ch. 5). These results can then be used to predict the CYP3A4 content in the liver and perhaps even the *in vivo* clearance of midazolam to the major metabolite, 1′-OH MDZ [Thummel et al., 1994]. When midazolam product turnover rates are measured from 4 minute incubations at concentrations including those ≥ 10 μM, CYP3A4

inactivation appears to have a significant effect on the rates of formation of 1′-OH MDZ. The substrate concentration dependent changes in midazolam kinetics can be at least partially explained by the inactivation of CYP3A4. However, the difference between the apparent K_ms of the two metabolites also contributes to the substrate dependent changes in midazolam product formation kinetics. Future steady-state experiments, including those designed to address the differing apparent K_ms that appear to accompany midazolam product formation kinetics catalyzed by CYP3A4, should be conducted at ≤ 4 μM midazolam to avoid complications by inactivation. Additionally, the further development of midazolam as a probe of CYP3A4 could continue in another direction. Studies utilizing midazolam at high concentrations to study the mechanism of inactivation could yield unique insights into the structure and function of CYP3A4.

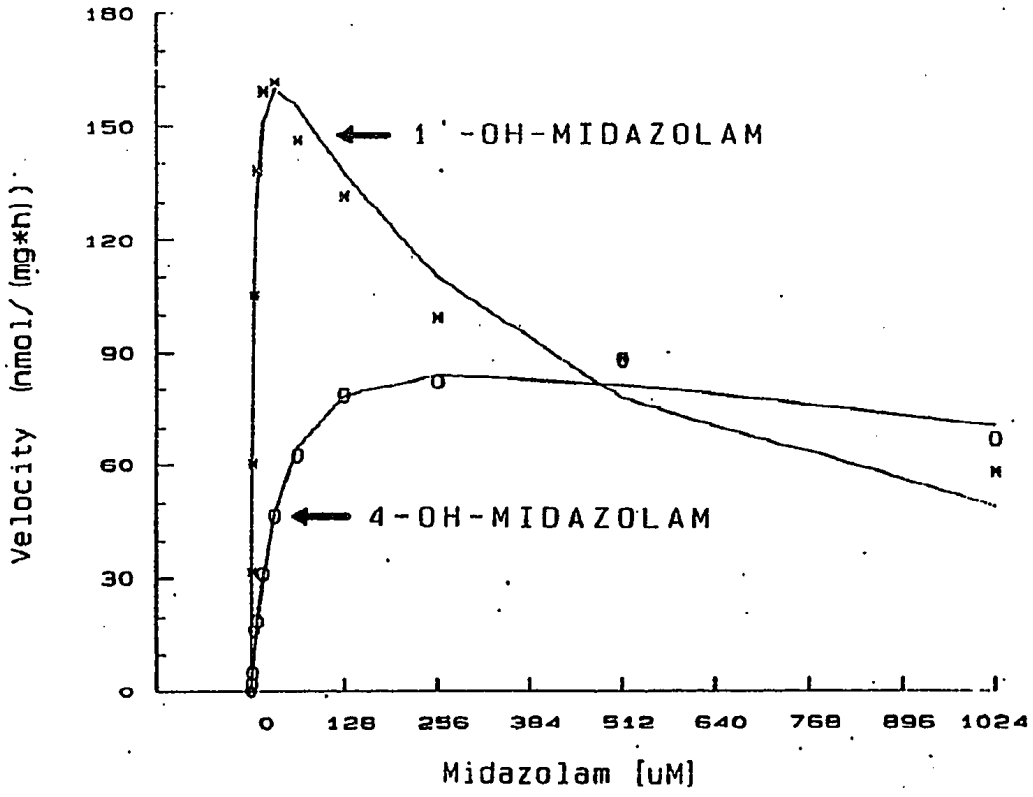

Figure 6.1. Velocity vs. substrate concentration curve for the formation of 1´-OH MDZ and 4-OH MDZ during a 10 minute incubation in human liver microsomes presented by Kronbach et al. [Kronbach et al., 1989].

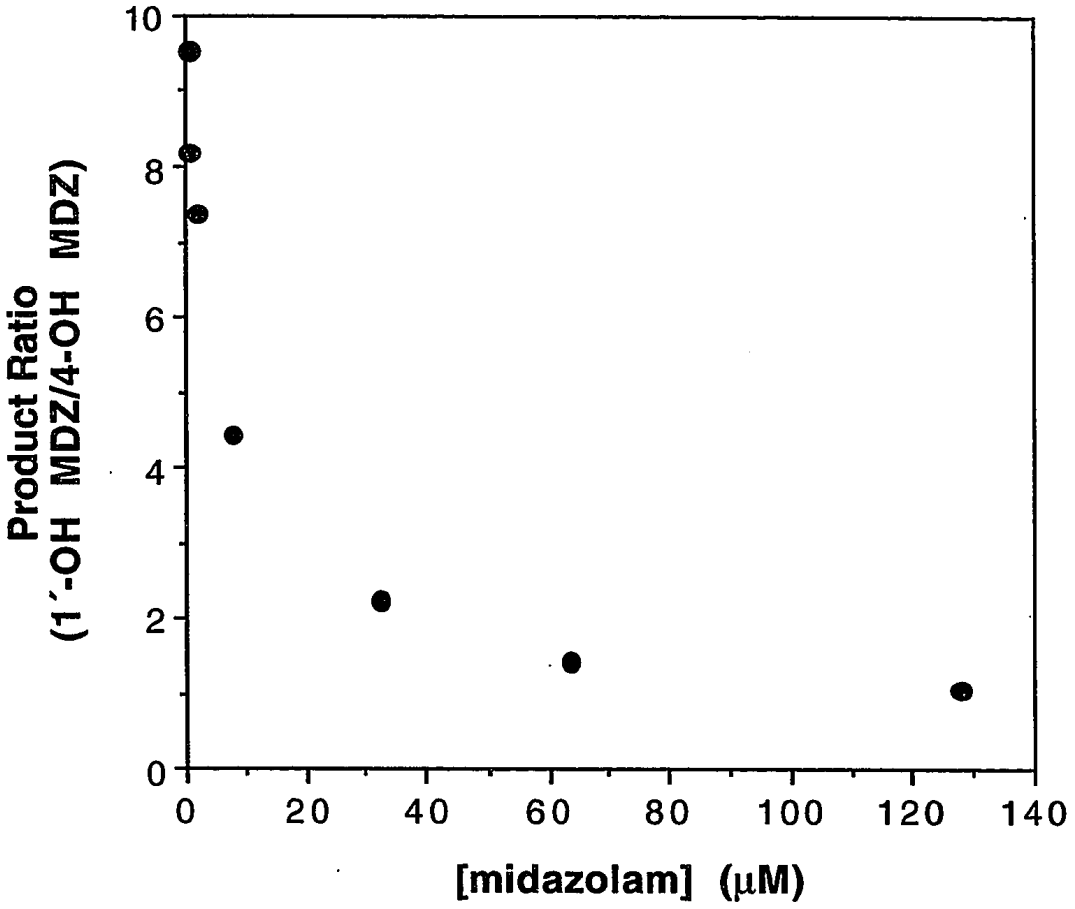

Figure 6.2. Changing ratio of 1´-OH MDZ to 4-OH MDZ as a function of midazolam concentration in a cDNA-expressed preparation of CYP3A4.

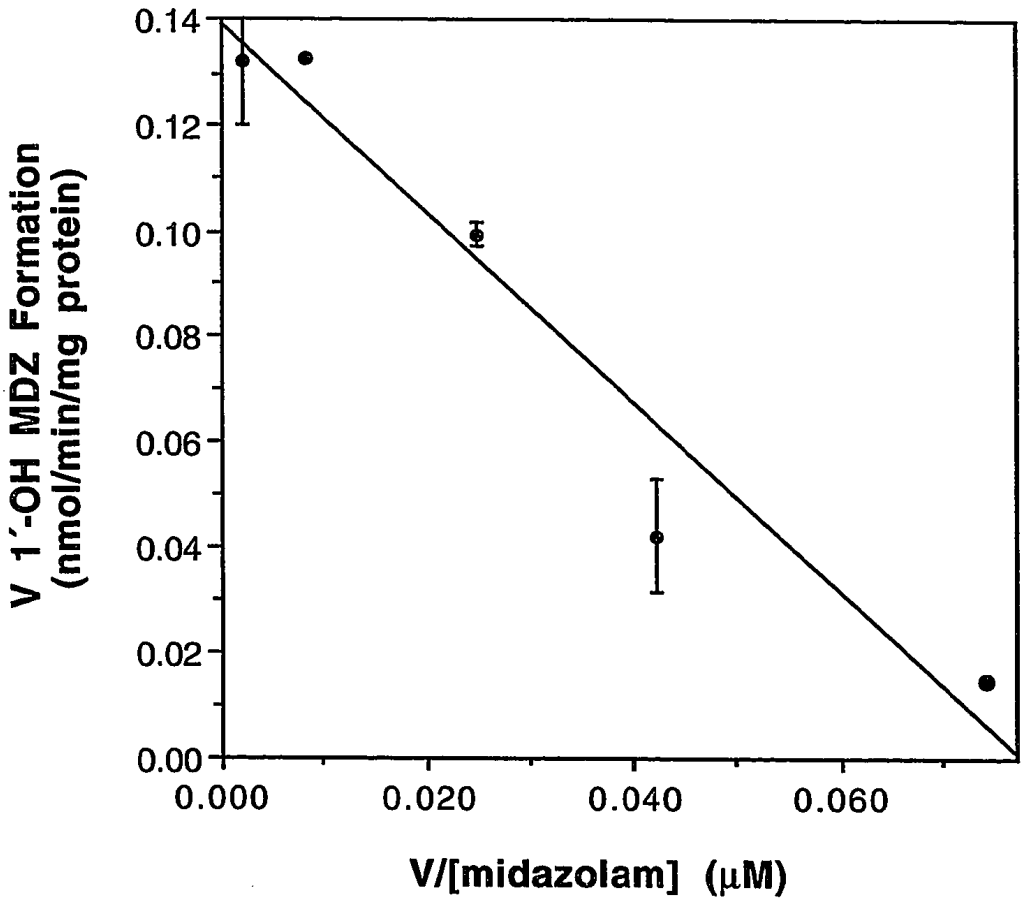

Figure 6.3. Eadie-Hofstee plot for the formation of 1´-OH MDZ from human liver biopsy sample D-8 at 0.2 to 64 μM midazolam. Error bars represent standard deviations of duplicate determinations at each concentration.

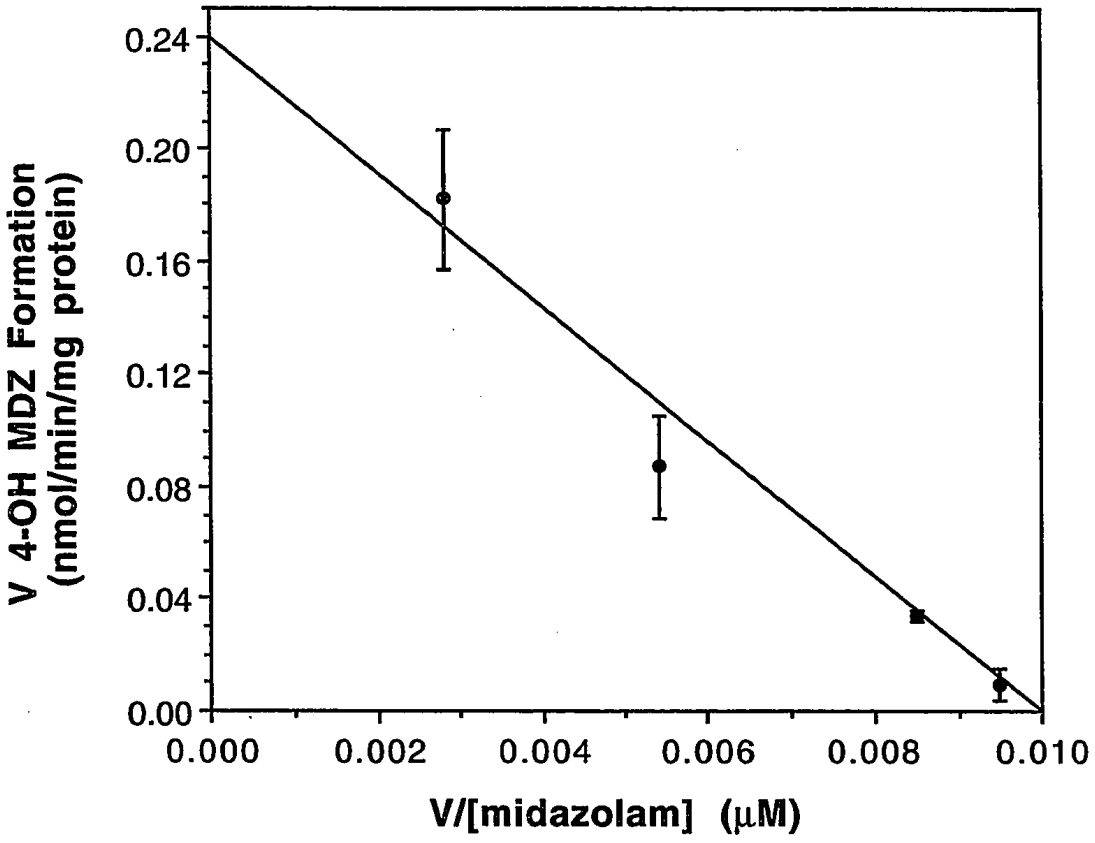

Figure 6.4. Eadie-Hofstee plot for the formation of 4-OH MDZ from human liver biopsy sample D-8 at 1 to 64 μM midazolam.

Table 6.1. Kinetic parameters for 1′-hydroxylation and 4-hydroxylation of midazolam in subcellular 13,000 × g supernates of human liver biopsy samples.

	1′-Hydroxylation		4-Hydroxylation	
Sample	K_m (μM)	V_{max}* (nmol/min/nmol)	K_m (μM)	V_{max}* (nmol/min/nmol)
R-6	1.52	13.3	19.4	25.3
D-8	1.79	14.7	21.9	23.9
D-17	1.68	11.2	17.4	15.0
av ± SD	1.66 ± 0.14	13.1 ± 1.8	19.6 ± 2.3	21.4 ± 5.6

* V_{max} parameters are reported as nmol product/min/nmol CYP3A4.

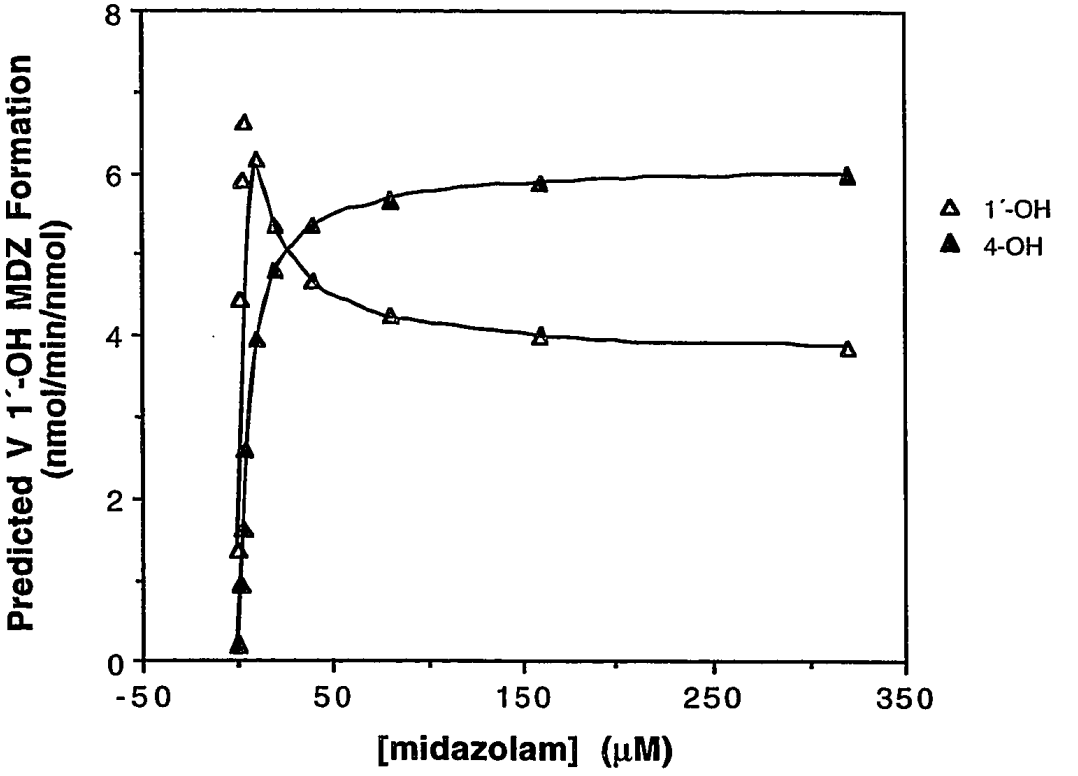

Figure 6.5. Predicted velocity vs. substrate concentration curve for the formation of 1´-OH MDZ and 4-OH MDZ during a 10 minute incubation.

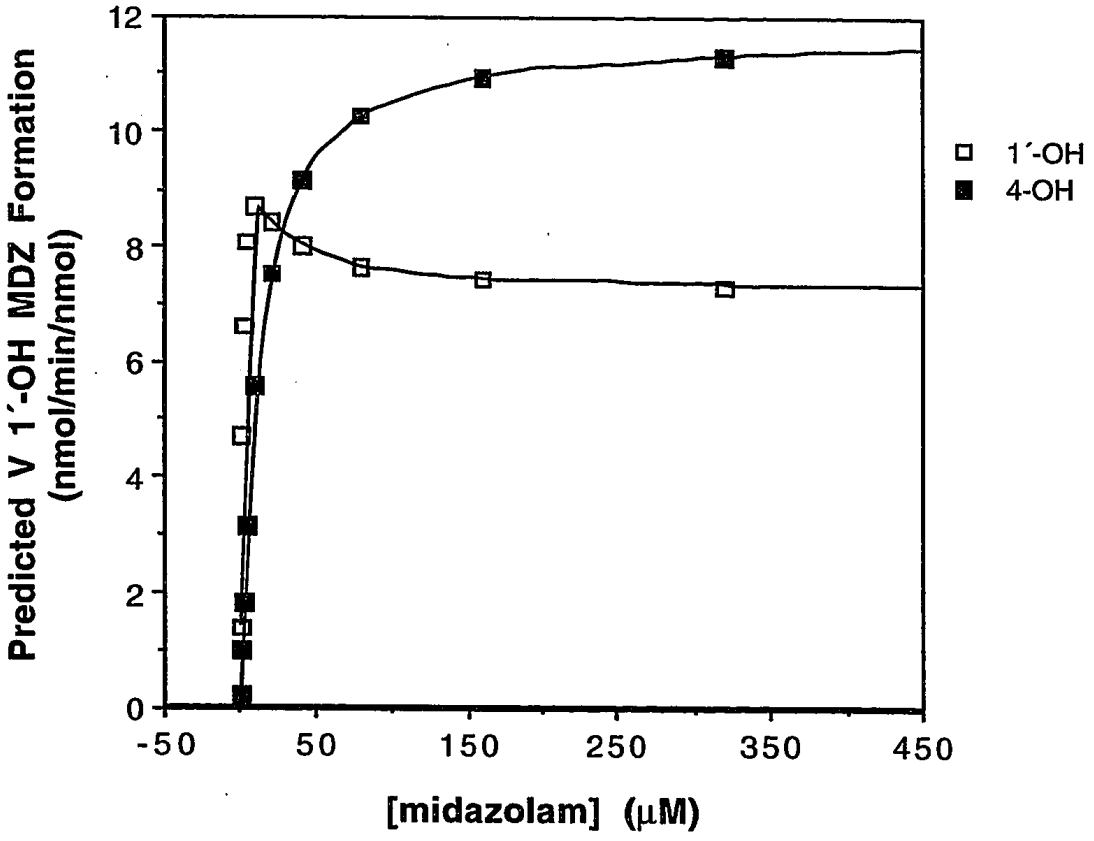

Figure 6.6. Predicted velocity vs. substrate concentration curve for the formation of 1´-OH MDZ and 4-OH MDZ during a 4 minute incubation.

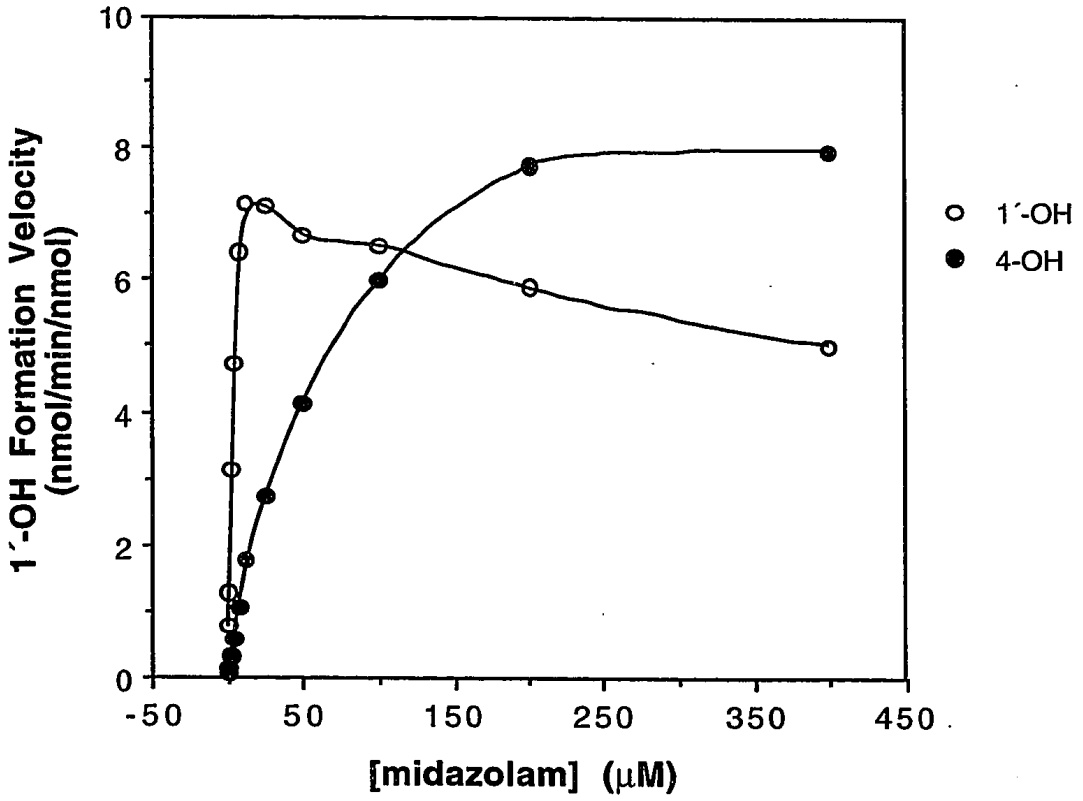

Figure 6.7. Velocity vs. substrate concentration curve for the formation of 1´-OH MDZ and 4-OH MDZ from HL #124 microsomes during a 4 minute incubation.

BIBLIOGRAPHY

Allonen, H., G. Ziegler, et al., *Clinical Pharmacology and Therapeutics* **30**(5): 653-661. (1981).

Aoyama, T., S. Yamano, et al., *The Journal of Biological Chemistry* **264**(18): 10388-10395. (1989).

Banzon, J. A., J. M. Kuo, et al., *Biochemistry* **34**(3): 743-749. (1995).

Beaune, P. H., D. R. Umbenhauer, et al., *Proc. Natl. Acad. Sci. USA* **83**: 8064-8068. (1986).

Bensoussan, C., M. Delaforge, et al., *Biochemical Pharmacology* **49**(5): 591-602. (1995).

Blackett, A., S. Dhillon, et al., *Journal of Chromatography* **433**: 326-330. (1988).

Bolt, H. M., H. Kappus, et al., *J. Endocrinol. Metab.* **39**: 1072-1080. (1977).

Bork, R. W., T. Muto, et al., *The Journal of Biological Chemistry* **264**(2): 910-919. (1989).

Budzikiewicz, H., *Mass Spectrometry Reviews* **5**: 345-380. (1986).

Darbyshire, J. F., J. R. Gillette, et al., *Biochemistry* **33**(10): 2938-2944. (1994).

DeKroon, I. F. I., P. N. J. Landendijk, et al., *Journal of Chromatography* **491**: 107-116. (1989).

Dixon, R., R. Lucek, et al., *Res. Commun. Chem. Pathol. Pharmacol.* **37**: 11-16. (1982).

Drayer, D. E., *Clin. Pharmacokin.* **1**: 426-431. (1976).

Dundee, J. W., N. J. Halliday, et al., *Drugs* **28**: 519-543. (1984).

Estabrook, R. W., S. Kawano, et al., *Acta Biol. Med. Germ.* **38**: 423-434. (1979).

Fabre, G., P. Crevat-Pisano, et al., *Biochemical Pharmacology* **37**(10): 1947-1953. (1988).

Fabre, G. e., R. Rahmani, et al., *Biochemical Pharmacology* **37**(22): 4389-4397. (1988).

Franklin, M. R., *Pharmac. Ther.* **A2**: 227-232. (1977).

Franklin, M. R. (1991). Cytochrome P450 metabolic intermediate complexes from macrolide antibiotics and related compounds. Methods in Enzymology. M. R. Waterman and E. F. Johnson. San Diego, Academic Press. **206:** 559-573.

Fraser, A. D., W. Bryan, et al., *Journal of Analytical Toxicology* **15**: 8-12. (1991).

Gascon, M. P. and P. Dayer, *European Journal of Clinical Pharmacology* **41**: 573-578. (1991).

Gibaldi, M. and D. Perrier (1982). Pharmacokinetics. New York, Marcel Dekker Inc.: 409-417.

Gillam, E. M. J., Z. Guo, et al., *Archives of Biochemistry and Biophysics* **317**(2): 374-384. (1995).

Gillette, J. R., *Annals of the New York Academy of Sciences* **179**: 43-66. (1971).
Gonzalez, F. J., B. J. Schmid, et al., *DNA* **7**(2): 79-86. (1988).

Gorski, J. C., S. D. Hall, et al., *Biochemical Pharmacology* **47**(9): 1643-1653. (1994).

Greenblatt, D. J., A. Locniskar, et al., *Anesthesiology* **55**: 176-179. (1981).

Guengerich, F. P., M. V. Martin, et al., *J. Biol. Chem.* **261**: 5051-5060. (1986).

Guengerich, F. P., D. Muller-Enoch, et al., *Molecular Pharmacology* **30**: 287-295. (1986).

Guengerich, F. P., *Molecular Pharmacology* **33**: 500-508. (1988).

Guengerich, F. P., *Critical Reviews in Biochemistry and Molecular Biology* **25**(2): 97-139. (1990).

Guengerich, F. P., *Chemical Research in Toxicology* **3**(4): 363-371. (1990).

Guengerich, F. P. and C. G. Turvey, *J. Pharmacol. Exp. Ther.* **256**: 1189-1194. (1991).

Ha, H. R., K. M. Rentsch, et al., *Therapeutic Drug Monitoring* **15**: 338-343. (1993).

Heizmann, P. and W. H. Ziegler, *Arzneim. Forsch./Drug Res.* **31**: 2220-2223. (1981).

Horsmans, Y., J. P. Desager, et al., *Parmacol. Toxicol.* **71**: 258-261. (1992).

Itoh, S., T. Yanigimoto, et al., *Biochem. Biophys. Acta* **1130**: 133-138. (1992).

Johnson, E. F., G. E. Schwab, et al., *The Journal of Biological Chemistry* **263**(33): 17672-17677. (1988).

Kharasch, E. D. and K. E. Thummel, *Anesth Analg* **76**: 1033-1039. (1993).
Kitz, R. and I. B. Wilson, *The Journal of Biological Chemistry* **237**(10): 3245-3249. (1962).

Knight, G. C. and S. G. Waley, *Biochem. J.* **225**: 435-439. (1985).
Koley, A. P., J. T. M. Buters, et al., *The Journal of Biological Chemistry* **270**(10): 5014-5018. (1995).

Komori, M., K. Nishio, et al., *Biochemistry* **29**: 4430-4433. (1990).

Kronbach, T., Daniel Mathys, et al., *Molecular Pharmacology* **36**: 89-96. (1989).

Kronbach, T., V. Fischer, et al., *Clin. Pharmacol. Ther* **43**: 630-635. (1988).

Kunze, K. L. and W. F. Trager, *Chemical Research in Toxicology* **6**(5): 649-656. (1993).

Kuthan, H. and V. Ullrich, *European Journal of Biochemistry* **126**: 583-588. (1982).

Labroo, R. B., K. E. Thummel, et al., *Drug Metabolism and Disposition* **23**(4): 490-496. (1995).

Laemmli, U. K., *Nature (Lond.)* **227**: 680-686. (1970).

Lavrijsen, K. L. M., J. M. G. Van Houdt, et al., *Anesthesiology* **69**: 535-540. (1988).

Levin, W., A. Y. H. Lu, et al., *Archives of Biochemistry and Biophysics* **158**: 842-852. (1973).

Lillibridge, J. A., B. M. Amore, et al., *Drug Metabolism and Disposition* . In press. (1996).

Lown, k. S., J. C. Kolars, et al., *Drug Metabolism and Disposition* **22**(6): 947-955. (1994).

Mastey, V., A.-C. Panneton, et al., *Journal of Chromatography B: Biomedical Applications* **655**: 305-310. (1994).

McClune, G. J., J. A. Fee, et al., *J. Am. Chem. Soc.* **99**: 5220-5222. (1977).

Molowa, D. T., E. G. Schuetz, et al., *Proc. Natl. Acad. Sci. USA* **83**: 5311-5315. (1986).

Nelson, D. R., T. Kamataki, et al., *DNA and Cell Biology* **12**(1): 1-51. (1993).

Ortiz de Montellano, P. R., Ed. (1986). Cytochrome P-450. New York, Plenum.

Ortiz de Montellano, P. R., *Progress in Drug Metabolism* **11**: 99-148. (1988).

Paine, M., et al., *ISSX Proceedings* **8**: 298. (1995).

Pessayre, D., V. Descatoire, et al., *Biochemical Pharmacology* **30**: 553-558. (1981).

Peter, R., R. B¬ocker, et al., *Chemical Research in Toxicology* **3**(6): 566-573. (1990).

Porter, W. R., R. V. Branchflower, et al., *Biochemical Pharmacology* **26**: 549-550. (1977).

Puglisi, C. V., J. C. Meyer, et al., *Journal of Chromatography* **145**: 81-96. (1978).

Puglisi, C. V., J. Pao, et al., *Journal of Chromatography* **344**: 199-209. (1985).

Purba, H. S., J. L. Maggs, et al., *Br. J. Clin. Pharmacol.* **23**: 447-453. (1987).

Ramsdell, H. S., A. Parkinson, et al., *Toxicol. Appl. Pharmacol.* **108**: 436-441. (1991).

Rettie, A., K. Korzekwa, et al., *Drug Metabolism and Disposition* **17**: 265-270. (1989).

Rettie, A. E., K. R. Korzekwa, et al., *Cemical Research in Toxicology* **5**: 54-60. (1992).

Rubio, F., B. J. Miwa, et al., *Journal of Chromatography* **233**: 157-165. (1982).

Sattler, M., F. P. Guengerich, et al., *Drug Metabolism and Disposition* **20**(5): 753-761. (1992).

Schaefer, W. H., T. M. Harris, et al., *Biochemistry* **24**(13): 3254-3263. (1985).

Schuetz, J. D., D. L. Beach, et al., *Pharmacogenetics* **4**: 11-20. (1994).

Schuetz, J. D., D. T. Molowa, et al., *Archives of Biochemistry and Biophysics* **274**(2): 355-365. (1989).

Schwab, G. E., J. L. Raucy, et al., *Molecular Pharmacology* **33**: 493-499. (1988).

Shah, V. P., K. K. Midha, et al., *European Journal of Drug Metabolism and Pharmacokinetics* **16**(4): 249-255. (1991).

Shou, M., J. Grogan, et al., *Biochemistry* **33**: 6450-6455. (1994).

Silverman, R., (1988). Mechanism-Based Enzyme Inactivation: Chemistry and Enzymology. Boca Raton, FL, CRC Press.

Silvers, K. J., T. Chazinski, et al., *Cancer Research* **52**: 6237-6243. (1992).

Tatsunami, S., N. Yago, et al., *Biochimica et Biophysica Acta* **662**: 226-235. (1981).

Thummel, K. E., C. A. Lee, et al., *Biochemical Pharmacology* **45**(8): 1563-1569. (1993).

Thummel, K. E., D. D. Shen, et al., *Journal of Pharmaceutics and Experimental Therapeutics* **271**(1): 549-556. (1994).

Thummel, K. E., D. D. Shen, et al., *Journal of Pharmaceutics and Experimental Therapeutics* **271**(1): 557-566. (1994).

Tudela, J., F. G. Canovas, et al., *Biochimica et Biophysica Acta* **912**: 408-416. (1987).

Vasiliades, J. and T. Sahawneh, *Journal of Chromatography* **228**: 195-203. (1982).

Waley, S. G., *Biochem. J.* **185**: 771-773. (1980).

Waley, S. G., *Biochem. J.* **227**: 843-849. (1985).

Walker, D., J.-P. Flinois, et al., *Biochemical Pharmacology* **47**(7): 1157-1163. (1994).

Walsh, C., T. Cromartie, et al., *Methods Enzymol.* **53**: 437-448. (1978).

Wandel, C., R. Bocker, et al., *British Journal of Anaesthesia* **73**(5): 658-661. (1994).

Wang, P. P., P. Beaune, et al., *Biochemistry* **22**(23): 5375-5383. (1983).

Watkins, P. B., S. A. Wrighton, et al., *Proc. Natl. Acad. Sci.* **82**: 6310-6314. (1985).

Waxman, D. J., C. Attisano, et al., *Archives of Biochemistry and Biophysics* **263**(2): 424-436. (1988).

Waxman, D. J., D. P. Lapenson, et al., *Archives of Biochemistry and Biophysics* **290**(1): 160-166. (1991).

White, I. and U. Muller-Eberhard, *Biochem. J.* **166**: 57-64. (1977).

Wilkinson, G. R., *Pharmacological Reviews* **39**(1): 1-47. (1987).

Williams, R. T., (1959). Detoxication Mechanisms. New York, Wiley.

Williams, R. T. (1971). . Concepts in Biochemical Pharmacology, Part 2. B. B. Brodie and J. R. Gillette. Berlin, Springer-Verlag: 226-232.

Winkler, K., S. Keiding, et al. (1973). Clearance as a Quantitative Measure of Liver Function. The Liver: Quantitative aspects of structure and function. G. Paumgartner and R. Preisig. New York, S. Karger: 144-155.

Wrighton, S. A., P. Maurel, et al., *Biochemistry* **24**: 2171-2178. (1985).

Wrighton, S. A., B. J. Ring, et al., *Molecular Pharmacology* **36**: 97-105. (1989).

Wrighton, S. A., W. R. Brian, et al., *Molecular Pharmacology* **38**: 207-213. (1990).

Yang, H. L., Q. P. Lee, et al., *Molecular Pharmacology* **46**: 922-928. (1994).

Yun, C., R. A. Okerholm, et al., *Drug Metabolism and Disposition* **21**(3): 403-409. (1992).

Yun, C.-H., M. Wood, et al., *Anesthesiology* **77**: 467-474. (1992).

VITA

Terry Dean Podoll, sixth child of Harvey J. Podoll and Bonnie J. Podoll, was born on July 28, 1965 in Madison County, Nebraska. He graduated from Norfolk Senior High School (NE) in May 1983. That fall he entered the University of Texas at Austin. He was a Robert A. Welch Undergraduate Fellowship Award recipient in the Summer of 1989, and in December of 1989 he graduated with a Bachelor of Science degree in Chemistry. He then entered the graduate program in Chemistry at the University of Washington. After graduating with a Master of Science degree in Organic Chemistry in June of 1991, he entered the graduate program in Medicinal Chemistry at the same university. He was Summer Research Fellow at the Upjohn Research Laboratories in 1992, and was a Gordon Research Conference Travel Award recipient in 1994. Terry received the Doctor of Philosophy in Medicinal Chemistry in the Winter of 1996.